2014-04-04

Effect of macrophage depletion on avian infectious bronchitis coronavirus infection

Kameka, Amber Marie

UNIVERSITY OF CALGARY

Effect of macrophage depletion on avian infectious bronchitis coronavirus infection

by

Amber Marie Kameka

A THESIS

SUBMITTED TO THE FACULTY OF GRADUATE STUDIES

IN PARTIAL FULFILMENT OF THE REQUIREMENTS FOR THE

DEGREE OF MASTER OF SCIENCE

VETERINARY MEDICAL SCIENCES GRADUATE PROGRAM

CALGARY, ALBERTA

APRIL, 2014

Abstract

Infectious bronchitis virus (IBV) causes severe respiratory tract infections in young chickens and has significant negative impact on the poultry industry. Information on the functional roles of macrophages in response to IBV infection is scarce. Objectives of the work described in the thesis were to 1) establish an effective means of depleting macrophages within the respiratory tract of chickens using clodronate encapsulated-liposomes, 2) determine the effects of IBV infection on macrophage numbers *in vivo*, and 3) the effect of macrophage depletion on the replication of IBV and resulting pathogenesis. We found that clodronate encapsulated-liposomes were effective in significantly depleting macrophages in the respiratory tract. We also observed that an infection with the Conn strain IBV results in an increase in macrophage numbers in trachea and lung, and that clodronate encapsulated-liposome treated trachea have a higher IBV genome load at the beginning of infection when compared to untreated tissues. Our data suggests that respiratory macrophages may play an important role in limiting the replication of IBV within respiratory tissues.

Key words: infectious bronchitis virus, macrophages, clodronate, respiratory tract

Preface

This thesis is based on the studies done at the Department of Ecosystem and Public Health, Faculty of Veterinary Medicine, University of Calgary, Alberta, Canada from May 2012 to April 2014. Chapters three and four of this thesis contain materials that were previously published as follows:

Kameka, A.M., Haddadi, S., Kim, D.S., Cork, S.C., Abdul-Careem, M.F., 2014. Induction of innate immune response following infectious bronchitis corona virus infection in the respiratory tract of chickens. Virology 450-451, 114-121.

Kameka, A.M., Haddadi, S., Jamaldeen, F.J., Moinul, P., He, X.T., Nawazdeen, F.H.P., Kim, D.S., Bonfield, S., Sharif, S., van Rooijen, N., and Abdul-Careem, M.F., 2014. Clodronate treatment significantly depletes macrophages in chickens. Canadian Journal of Veterinary Research, in Press.

Acknowledgements

First of all I would like to acknowledge the Faculty of Veterinary Medicine, University of Calgary for providing me with the opportunity to conduct my MSc studies. The research and my stipend were funded by Natural Science and Engineering Council (NSERC) of Canada.

I would like to thank Dr. Faizal Careem for being my supervisor and mentor for these last 2 years. He's helped me to stand on my own two feet, problem solve, and feel confident in my abilities in the lab. He also took a chance on me since I had no previous background in research work before coming to the University of Calgary, and I hope he also feels a sense of accomplishment in all that we've done in my masters program.

I would also like to thank my co-supervisor, Dr. Susan Cork, for her relaxed nature and helpful advice during the start of my program, as well as her continuing enthusiasm in my progress as a student. My committee members Drs. Markus Czub and Robin Yates have also been extremely accessible and provided me with useful creative criticism and access to information in their own areas of research, which helped me to expand on any issues I was having with my own.

I would like to thank all of the previous summer students: Jasmine, Jesreen, Hafsa, Prima, and Tim for their help with the preliminary immunohistochemical staining of tissue sections, and the light hearted attitude that came from working as a team. Siamak Haddadi and Dae-Sun Kim were particularly helpful with my in lab training, animal care, and tissue collection. They also provided me with someone to talk too, if things were getting too overwhelming at times. I would also like to acknowledge my friend and current lab partner Simrika Thapa, whose positive attitude and helpful and

kind personality made working in the lab all the more fun. Finally, I would like to show my gratitude to Steven Bonfield and Sandeep Atwal, who helped me learn about the intricate system of ordering products and using machines on campus, as well as providing their time to look over manuscript submissions and troubleshoot any data analysis problems I had.

My thanks also goes out to all the on and off campus facilities that aided our lab in this research, especially Brenda Roszell and Dr. Greg Muench of the Veterinary Science Research Station at Spy Hill, University of Calgary for experimental animal management and support in performing animal procedures respectively. I would like to thank the staff at the Histopathology Diagnostic Services Unit for providing their services in sectioning tissues and histological staining. Also, Lauren Kennedy and Yui Ipliu for their flexibility and expertise in flow cytometry sample sorting. A big thanks to all the members of the Czub, van Marles, Van der Meer, Schaetzl, Glich, and Coffin labs for their help, support, and all around experience.

I would like to conclude that I never would have made it to this point if it wasn't for the love, help, and support provided to me by my mom and dad. They have always been there for me from the very beginning and are a constant reminder of what the will to succeed can bring about with support and love behind it.

Thank you all,

Amber Marie Kameka

Table of Contents

List of Tables

List of Figures and Illustrations

List of Abbreviations

ANOVA	Analysis of variance
APC	Alloplycocyanin
$AppCl_2p$	Adenosine-5'-[β, γ-dichloromethylene]triphosphate
Ark	Arkansas
ATP	Adenosine triphosphate
BALT	Bronchus associated lymphoid tissue
B cell	B lymphocyte
BCoV	Bovine coronavirus
BSA	Bovine serum albumin
CD	Cluster of differentiation
cDNA	Complementary DNA
CEK	Chicken embryonic kidney
Cl_2MBP or Clod	Clodronate
Conn	Connecticut
CpG ODN	CpG oligodeoxynucleotides
DC	Dendritic cell
dpi	Days post-infection
dpt	Days post-treatment
dsRNA	Double-stranded RNA
E	Envelope
EDTA	Ethylenediaminetetraacetic acid

EID_{50}	Egg infectious dose 50
ELISA	Enzyme-linked immunosorbent assay
ER	Endoplasmic reticulum
FARM	Free avian respiratory macrophage
FBS	Fetal bovine serum
FIPV	Feline infectious peritonitis virus
H & E	Haematoxylin and eosin
HBSS	Hank's balanced salt solution
HDSU	Histopathology Diagnostic Service Unit
HPAI	Highly pathogenic avian influenza
hpi	Hours post-infection
HPS	Hypopericardium syndrome
HSV	Herpes simplex virus
IB	Infectious bronchitis
IBV	Infectious bronchitis virus
IFN	Interferon
IL-	Interleukin
ILTV	Infectious laryngotracheitis virus
iNOS	Inducible nitric oxide synthase
LPS	Lipopolysaccharides
LTA	Lipoteichoic acid
M	Membrane

Mass	Massachusetts
MDV	Marek’s disease virus
MHC	Major histocompatibility complex
MHV	Mouse hepatitis virus
MPS	Mononuclear phagocyte system
mRNA	Messenger RNA
MyD88	Myeloid differentiation primary response gene 88
N	Nucleocapsid
NK	Natural killer
NO	Nitric oxide
nsp	Non-structural protein
OCT	Optimal cutting temperature
PAMP	Pathogen associated molecular pattern
PBS	Phosphate buffered saline
PCR	Polymerase chain reaction
PE	Phycoerythrin
PRR	Pathogen recognition receptor
qPCR	Quantitative PCR
(-)ssRNA	Negative single-stranded RNA
(+)ssRNA	Positive single-stranded RNA
RNP	Ribonucleoprotein
ROS	Reactive oxygen species

S1, S2, and S protein	Spike
SARs-CoV	Severe acute respiratory syndrome virus
SAT	Spontaneous autoimmune thyroiditis
SEM	Standard error of the mean
SPF	Specific pathogen free
ssRNA	Single-stranded RNA
T cell	T lymphocyte
TLR	Toll-like receptor
TRIF	TIR-domain-containing adapter-inducing interferon-β
VSRS	Veterinary Science Research Center

Chapter One: Introduction

1.1 General Introduction

The respiratory mucosa is under constant challenge from airborne particles and potential pathogens. Given this risk, alveolar macrophages and other components of the innate immune system have a critical role in primary immune defence in the respiratory tract mucosa. Respiratory macrophages play an important role in both innate and adaptive immune systems, with functions ranging from phagocytic clearance of pathogens and cellular debris, antigen processing and presentations and immune activation (Roscic-Mrkic *et al.*, 2001; Tate *et al.*, 2010). Macrophage response to invading pathogens varies according to the types of pathogen involved, including dengue virus (Fink *et al.*, 2009), influenza virus (Tate *et al.*, 2010), and some adenovirus infections (Nakamura *et al.*, 2001).

Although the role of alveolar macrophages in many viral-host interactions is known, specific information on the interaction of avian respiratory macrophages with infectious bronchitis virus (IBV) infection is scarce, and further research is required to provide a better understanding of how macrophages play a role in the pathogenesis of infectious bronchitis (IB) in chickens (Jeurissen *et al.*, 1998; Quere *et al.*, 2003; Rivas *et al.*, 2003). The research outlined in this thesis was developed to study some aspects of the interaction between avian respiratory macrophages and IBV infection in the respiratory tract of chickens. The approach used included the establishment of a method of depleting respiratory tract macrophages using clodronate encapsulated-liposomes due to their high efficiency and specificity in depleting avian macrophages and minimal toxic effects

against the host (van Rooijen and Hendrikx, 2010; van Rooijen and Sanders, 1994). This chapter of the thesis provides an overview of the pathogenesis of IBV, including its replication cycle, tissue tropisms, and the problems with past attempts at controlling IB in the poultry industry. Information on avian macrophages in terms of their location within the respiratory tract, and their common response to viral infection are also discussed along with different macrophage depletion techniques. The mechanism of clodronate-mediated depletion is expanded on, and the hypotheses and aims of this thesis are summarized.

1.2 Infectious Bronchitis Virus

1.2.1 *History*

Researchers Schalk and Hawn first reported clinical signs of IBV in 1931, characterizing the disease as a respiratory infection prominent in chickens ranging from 2 days to 3 weeks of age, with a high mortality rate (40-90%) and post-mortem examination revealing congested respiratory pathways, including the para-bronchioles and trachea of the bird (Shalk and Hawn, 1931). A serum neutralization test using embryonated eggs was later developed for the detection of IBV in infected flocks (van Roechel *et al.*, 1942a). This became particularly important after the discovery of an IBV infection in adult and young chickens in Rhode Island, indicating that IBV infection is not limited to young chickens alone (Delaplane and Stuart, 1939).

IBV infections in older chickens are characterized by mild respiratory symptoms, but also leads to a subsequent loss in egg production in layers (Delaplane and Stuart, 1939). Laboratory studies by van Roeckel *et al.* (1942b) later confirmed these

observations and lead to the introduction of a “planned exposure” program. In this approach, growing chickens were protected from natural IBV infection by the immunization of a few birds with avirulent egg-propagated virus, which were then released into the flock to naturally expose the rest of the flock and propagate the attenuated protective strain of the virus (van Roeckel *et al.*, 1942b). However, the implementation of commercially produced North America vaccines, including the those for the Mass (Holland strain), Mass (1-L strain), and Ark strains or combinations thereof against IBV infection had limited effect in cross-protecting the birds against different IBV serotypes and/or strains, and in maintaining a successful disease control program against its spread in the poultry industry due to a loss in vaccine-induced protection alone and an increase in virulence (Cook *et al*., 1999c).

1.2.2 *Molecular and biological characteristics of IBV pathogenesis*

IBV is a positive-sense single-stranded (ss)RNA virus of 120 to 160 nm in diameter and belongs to the Order *Nidovirales*, Family *Coronaviridae.* It is part of the Group 3 *Coronaviruses* that specifically infect avian hosts such as chickens, pheasants, and galliforms (Siddell and Snijder, 2008). IBV has a genome length of 27.6Kb and these virions are generally pleomorphic in shape, enveloped, with a genome encoding both structural proteins; spike (S1 and S2), membrane (M), envelope (E), and nucleocapsid (N), and the non-structural proteins (Nsps) that are important for the proliferation or replication of the virus, as illustrated in Figure 1.1.

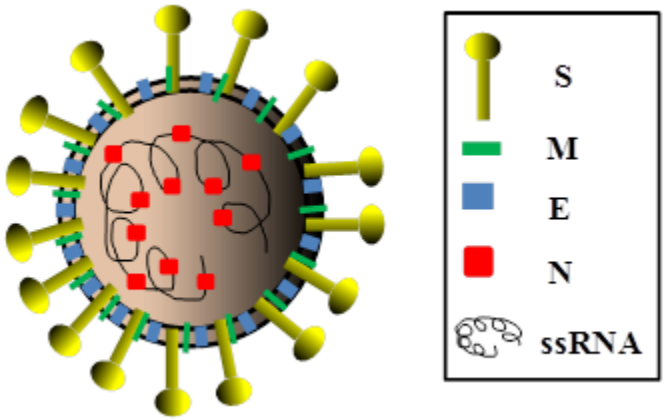

Figure 1.1. Illustration of the IBV viral particle and associated structural proteins. Adapted from Houge and Machamer (2008).

S proteins are found on the surface of the viral envelope and assist in host-cell attachment (Huang *et al.*, 1994). The S protein has a cleaved form with S1 and S2 subunits; the S1 subunit is the determined inducer of immune response against IBV in chickens, while S2 is responsible for fusion of the virus with the host's cells (Huang *et al*., 1994). Differences as small as 2 to 3% in the amino acid residues within the S1 protein have resulted in changes in IBV serotype, leading to the problem of diminished cross-protection with serotype specific vaccination (Cavanagh *et al*., 1997). There are hundreds of different IBV strains and/or serotypes existing in the world today, although most only differ from each other by 20-25% of S1 amino acids (Cavanagh *et al*., 1992; Huang *et al*., 1994; Kant *et al.*, 1992; Koch *et al.*, 1990). To clarify any confusion between the terms "serotype" and "strain", IBV serotypes are determined based on the results of virus neutralization tests using IBV and embryonated chicken eggs or chicken tracheal organ cultures and are dependent on the different external antigens expressed by each serotype that bind with the antibodies used in the assays (Dolz *et al.*, 2006).

Different strains of IBV are determined using real-time quantitative polymerase chain reaction (qPCR) or by nucleotide sequencing, and are thus dependent on differences within the coding sequence of the viral genome (Callison *et al.*, 2001).

The M glycoprotein is embedded in the viral lipid bi-layer, with a small protruding portion on the outer surface (Cavanagh, 1983), while E is a much smaller membrane associated non-glycosylated protein; both proteins are important for virus particle formation during replication (Nauciel *et al.*, 1974). Specifically, the E protein has the role of forming cation-selective ion channels within the host membrane to enhance viral morphogenesis and assembly (Wilson *et al.*, 2004). Results from enzyme-linked immunosorbent assays (ELISAs) have indicated that the M protein is the least immunogenic of the structural proteins (Ignjatovic and Galli, 1995), and shows little cross-reactivity in antibodies between itself and the S1, S2, and N proteins produced during an *in vivo* immunization with both virulent or avirulent strains of IBV vaccines (Ignjatovic and Galli, 1995).

The N protein is closely associated with the RNA genome of IBV, forming a structure termed the ribonucleoprotein (RNP) (Biebricher *et al.*, 1984). The N protein is generally localised within the cytoplasm of the host cell, but may also migrate to the host cell nucleolus as a strategy to control host and viral transcription of subgenomic RNA, due to the high concentration of host ribosomes available during the interphase portion of the cell cycle (Hiscox *et al.*, 2001). There is also evidence that suggests that the N protein is involved in inducing cell cycle arrest to help increase the possibility of the virus to subvert the host cells machinery to help further its replication (Wurm *et al.*, 2001). Both Nsp3 and the N glycoprotein have been implicated in the immunosuppressive tactics of a

number of different coronavirus species (Clementz *et al.*, 2010), including IBV, with the N protein also possessing multiple T lymphocyte (T cell) epitopes for the stimulation of cell-mediated immune responses against IBV infection in chickens (Chubb *et al.*, 1987; Cook *et al.*, 1992; Darbyshire and Peters, 1984).

1.2.3 *IBV replication*

The replication cycle of IBV is similar to that of other coronaviruses, as illustrated in Figure 1.2. The S protein binds to the specific target receptors of the cells that encompass the tissue tropism of that particular IBV strain (Binns *et al.*, 1999). It is unclear if the virus is internalized by either receptor-mediated endocytosis or by fusion with the host cell membrane (Bom *et al.*, 1999). The positive- (+)ssRNA of the virus is used as a template by the host polymerase to synthesizes the viral RNA polymerase directly, in order to further recognize and replicate viral RNAs by producing negative-stranded (-)ssRNA, using the (+)ssRNA as a template (Boyle *et al.*, 1999; Wang *et al.*, 1999). Subgenomic mRNA is also produced, and leads to the process of discontinuous transcription, whereby transcription occurs at the short leader sequences found at the 3' end and allows for elongation either up to the first transcription-regulating sequence and stops synthesis, or to skip over this sequence to continue to elongate the nascent strand (Siddell and Snijder, 2008). The (-)ssRNA is used to synthesize the other proteins of the virus, as well as becoming the subsequent template for the generation of new (+)ssRNA (Boyle *et al.*, 1999). The N protein then binds to the newly synthesized RNA, alongside the integration of the M and E proteins into the membrane of the endoplasmic reticulum

(ER) of the host cell (Casler and Cook, 1999). After the N protein binds to the RNA, it twists into a helical structure, buds into the ER, and is encased within its membrane (Casler and Cook, 1999). The newly formed virions are then transported to the cell surface via the Golgi transport apparatus, and released from the cell by exocytosis (Casler and Cook, 1999).

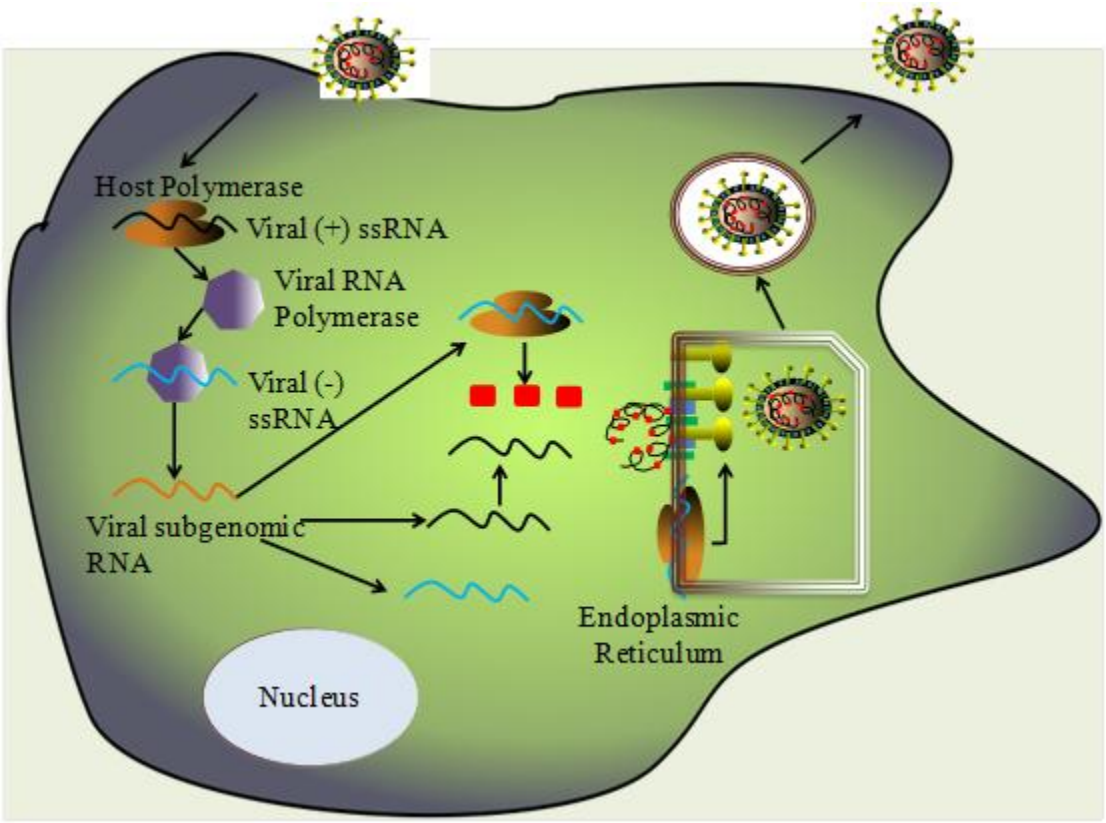

Figure 1.2. IBV replication cycle in infected host cell. IBV replication relies on the host polymerase to generate the viral RNA polymerase, translating the (+)ssRNA into (-)ssRNA, which serves to transcribe the smaller structural proteins (M, E, and S) and as a template for more (+)ssRNA. The virus is enveloped in the host ER, and then is released from the cell via exocytosis while encased in the ER membrane. Adapted from Lai (1987).

1.2.4 *Pathogenesis of IBV*

Depending on the strain, IBV primarily targets epithelial cells in the domestic chicken (*Gallus gallus domesticus*), including those of the upper respiratory tract, kidneys, gastrointestinal tract, and the female reproductive tract, depending on the strain (Cavanagh, 2003). Infection of layer chickens at a young age is characterized by damage to the oviducts, resulting in a significant decrease in both egg quality and numbers, and the production of "false" layers who are unable to lay eggs due the formation of cysts within the oviducts (Jones and Ambali, 1987). Layer chickens have also been found to remain persistently infected, with no viral particles detected after initial infection at a young age (Jones and Ambali, 1987). However, when these persistently infected individuals reach 19 weeks of age, the stress conditions associated with egg production result in a re-excretion of viral particles. This is most likely from the kidneys, alimentary tract, and cecal tonsils, and results in a spread of infection to other flock members through periodic shedding in nasal excretions and faeces (Cavanagh and Naqi, 2003; Chong and Apostolov, 1982; Jones and Ambali, 1987). Recently, IBV has also been identified in the testes of cockerels, indicating a potential expansion in the tissue tropism for some strains of IBV, and the resulting danger of infertility in males if replication of IBV occurred in the spermatozoa producing cells of the testes (Boltz *et al*., 2004).

Damage to the kidneys occurs in infections with the nephropathogenic strains of IBV, with the virus targeting the epithelial cells of all the segments of the tubules and ducts of the kidneys for replication (Paul-Clark *et al*., 2001). Nephropathogenic infections are commonly seen in broiler chickens harvested for meat, and can result in

high mortality in younger birds, as well as a loss of body mass and growth retardation during development (Casais *et al*., 2003).

The research outlined in this thesis focussed specifically on the Connecticut (Conn) strain of IBV, as its replication is limited to the respiratory tract of chickens (Uenaka *et al.*, 1998; Winterfield and Albassam, 1984). Infections of IBV in the upper respiratory tract show the highest viral titres within three days of infection and clearance occurring only after a further five days of infection (Ambali and Jones, 1990). The resulting histopathology includes de-ciliation in the cells of the nares and trachea and inflamed lung tissue as well as thickened and cloudy air sacs, and an infiltration of mononuclear cells into the surrounding mucosal layers (Cavanagh, 2003). Clinical signs of IBV respiratory infection include coughing, sneezing, depression, rales, nasal and ocular discharge, and lethargy (Capua *et al.*, 1994). Viral particles are spread horizontally between members of a flock by contact with the nasal and ocular discharges of infected individuals (Bond *et al*., 1979), and ingestion of faeces or contaminated feed and drinking water (Cavanagh, 2003). IBV can also be spread between farms due to the virus's ability to survive for long periods of time in infected faeces (Cavanagh, 2003). Both contaminated litter, footwear, equipment, personnel, and even strong prevailing winds can result in a spread of IBV between farms (Erbeck and McMurray, 1998)

Whereas macrophages are a source of replication and a means of spreading to other sites in the body by other species of coronavirus such as severe acute respiratory syndrome corona virus (SARs-CoV) (Nicholls *et al.*, 2003); feline infectious peritonitis virus (FIPV) (Yount *et al.*, 2002); murine hepatitis virus (MHV) (Perkins *et al.*, 1999); bovine coronavirus (BCoV) (Borucki *et al*., 2013) and other avian viral diseases such as

infectious laryngotracheitis virus (ILTV) (Calnek *et al.*, 1986; Loudovaris *et al.*, 1991) and Newcastle disease virus (Joiner *et al.*, 2005; Rosenberger and Gelb, 1978), this does not appear to be the case for IBV (von Bulow and Klasen, 1983). The spread of IBV from the respiratory tract to other areas of the body is believed to be accomplished through the process of viremia (Foltz, 2008); complete viral particles enter the bloodstream after being released from the infected respiratory epithelium, where they then travel suspended in the plasma alongside the red blood cells to other areas of the body, such as the kidneys, reproductive tract, and other organs, whereby the epithelial cells of these tissues become infected (Champoux *et al.*, 2004).

1.2.5 *Limitation of the control of IBV in the poultry industry*

IB is a disease common worldwide and can result in significant economic losses (Cavanagh and Naqi, 2003). Canada's poultry industry has been valued at around $3 billion (2009) with 176 million meat birds and more than 7 billion eggs produced annually. Thus far, the main form of control against the different strains of IBV has involved stimulating the adaptive immune responses (ie. stimulation of antibody production or cell mediated immune response). In the early 1950s, the first vaccines for IB were developed, with the same technique of production still used today. This involves the passing of IBV field strains through the embryonated eggs of domestic chickens to naturally attenuate them before vaccinating poultry with live attenuated strains (Cavanagh et al., 1997; Cavanagh et al., 1999). While vaccines are useful in that they have been developed in the form of aerosols sprays or can be administered in drinking

water in order to immunize a large numbers of animals at once, there are significant limitations in the use of vaccines alone against multiple IBV serotypes and/or strains (Cook *et al.*, 1999). Key limitations include the influence of intrinsic factors such as the chicken's age, breed, nutrition, and its living environment, and variation and potential reversion of attenuated viral strains of IBV to virulence.

Since the 1950s, IBV outbreaks in North America have been mainly attributed to the Massachusetts (Mass), Conn, and Arkansas (Ark) strains of the virus (Mondal *et al.*, 2012). Outbreaks of the different strains of IBV are generally attributed to two aspects of coronavirus biology: mutation and recombination. Due to the use of an RNA polymerase in replicating the genome, IBV virions experience 10^{-3} to 10^{-5} errors per replicating cycle, or three mutations per newly synthesized genome (Manrubia *et al*., 2005). This leads to the generation of genetically variable members of the species, which can further contribute to the virus's ability to increase its tropism and respond faster to changes in selective pressures (Biebricher and Eigen, 2006; Sekimura *et al*., 1999; Vignuzzi *et al*., 2006). Recombination is the second aspect of coronavirus biology that contributes to their high adaptability. IBV has been found to undergo homologous recombination with either other infecting strains (Cavanagh *et al.*, 1990; Jia *et al.*, 1995; Kusters *et al.*, 1990), and also with vaccine strains (Lee and Jackwood, 2001; Smati *et al.*, 2002; Wang *et al.*, 1993). The result is the generation of new serotypes and/or strains of IBV, which are frequently resistant to vaccine mediated protection.

'Vaccine failure' is a term used to describe a vaccine's inability to protect a chicken against more than one strain/serotype of a virus (Casais *et al*., 2003; Cavanagh *et al.*, 1997). In terms of IBV, this is believed to be the result of recombination occurring

between two different strains of IBV infecting the host cell, specifically within the genes that code for the S1 amino acids which then alters their protective-inducing epitopes and changing the virus's serotype in the process (Cook *et al.*, 1999b). This was the case seen with the loss of protection by Mass-like IBV vaccine against a recombination event between strains of Ark-like and Mass-like IBV that produced a unique S1 protein (Wang *et al.*, 1993). The manufactures of vector vaccines have attempted to combat this problem by generating a recombinant non-pathogenic strain of another avian virus, such as the fowlpox virus, that can express the IBV S1 gene (Wang *et al.*, 1994). The results have been promising in that protection against IBV was found to be maintained around 90-100% in vaccinated chickens, but thus far only experimental data are available (Johnson *et al.*, 2003; Wang *et al.*, 1994).

Clinical disease caused by IBV is more severe and economically important in young chickens than in adults. This is because as their age increases, the chickens become more resistant to the formation of lesions in the tissues that the specific strains of IBV target, and mortality rate decreases considerably (Albassam *et al.*, 1986; Crinion and Hofstad, 1972; Smith *et al.*, 1985). As a result, live vaccinations of layer chickens occurs at two to three weeks of age, followed by an immunization of an attenuated IBV vaccine near the start of laying; the more short lived broilers are vaccinated the one time with only the live vaccine, on the day of hatch (Cavanagh and Naqi, 2003). However, this protection has been found to be short-lived; chickens that were vaccinated against IBV showed a decline in protection after nine weeks and required revaccinations later in life (Darbyshire and Peters, 1984; Gough and Alexander, 1979).

1.2.6 *Factors contributing to IBV susceptibility/resistance*

Certain breeds of chicken are more susceptible to IBV. For example, evidence suggests that light breeds, such as the White Leghorns, are more susceptible to the nephropathogenic strains of IBV than the heavy breeds, such as the Rhode Island Reds (Cumming and Chubb, 1988). In addition, two inbred lines of White Leghorn chickens (one susceptible breed, one resistant breed) indicated that while the virus can propagate within both lines equally during infection, the more susceptible breed had a much slower viral clearance and the cytopathic effects seen within the trachea occurred much earlier during infection as well (Otsuki *et al.*, 1990). These observed differences in protection are believed to be influenced by the differences in the major histocompatibility complex (MHC) expressed between the different breeds (Bacon *et al.*, 2004), although it is uncertain if significant variation also exists within individuals of the breeds themselves. As a result, there can be variability in the effectiveness of live vaccines amongst different inbred lines of chickens (Otsuki *et al.*, 1990; Pensaert and Lambrechts, 1994). This limits the production of a breed-wide efficacious vaccine for the protection against IBV.

Environmental factors can also influence the susceptibility of chickens to IBV, therefore making the less effective vaccines redundant. The current farming conditions of poultry can also influence a chicken's susceptibility to respiratory disease; environmental stresses such as high levels of ammonia from a buildup of faeces (Anderson *et al.*, 1966; Anderson *et al.*, 1968; Davis and Morishita, 2005), bacterial contamination of food or water (Cooke *et al.*, 1999), and extreme heat (McFarlane *et al.*, 1989) or cold stress (Ratanasethakul and Cumming, 1983), can result in either permanent or transient

immunosuppression and increase a chicken's susceptibility to IBV infection. In comparison, chicken immune responses have been found to be stimulated through the use of treatments involving various immunostimulants, including CpG oligodeoxynucleotides (CpG ODN) (Gomis *et al*., 2003); lipoteichoic acid (LTA) (Farnell *et al.*, 2003); and lipopolysaccharide (LPS) (Parvizi *et al.*, 2014).

1.2.7 *Issues with antiviral therapy*

Other ways of inhibiting coronavirus replication includes targeting the main proteinase used by coronaviruses for virion replication using antiviral drug therapy. Research has shown that the use of cysteine-proteinase inhibitors in cell cultures have inhibited the replication of many species of coronavirus, including IBV (Hiscox *et al*., 2001). Another possible antiviral drug target would be the proteins used in viral RNA synthesis, such as the surface glycoproteins used in the fusion of the virus with the host cell membrane; results have been promising in that the use of the fusogenic inhibitor enfuvirtide inhibits human immunodeficiency virus (HIV) replication by interfering with the conformational rearrangement of structures within carboxy-proximal region of the S protein (Siddell, 2008). However, researchers are still far from developing an antiviral drug that is safe, effective, and can be applied across a wide spectrum of coronavirus species. Therefore, there is a need for more effective disease control strategies to mitigate the effects of IBV infection in the poultry industry. To achieve this, we need to have a greater understanding of the largely unexplored innate immune responses elicited by IBV infection.

1.3 Avian innate immune response

Vertebrate host responses are generally divided into two pathways: the innate and the adaptive immune responses. The adaptive immune response slower than the innate system, but also produces memory B lymphocytes (B cells) and T cells that allows for a rapid secondary response against a pathogen. The B cells mature within a specialized organ of the chickens called the bursa of Fabricius, while the T cells of both mammals and birds mature within the thymus (Koskela *et al.*, 2004; Shanmugasundaram and Selvaraj, 2013). Both B and T cells allow for specific immune responses as they recognize to a particular target antigen that has been processed and presented by the various antigen presenting cells of the immune system (Coleman *et al.*, 1999). In contrast, the innate immune response is more rapid as it is non-specific and the cells involved can recognize a variety of microbial and foreign antigens. It also lacks a memory component, so that a secondary response to the pathogen is mounted at the same speed and intensity as the primary response.

The non-specific immune response is mediated by the binding of cellular pattern recognition receptors (PRRs) to the pathogen associated molecular patterns (PAMPs) of pathogens; PAMPs are targeted as they are conserved among different kinds of pathogens and are not expressed by the host cells (Cook, 1999). An important PRR which is expressed in and on host cells and is involved in the protection against viruses includes the toll-like receptors (TLRs). The interaction between PRRs and PAMPs induces a signalling cascade that results in the recruitment and activation of various adaptor proteins that help to form the large protein complexes that drive the cascade itself. In

chickens, recognition of viral infection is attributed to TLR3 and TLR7, which are orthologous to their mammalian counterparts (Cook *et al*., 1999a). Within the endosomal compartments of the host cell, TLR3 recognizes and binds to the dsRNA intermediates produced during viral replication (Alexopoulou *et al.*, 2001; Higgs *et al*., 2006; Iqbal *et al*., 2005). Stimulation of TLR3 leads to activation of TIR-domain-containing adapter-inducing interferon-β (TRIF) adaptor protein-mediated pathway, whereas TLR7 responds to ssRNA produced during intracellular viral replication, activating the myeloid differentiation primary response gene 88 (MyD88) mediated-pathway (Akira, 2001; Watters et al., 2007). The end products of these signalling cascades are pro-inflammatory cytokines, chemokines, and antiviral type I and II interferons (IFNs) (Guillot *et al*., 2005). The different cells of the avian innate immune response to viral infections are described below.

1.3.1 *The importance of avian macrophages in response to viral infection*

The main cells of the avian innate immune response to viral infections include heterophils (orthologous to mammalian neutrophils), natural killer (NK) cells, dendritic cells (DCs), and macrophages. Heterophils are usually the first cells to be recruited to the site of infection. Experimental studies using respiratory lavage analysis have demonstrated that there is a dramatic increase in heterophils numbers during IBV infection from 24-72 hours post-infection (hpi) (Fulton *et al*., 1993). Heterophils are highly phagocytic and express most of the TLRs found in chickens, although they lack the expression of MHC class I and II molecules that are expressed in other chicken innate

immune cells (Brune *et al.*, 1972). Heterophils are believed to be responsible for the destruction of IBV-infected cells during initial infection through phagocytosis and oxidative burst (Brune *et al.*, 1972; Fulton *et al.*, 1993; Fulton *et al.*, 1997).

NK cells are also significant defenders against viral infections and are a major source of IFNγ production, the latter a cytokine involved in inhibiting the spread of the virus to surrounding cells and thus improving the success of the host immune response (Gobel *et al*., 1994). Recent research has shown that upon infection with Mass41 strain of IBV, NK cell numbers increased by 1 day post-infection (dpi), in conjunction with a significant increase in IFNγ production by 4 dpi (Vervelde *et al.*, 2013). Unlike macrophages and DCs, NK cells are incapable of phagocytosis and do not express MHC class II molecules (Gobel *et al.*, 1994).

The DCs of the chicken possess both phagocytic and antigen presenting capabilities, with resident DCs maturing by increasing the expression of the MHC class I and II molecules on their surface in response to antigens from invading pathogens (Wu *et al.*, 2011). Unlike mammals, chickens do not possess lymph nodes, but instead express bronchus-associated lymphoid tissue (BALT) and interstitial follicles between the para-bronchi of the lung, which is where the phagocytosed material is presented by the DCs (Fagerland and Arp, 1993).

Macrophages play an essential role in innate immune responses when protecting animals from deleterious effects of microbial infections and potentially harmful substances. As in mammals, chicken macrophages originate from the bone marrow stem cells, from where they travel via the circulatory system in the form of monocytes to the organs of the body, further differentiating into resident tissue macrophages upon

exposure to colony stimulating factors (Qureshi *et al.*, 1986). The phagocytic functions of macrophages occur as early as 12 days in chicken embryonic development, and are fully functional at the time of hatching (Jeurissen and Janse, 1989).

Unlike in mammals, macrophages are not found within the lumen of the conducting pathways of avian lungs (Cook and Wilkie, 1999). The free avian respiratory macrophages (FARMs) are found in relatively low numbers on the mucosal surface of avian lungs as opposed to the high percentage found in mammals, but greatly increase within the air sacs in response to infection, with bacterial clearance rates of 24-48 hours in healthy chickens (Ficken *et al.*, 1986; Nagaraja *et al.*, 1984). In comparison, avian respiratory macrophages are present within the parenchyma of the lung, lining the atria and infundibulae in order to clear the air of inhaled particles (<5μm) before they reach the capillaries (Ramsey *et al*., 1999).

Macrophage and monocyte chemotaxis to the area of infection is regulated by the production of chemokines by the other innate immune cells. This includes the chicken-restricted chemokine 9E3/CEF4 (Bedard *et al.*, 1987; Sugano *et al*., 1987), interleukin (IL)-1β (Babcock *et al*., 2008; Sick *et al.*, 2000), and K60 (orthologous to mammalian chemokine IL-8) (Sick *et al.*, 2000). Chicken macrophages also have the ability to process and present antigens and produce several cytokines and chemokines in response to microbial infections (Fink *et al.*, 2009; Reyes *et al*., 2010; Roscic-Mrkic *et al.*, 2001; Tate *et al.*, 2010). Macrophages also have higher levels of proteolytic activity than DCs, and as a result have more limited antigen-presenting capabilities in mammals (Delamarre *et al.*, 2005). However, macrophages aid in the removal of antigens (including infectious

agents) and in stimulating adaptive immune responses, including antibody production and cell mediated immune responses.

1.3.2 *Macrophage response to viral infection*

The specific responses of macrophages to viral infections have been characterized in various animal models. In the case of viral infections that use macrophages to replicate (ie. measles, (Roscic-Mrkic *et al.*, 2001); influenza virus (Tate *et al.*, 2010), dengue virus, (Fink *et al.*, 2009), such depletion can have a severe impact on the replication of the virus. For example, depletion of murine macrophages has shown a rapid increase in the number of DCs infected with the measles virus within the spleen of animals and a subsequent increase in the viral genome load as the virus targets cells other than the macrophages, primarily the DCs, as a site of replication. (Roscic-Mrkic *et al.*, 2001). In addition, the depletion of airway macrophages from mice during an infection of influenza virus involved a dramatic decrease in early protective cytokine response, leading to enhanced virus replication, inflammation, edema, and vascular leakage within the tissue of the infected lungs (Tate *et al.*, 2010). A similar pattern was noted during infection with dengue virus, in the clearance of both macrophages and blood monocytes from murine blood plasma, leading to enhanced dengue virus replication by 3 or 4 dpi within the blood cells or the peripheral tissues of blood vessels (Fink *et al.*, 2009).

Some viral avian respiratory infections are also known to use macrophages for replication. In the instance of highly pathogenic avian influenza (HPAI) virus (H5N1) infection, a significant drop in the macrophage population, followed by a subsequent

decrease in the production of pro-inflammatory and anti-viral cytokines such as IL-18 and IFNα was seen 48 hpi, and is thought to be the cause of the chicken's inability to fight the infection effectively (Suzuki *et al.*, 2009). A similar situation was seen with an infection of H6N1 influenza virus infection in turkeys, with a decrease in both phagocytosis and antimicrobial cytokine production at 10 dpi in the lungs (Kodihalli *et al.*, 1994). However, an infection of Marek's disease virus (MDV) in chicken lungs shows markedly different results. While MDV replicates within the host's macrophages, an up-regulation in the expression of pro-inflammatory cytokine genes (ie. IL-1β, IL-8, and inducible nitric oxide synthase (iNOS) was seen during the initial phase of infection (48 to 72 hpi), along with a significant increase in macrophage numbers from 12 to 168 hpi in MDV infected animals (Abdul-Careem *et al.*, 2009). This is expected as macrophages are still an important innate immune cell in the response against the MDV infection, so while some are being used as a site of replication, others are responding normally to help clear the infection and stimulate the adaptive immune response against MDV (Abdul-Careem *et al.*, 2009; Animas *et al.*, 1994).

Adenovirus infections in chickens were found to increase the proliferation and phagocytic activity of macrophages (Nakamura *et al*., 2001). This was also observed with an infection of hydropericardium syndrome (HPS) virus, which showed a marked systemic proliferation of macrophages instead of being limited to the site of infection within the lung, although there was an increase in lung lesions during viral replication as well (Nakamura *et al.*, 2001). This trend in innate immune response can also be seen when treating chickens with viral antigen-coated beads; influenza A coated-beads induced a significant increase in macrophages within the para-bronchial wall of the lung,

and an increase in the phagocytosis of the beads when compared to uncoated beads (de Geus *et al.*, 2012).

1.4 Macrophage depletion techniques

There have been few studies in chickens to deplete macrophages alongside experimental viral infections. In chickens, clodronate-mediated depletion has only been shown in depleting monocytes from the blood (Hala *et al.*, 1998), and macrophages from the spleen (Jeurissen *et al.*, 1998) and cochlea of the chicken ear in order to ascertain what impact there was on the sensory regeneration within the ear (Warchol *et al.*, 2012). Based on previous results for both avian and mammalian systems, we can summarize that macrophage depletion is potentially a useful tool for identifying the role of macrophages in the innate immune response. An experimental model for macrophage depletion has the potential to allow an assessment of the role of macrophages on the replication success of a variety of different viral pathogens. Many different forms of macrophage depletion have been attempted in both mammalian and chicken immune systems, each treatment with varying pros and cons.

1.4.1 *Use of silica dioxide and related compounds*

One of the most common methods is the use of silica dioxide injections. Silica dioxide is a naturally occurring mineral in the form of a compact particle. This mineral can exist in either a non-crystalline (amorphous) or crystalline form. Both the chemical and physical properties of silica have been implicated in its ability to deplete

macrophages, both *in vivo* and *in vitro* (Vallyathan *et al.*, 1988). Ingestion of silica by mammalian alveolar macrophages results in cell death, followed by release of intracellular silica in apoptotic bodies, that is then taken up by other neighboring macrophages (Balaan and Banks, 1998). One problem with this method is that due to the cycle of phagocytosis and cell death, there is an increase in the inflammatory response, most likely through the release of proteases, reactive oxygen species (ROS), or production of pro-inflammatory cytokines (Gilmour *et al.*, 1995), which could possibly mask the actual effects present during viral infection if used alongside silica dioxide treatment. It has been proposed that this over secretion of pro-inflammatory cytokines is a result of either abnormalities in the clearing of secondary apoptotic bodies, or secondary necrosis of these bodies that result in toxin production that stimulates cytokine production (Savill and Haslett, 1995).

Also, previous research into the depletion of macrophages from a heterogeneous cell population via administration of silica has often observed undesired effects on non-phagocytic cells (Martinet *et al*., 2007), as well as a decrease in silica toxicity if particles are not homogenous in size within the administered treatment (Kagan and Hartmann, 1984). Silica has mainly been used for the removal of monocytes from peripheral blood leukocyte suspension and in studying the effects of removing macrophages from immune cell populations *in vitro* (Martinet *et al.*, 2007). Silica dioxide use in chickens has shown depletion of macrophages and the resulting negative impact on the pathogenesis of the macrophage infecting MDV (Gross and Colmano, 1971), and the onset of spontaneous autoimmune thyroiditis (SAT) in obese strains of chickens (Hala *et al.*, 1996). Other common treatments involve the use of carrageen and asbestos. In mammals, use of these

chemicals has resulted in incomplete macrophage depletion, damage to bystander cells, and depletion of non-pathogenic cells (Kagan and Hartmann, 1984; Shek and Lukovich, 1982; van Rooijen and Sanders, 1994). Asbestos has also been found to not be suitable for macrophage depletion *in vivo*, as studies of intra-abdominal inoculations in mice show an increase in macrophage numbers to the surrounding area, rather than a decrease from lethal exposure to the chemical (Donaldson *et al*., 1982).

1.4.2 *Use of monoclonal antibodies*

Another way to target macrophages for depletion is through the use of monoclonal antibodies against macrophage-specific surface markers. In mammals, antibodies have been developed that can target cluster of differentiation (CD)11b/CD18 integrins, and stimulate macrophage depletion through complement-mediated lysis (Wang *et al*., 2005). One advantage to using antibodies is that due to their small dimensions, they can easily pass through the endothelial cell barrier of the blood vessels and enter the tissues that house resident macrophages (Alberts *et al.*, 2002), and be administered at highly concentrated doses without any unwanted side effects alongside a sufficient level of complement protein to implement lysis (Ho and Springer, 1984). Antibody-mediated depletion can also be further enhanced through the conjugation of antibodies with cytotoxic drugs, which enter the cell via endocytosis after the selective binding of the antibody to the macrophage (van Roon *et al.*, 2005).

Unfortunately, few antibodies have been developed that specifically target macrophages in chickens. Avian antibodies discovered include K1, which binds to both

chicken thrombocytes and macrophages via the recognition of a MHC class II molecule that they appear to share, which is also absent on the avian T and B cells (Kaspers *et al.*, 1993). Another macrophage specific antibody is CV1-68.1, which has been found to bind the cells of the macrophage/microglia lineage within the central nervous system of chickens and quail (Cuadros *et al*., 2006; Jeurissen *et al*., 1988). The antibody that best labels macrophages and monocytes is the KUL01 antibody, which targets a different epitope than that of CV1-68.1 antibodies, recently discovered to be a macrophage-specific mannose receptor found on the avian macrophage surface (Mast *et al*., 1998; Staines *et al*., 2012). One drawback to the use of antibody-mediated macrophage depletion is that not all antibodies are efficient in depleting macrophages, and can require several rounds of treatment to completely lyse the target cells (Martinet *et al.*, 2007), making this approach cost prohibitive.

1.4.3 *Use of scavenger receptor manipulation*

A third technique is the attachment of cytotoxic agents to scavenger receptor ligands, such as maleylated bovine serum albumin conjugated to the photosentizer chlorine, to increase the potency of selective macrophage cell depletion while leaving bystander cells unharmed (Rafla and Cook, 1999). Scavenger receptors are expressed in large numbers by macrophages and provide a direct and cell specific route for the delivery of the toxic chemicals to the endocytic compartments of the cells (Martinet *et al*., 2007). One problem with using this technique is that the dye conjugated to the photosentizer can bind with non-covalent complexes as well as the conjugates, thus

making it difficult to separate out pure conjugate and unbound dye during analysis (Cavanagh *et al*., 1999; Mew *et al*., 1983).

Based on the information above, we have access to a variety of different depletion techniques to be used in removal of macrophages from the avian immune system for analysis of their various roles in response to IBV replication. However, findings from researchers that used clodronate (dichloromethylene bisphosphonate or Cl_2MBP) encapsulated-liposome mediated depletion appear to be able to address the different limitations associated with the previously mentioned techniques, and have been used to deplete avian macrophages *in vivo* in a variety of tissues. The mechanism of this technique is detailed below.

1.4.4 *Mechanism of macrophage depletion by clodronate*

The use of clodronate encapsulated-liposomes results in macrophage depletion *in vivo* (van Rooijen and Sanders, 1994). The initial use of clodronate was for the targeting of osteoclasts, members of the mononuclear phagocyte system (MPS), in the treatment of osteoporosis in humans (Van Beek *et al.*, 2002). As macrophages are also members of the MPS, their depletion using clodronate encapsulated-liposomes was first implemented in murine test models by van Rooijen and Nieuwmegen in 1984, resulting in successful depletion of spleenocytes (van Rooijen and Nieuwmegen, 1984). The liposomes are multilamellar phospholipid structures that prevent the escape of the strongly hydrophilic clodronate once encapsulated (van Rooijen and Sanders, 1996). Only macrophages and their monocyte predecessors will phagocytose the liposomes; this is based on the belief

that liposomes of the size >200nm will not be internalized by non-phagocytic cells and other immune cells such as granulocytes, however this hasn't been properly investigated yet (Claassen *et al*., 1990). DC populations are also found not to be depleted upon administration of clodronate encapsulated-liposomes (van Rooijen and Hendrikx, 2010).

The mechanism for depletion of macrophages by clodronate encapsulated-liposomes is as illustrated in Figure 1.3; 1) The macrophages engulf the liposomes via phagocytosis, where they are internalized within the cytoplasm of the cell, 2) the phospholipids of the liposome are disrupted through the fusion of the liposome with the cell's lysosomes, which contain enzymes such as phospholipase (van Rooijen *et al*., 1996). 3) Clodronate is then released into the cytoplasm, with levels building up as the macrophage engulfs more liposomes (van Rooijen *et al.*, 1996).

Apoptosis is induced within the macrophages when the phosphate-carbon-phosphate backbone of the clodronate is incorporated into the β, γ positions of adenosine triphosphate (ATP) to generate the toxic metabolite adenosine-5'-[β, γ-dichloromethylene]triphosphate ($AppCl_2p$) (Auriola *et al*., 1997). This metabolite subsequently inhibits the mitochondrial adenine nucleotide translocase, which is important for mitochondrial respiration, thus killing the cell (Lehenkari *et al*., 2002). Any free clodronate released from the apoptotic macrophages has an extremely short half-life, on the order of minutes, and will be cleared from circulation by the renal system before having a chance to negatively impact the host (Sahni *et al.*, 1993). The toxicity of bisphosphonates in variable, but generally low; acute toxicity is usually due to the hypocalcaemia from high doses (5 mg/kg) of bisphosphonates (Okojie and Cook, 1999).

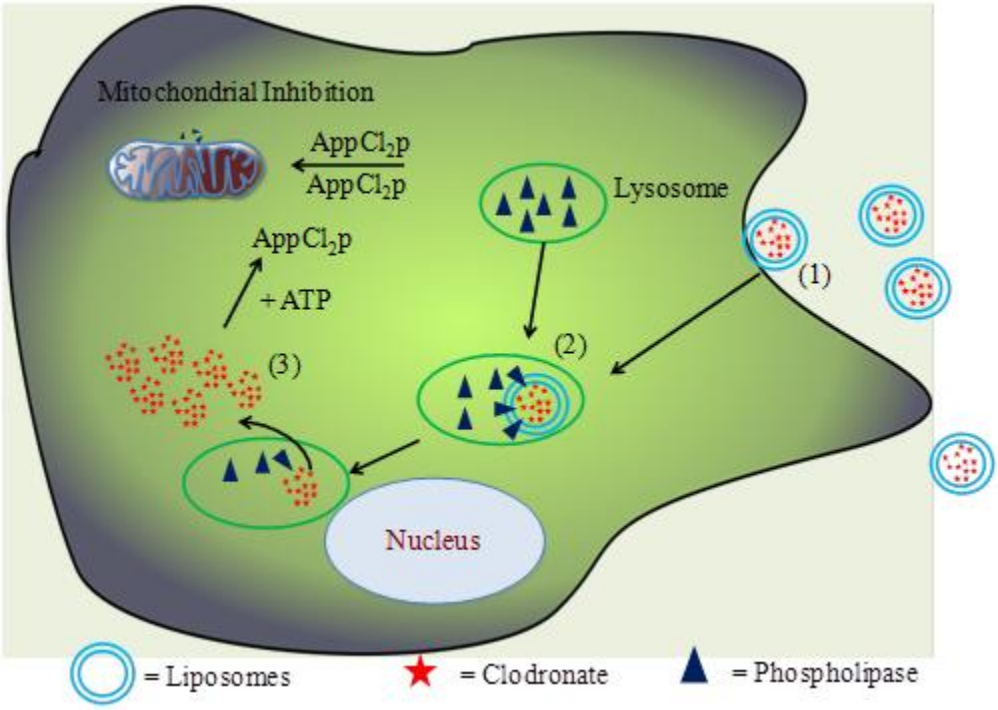

Figure 1.3. Illustration of the process by which macrophages are depleted using clodronate encapsulated-liposomes. Adapted from van Rooijen and Sanders (1994).

The use of clodronate encapsulated-liposomes is considered the best and most efficacious approach for macrophage depletion in mammals, due to minimal toxicity and maximum depletion efficiency (van Rooijen and Hendrikx, 2010; van Rooijen and Sanders, 1994, 1996), and clodronate encapsulated-liposomes have been used in various studies (Abdul-Careem *et al.*, 2011; Fink *et al.*, 2009; Reyes *et al.*, 2010; Roscic-Mrkic *et al.*, 2001; Tate *et al.*, 2010). One limitation in the use of these compounds is that any physical barriers between the injection site and the target area, such as the endothelial walls of blood-vessels or the alveolar epithelial cells of the lungs, will prevent the large multilamellar liposomes from reaching their destination (van Rooijen and Hendrikx, 2010). One way to circumvent this is to administer the clodronate encapsulated-

liposomes intravenously or intra-abdominally. The monocytes present within the bloodstream will then become depleted, and be unable to replenish the macrophages present within the parenchyma that naturally deplete overtime (Sunderkotter *et al*., 2004). Although research into proliferating alveolar macrophages has shown monocyte-independent expansion in the number of macrophages during chronic inflammation in mammalian lungs (Bitterman *et al*., 1984), no studies have been conducted in avian models, which have fewer FARMs than mammals to begin with (Cook and Wilkie, 1999).

Macrophage depletion in chickens through the use of clodronate encapsulated-liposomes has shown the efficacy of macrophage depletion through indirect means, such as a decrease NO production or a change in viral tumour disease progression (Lane *et al.*, 1997; Rivas *et al.*, 2003). Jeurissen and colleagues have qualitatively shown immunohistochemical evidence of macrophage depletion in clodronate encapsulated-liposome treated spleens after both 1 and 4 days post-treatment (dpt) (Jeurissen *et al*., 1998). However, due to a lack of quantitative data on macrophage depletion following clodronate encapsulated-liposome treatment, the effectiveness involved in depleting chicken macrophages using clodronate encapsulated-liposomes remains unclear. It is also unclear as to what effect macrophage depletion will have on the initial replication of IBV within the respiratory tissues of the chicken.

1.5 Statement of rationale

There are a range of diseases that impact poultry worldwide, but IBV is still an issue in most countries due to the limitations of vaccines available to protect both meat and egg laying chickens. Live attenuated and inactivated vaccines that are used for the control of IB and, in general, provide protection against field strains. However, the emergence of variant strains becomes a challenge and these heterogonous IBV strains lead to IB outbreaks in vaccinated flocks, leading to subsequent production losses. In addition, attenuated strains used for vaccination can spread among individual birds within the flock, change virulence during the bird to bird passage, and lead to disease and resultant production problems, such as a decrease in egg quality and quantity and a reduction in the size of meat birds. The interaction between host and IBV and the mechanisms which lead to virus clearance and disease pathogenesis are poorly understood. *In vivo* and *in vitro* host-virus models have demonstrated that immune system cells, particularly macrophages, are known to play a pivotal role in many host-virus interactions. To examine the potential role of macrophages in IBV infection in live chickens it was decided to develop a model system to deplete host alveolar macrophages.

1.5.1 Statement of hypotheses

In the studies described in this thesis, we tested the following hypotheses:

1) The replication of IBV in the trachea and lungs of the chicken (*Gallus gallus domesticus*) (White Leghorn) is associated with an increase in the number of macrophages in the respiratory mucosa.

2) The depletion of macrophages using clodronate encapsulated-liposomes will result in an increase in IBV replication in these tissues, which will influence the resultant pathological outcomes when compared to uninfected controls.

1.5.2 *Experimental approach*

Aim #1.1: Determine the macrophage depletion efficiency using a single treatment of clodronate encapsulated-liposomes using an *in vivo* model; as macrophages are influenced by other cells of both the innate and adaptive immune responses, we can gather a better understanding as to what the actual roles are *in vivo* rather than *in vitro*.

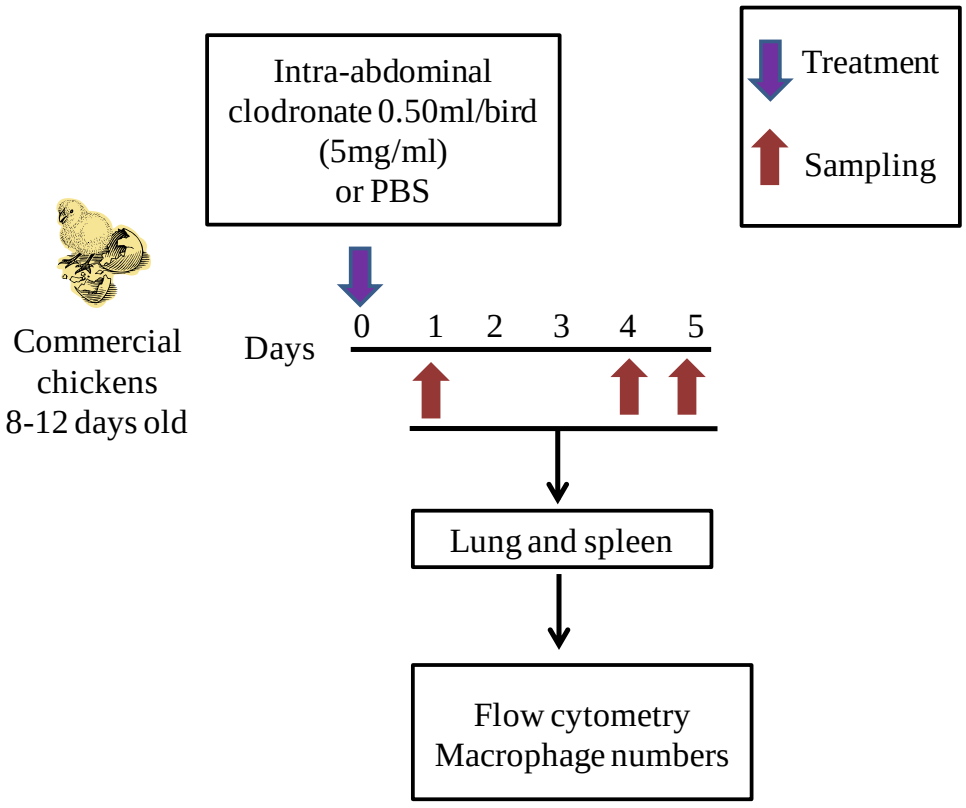

Figure 1.4. Experimental approach for Aim #1.1. Commercial chickens received a single treatment of clodronate or phosphate buffered saline (PBS) encapsulated-liposomes at the days post-treatment (dpt) indicated in the timeline. The spleen and lungs were collected at the indicated time points to determine macrophage depletion using flow cytometry analysis.

Aim #1.2: Determine macrophage depletion efficiency following two clodronate encapsulated-liposome treatments four days apart

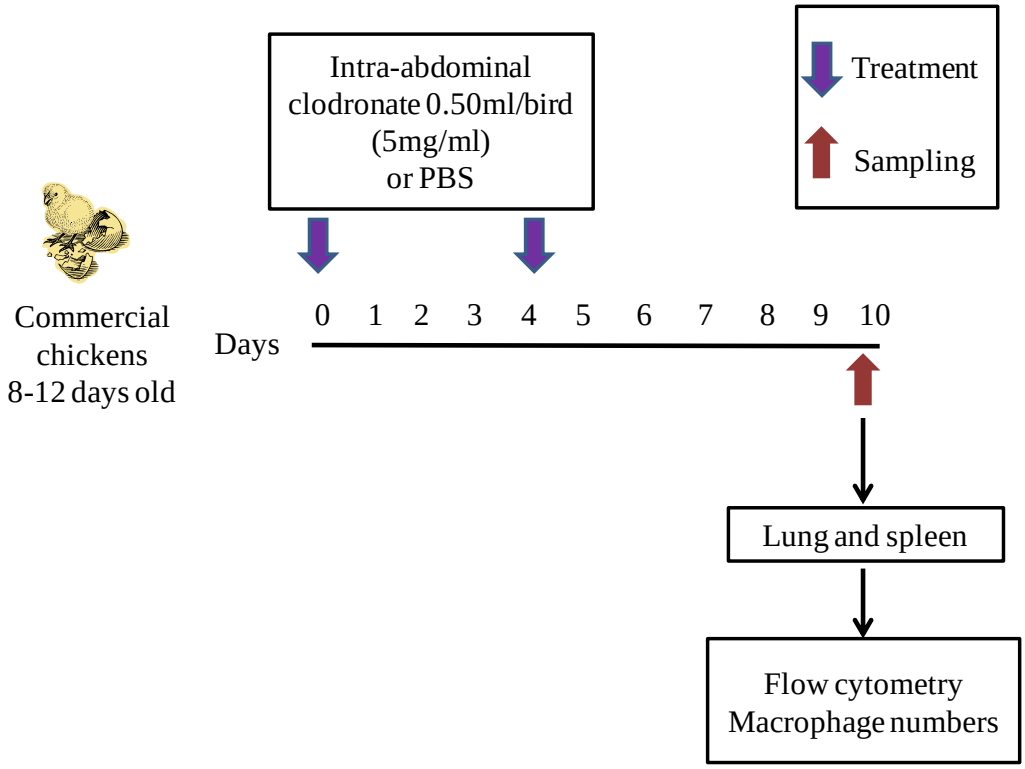

Figure 1.5. Experimental approach for Aim #1.2. Commercial chickens were treated with either clodronate or PBS encapsulated-liposomes two times, with the second treatment four days after the first. The lung and spleen were then sampled six days from the last treatment and macrophage depletion in the tissues were determined using flow cytometry analysis.

Specific Aim #2.1: Establishment of an *in vivo* IBV infection model

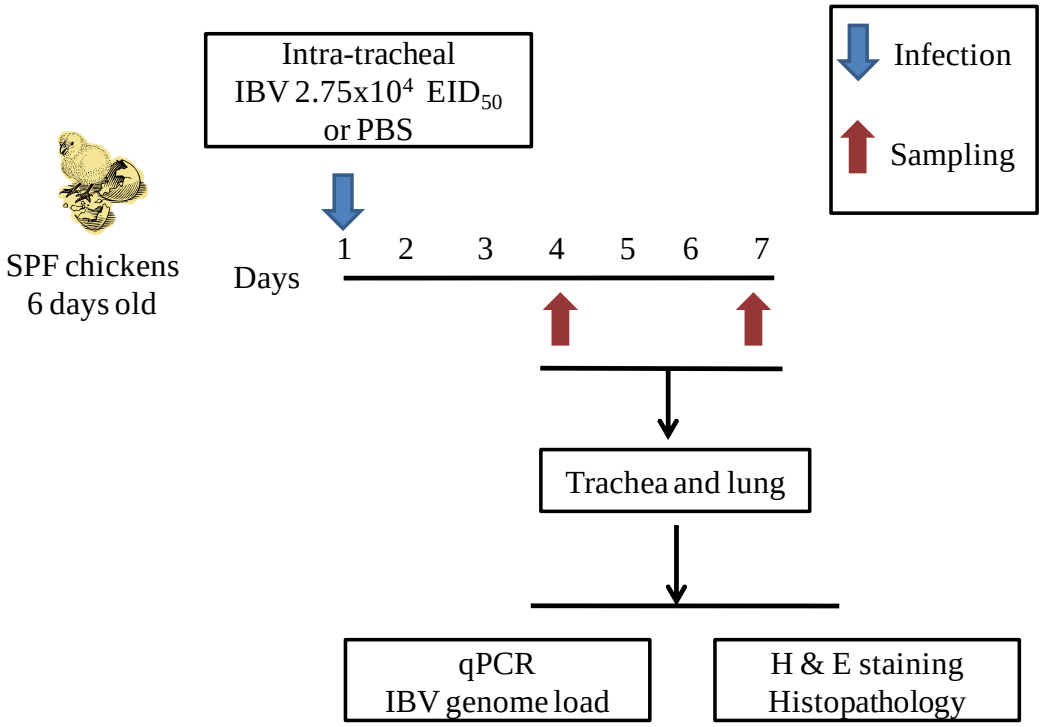

Figure 1.6. Experimental approach for Aim #2.1. Specific pathogen free (SPF) chickens were first infected with either IBV ($2.75x10^4$ egg infectious dose 50 (EID_{50})/bird or PBS at the dpi indicated in the timeline. qPCR was ran to determine changes in IBV viral genome load. Alongside this assay, the trachea and lung were also stained with haematoxylin and eosin (H & E) to observe any changes in histology.

Aim #2.2: Determine what effect IBV infection has on macrophage numbers in the trachea and lungs

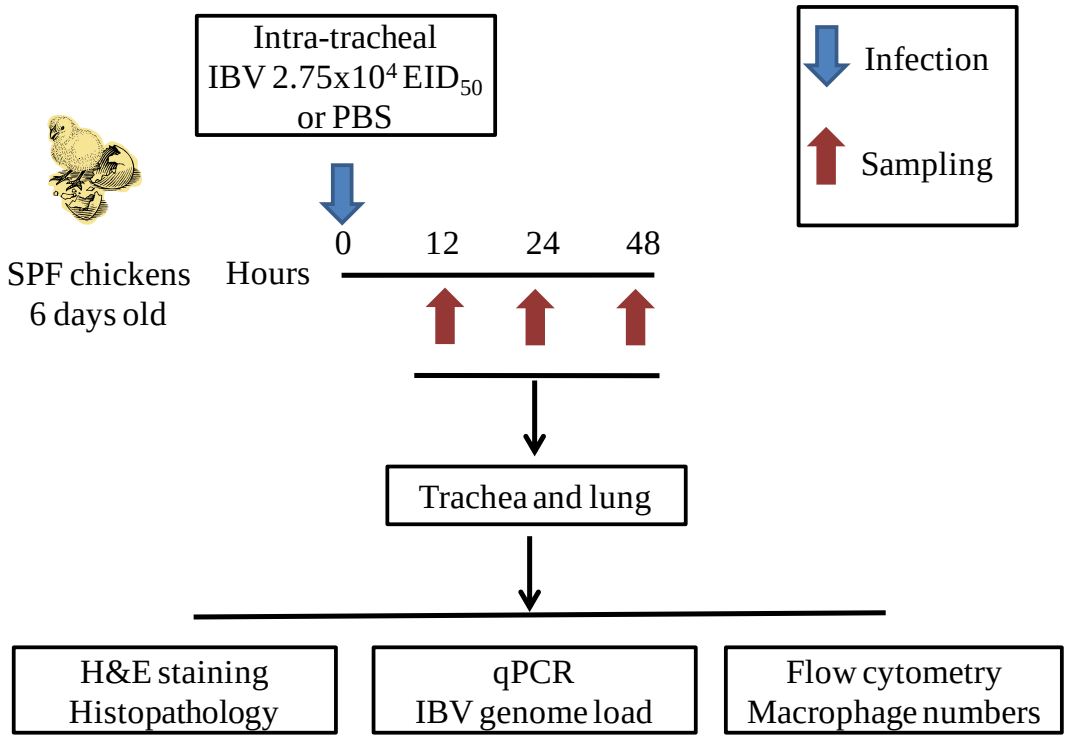

Figure 1.7. Experimental approach for Aim #2.2. SPF chickens were first infected with either IBV (2.75x10^4 EID$_{50}$)/bird or PBS at the hpi indicated in the timeline. Both trachea and lung were collected and qPCR used to determine changes in IBV viral genome load, any changes in macrophage numbers via flow cytometry, and semi-quantitative analysis of changes in histopathology using lesion scoring systems for both tissues.

Aim #3: Determine the effect of macrophage depletion on IBV infection in the trachea of chicken

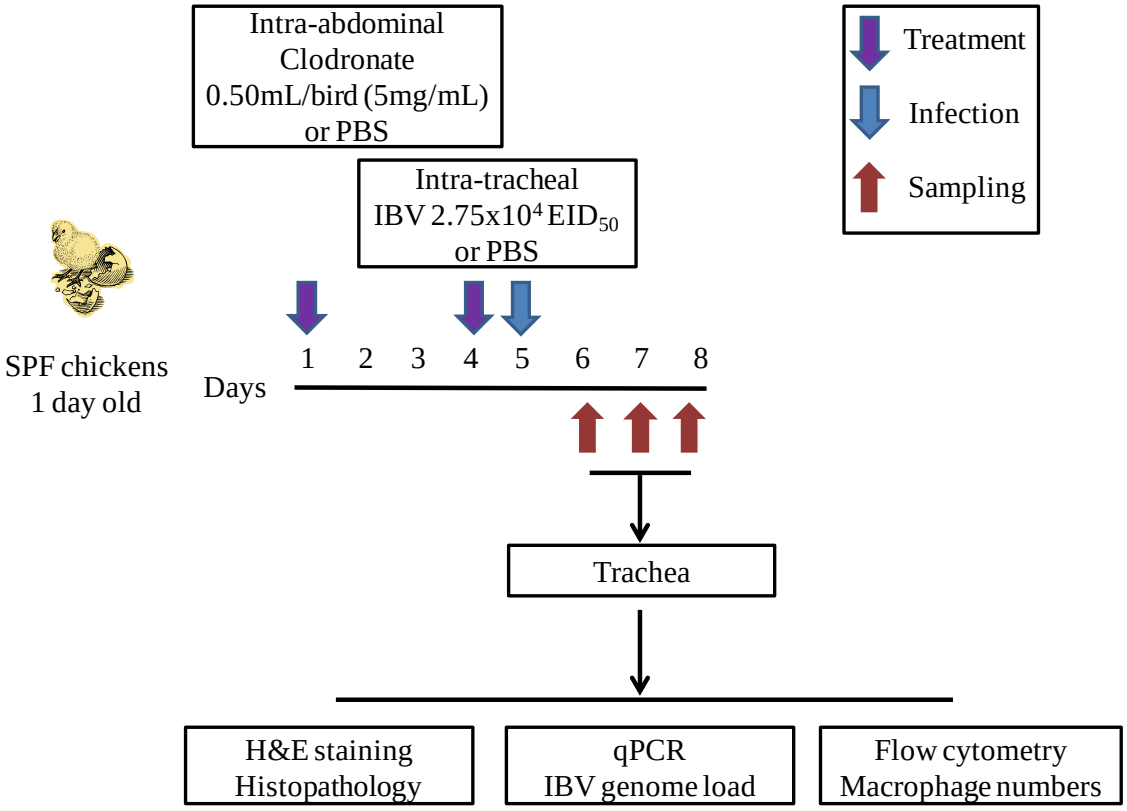

Figure 1.8. Experimental approach for Aim #3. SPF chickens were first treated with either clodronate or PBS encapsulated-liposomes twice, as per the timeline illustrated in Figure 1.7. The chickens were then infected with IBV (2.75x10^4 EID$_{50}$)/bird or PBS one day following the second liposome treatment, and the trachea collected at the dpi indicated in the above timeline. qPCR were used to determine changes in IBV viral genome load, any changes in macrophage numbers determined via flow cytometry, and semi-quantitative analysis of changes in histology using lesion scoring systems for H & E stained trachea.

Chapter Two: Materials and Methods

2.1 Animals

Unsexed specific pathogen free (SPF) layer chicks (White Leghorn) were obtained from Canadian Food Inspection Agency, Ottawa and used in experiments involved with IBV infection. Lack of previous exposure to IBV means in SPF chickens a lack of maternal antibodies present that would have been acquired from the laying mothers via the yolk sac, and thus be unable to influence the chickens immune response to the infection (Hamal et al., 2006). In addition, unsexed commercial layer chickens (White leghorn), were obtained from Rochester Hatchery (Westlock, AB, Canada) and used in experiments involved with only macrophage depletion via clodronate encapsulated-liposome treatments. The chickens were not immunized against any diseases. The chickens were housed in high containment poultry isolators (Figure 2.1) at the University of Calgary's Veterinary Science Research Center (VSRS), with ample access to food and water that was nutritionally complete and appropriate for the age of the chickens. Approval was given by the University of Calgary animal care committee and the correct animal care protocols were in place prior to the experiments. We used power calculation based on data of previous work to determine the number of animals required for each group (at 85% power and $P<0.05$). Throughout the thesis, "n" is defined as an individual animal (biological replicate) used in each respective experiment.

2.2 IBV infection

Conn A5968 strain of IBV was obtained from ATCC (Manassas, Virginia, United States). The chickens were infected intra-tracheally while under isoflurane anesthesia (Figure 2.2), following all University of Calgary's animal care and biosafety protocols.

Figure 2.1. High containment poultry isolators kept at the VSRS.

2.3 Experimental designs

Aim #1: Determine the macrophage depletion efficiency: In order to determine if macrophage depletion by clodronate encapsulated-liposomes would be effective in depleting macrophages from the respiratory tract of the chickens, we first needed an optimal protocol for macrophage depletion established before attempting depletion alongside IBV infection. In this way, we could determine how macrophage depletion

would influence IBV replication and the resulting pathogenesis within the body, and obtain a better understanding of the avian respiratory macrophage's role. Three separate experiments were performed to develop this optimal model. For Experiment #1, 28 days-old chickens had their spleens collected (n=2) and used in the optimization of the flow cytometry staining technique for macrophages. For Experiment #2, 8-12 days-old commercial chickens were injected intra-abdominally with either clodronate or PBS encapsulated-liposomes at a volume of 0.5 mL per bird (5 mg/mL). At 1 (n=7-10 per group), 4 (n=5 per group) and 5 (n=7-8 per group) dpt, the spleen and lung were collected from the chickens and macrophage numbers analyzed using flow cytometry. Spleen was collected to serve as a positive control for clodronate-mediated macrophage depletion, due to the high numbers of macrophages known to be found within the tissue. For Experiment #3, 8-12 days-old commercial chickens were injected intra-abdominally with either clodronate (n=5) or PBS (n=5) encapsulated-liposomes twice, four days apart, at a volume of 0.5 mL per bird (5 mg/mL). The spleen and lung tissues were collected six days following the second intra-abdominal injection and macrophage numbers analyzed using flow cytometry.

Aim#2: Establishment of an in vivo IBV infection model and determine the number of macrophages within the trachea and lung following IBV infection: Two separate experiments were performed. For Experiment #1, 6 days-old SPF chickens were infected intra-tracheally with either 30 µL of Conn strain of IBV ($2.75x10^4$ EID_{50})/bird or PBS, an optimal dose based on previously performed experiments (data not shown). At 4 (n=3 per group) and 7 (n=3 per group) dpi the trachea and lungs were collected and analyzed for

IBV genome load using qPCR and histopathology using H & E staining of tissue sections. For Experiment #2, 6 days-old SPF chickens were infected intra-tracheally with either 30 µL of Conn strain of IBV ($2.75x10^4$ EID_{50})/bird or PBS. On 12, 24, and 48 hpi, the trachea and lungs of the chickens were collected and analyzed for IBV genome load, histopathology using H & E staining, and macrophage numbers using flow cytometry. For qPCR analysis, on 12 hpi PBS n=5 and IBV n=6, and on 24 and 48 hpi PBS n=5 and IBV n=5 trachea and lung were collected. For flow cytometry analysis; on 12, 24 and 48 hpi PBS n=5 and IBV n=4 trachea and PBS n=3 and IBV n=3 lung were collected. For histopathology, on 12 hpi PBS n=5 and IBV n=5 trachea and lung were collected; on 24 hpi PBS n=2 and IBV n=5 trachea and lung were collected; on 48 hpi PBS n= 2 and IBV n=4 trachea and PBS n=2 and IBV n=5 lung were collected.

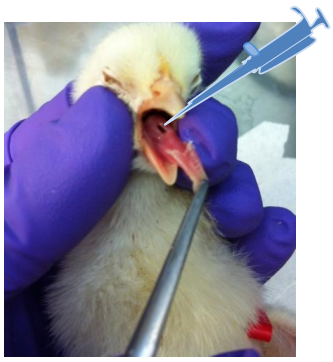

Figure 2.2. Intra-tracheal infection of IBV in chickens. To facilitate the infection, the chicken tongue is gently pulled out and downwards while under isoflurane anesthetic, exposing the glottis, the opening that connects to the larynx and leads to the trachea of the bird**.**

Aim #3: To determine the effect of macrophage depletion on IBV infection within the trachea of chickens: In order to ascertain if macrophage depletion results in an increase in both IBV replication and resulting pathology when compared to untreated controls, 1 day-old SPF chickens were injected intra-abdominally with either clodronate or PBS encapsulated-liposomes twice, four days apart, at a volume of 0.5 mL per bird (5 mg/mL). Twenty-four hours following the second treatment, the chickens were then infected intra-tracheally with either 30 µL of Conn strain of IBV ($2.75x10^4$ EID_{50})/bird or PBS. At 1, 2, and 3 dpi, the chicken trachea and lung were collected and analyzed for IBV genome load using qPCR, histopathology using H & E staining, and macrophage numbers using flow cytometry. At 1, 2, and 3 dpi, the following numbers of trachea were collected for each group: untreated and uninfected group n=4; untreated and IBV infected group n=5; macrophage depleted and uninfected group n=4 (on 3dpi, only n=2 tracheas were collected); and macrophage depleted and IBV infected group n=5.

2.4 Clinical signs and histopathology of trachea and lungs

The experimental chickens were observed daily for development of clinical signs. Portions of the lung and trachea of IBV infected and control chickens that were preserved in 10% formol saline and then sent to the Histopathology Diagnostic Services Unit (HDSU) at the University of Calgary, Faculty of Veterinary Medicine. The tissues were embedded in paraffin, sectioned at 5 µm, and stained with H & E. The histological changes observed in the trachea were scored as described previously (Grgic et al., 2008) (see Table 2.1). The histological changes observed in lungs were scored based on visible

changes in the para-bronchioles of the lung, as described in Table 2.2. All H & E stained sections were scored blindly except for those from the 4 and 7 dpi experiments.

2.5 Macrophage depletion technique

Clodronate, encapsulated in liposomes (5 mg/mL) was used to deplete macrophages in the chicken lung and trachea. Clodronate encapsulated-liposomes were purchased from Foundation Clodronate Liposomes, Amsterdam, the Netherlands.and had been prepared as described earlier (van Rooijen and Sanders, 1994). Control liposomes contained PBS only. Each animal received intra-abdominally 0.5 mL (5 mg of clodronate per 1 mL of the total suspension volume) of clodronate encapsulated-liposomes or PBS encapsulated-liposomes. For intra-abdominal administration, the birds were restrained so that the ventral side of the bird was up and a 28 gauge needle and 1 mL syringe was used to deliver the liposomes in the middle of ventral midline between scar of yolk sac attachment and cloaca.

Table 2.1. Scoring criteria used for determination of histological changes in trachea

Score	Criteria
1	No lesion
2	Epithelial hyperplasia and subepithelial lymphoid infiltration with occasional germinal centers and mucous glands are distorted and elongated
3	Epithelial hyperplasia with loss of cilia and moderate subepithelial lymphoid infiltration, with decrease in mucous gland size and edema of the lamina propria
4	Epithelial hyperplasia and subepithelial lymphoid infiltration, with superficial epithelial layer appearing flattened with a squamous appearance, and no mucous glands are detected.

2.6 Spleen and lung mononuclear cell isolation technique

The chicken spleen and lungs were dissected out from the animals and rinsed multiple times in cold Hank's balanced salt solution (HBSS) to ensure that they were free of blood. The spleens were crushed using a sterile syringe bottom, filtered through a 70 μm cell strainer (VWR, Edmonton, AB, Canada) and the cells were collected. Using sterile scalpel and forceps, the lungs were minced to approximately 5 mm fragments and soaked in 400 U/mL collagenase type I solution (Sigma-Aldrich, Oakville, ON, Canada) for 30 minutes at 37º C. Dispersed cells and tissue fragments were separated from larger pieces using a 40 μm cell strainer. The filtered lung and spleen cells were pelleted at 233

g for 10 minutes (4º C), followed by re-suspension in HBSS and carefully layered onto 4 mL Histopaque 1077 (GE Health Care, Mississauga, ON, Canada) in a 15 mL conical tube at room temperature (with a 1:1 ratio of cell suspension). The layered cells were spun 40 minutes at 400 g at 20°C. The cloudy layer, rich in mononuclear cells, was collected and pelleted, washed with HBSS, and the cells were suspended in complete RPM1 medium (RPMI medium 1640 supplemented with 2 mM/l L-glutamine, 1% penicillin-streptomycin and 10% heat inactivated fetal bovine serum (FBS) and the cells were counted using a haematocytometer.

2.7 Trachea total cell isolation technique

The trachea was cut into approximately 5 mm fragments with sterile scissors, suspended in 0.5mM EDTA (Ethylenediaminetetraacetic acid) + 5% FBS in 1% PBS in a 50 mL conical tube, and shook for 20 minutes at 0.28 g (100 RPM) (41°C). The dispersed cells and tissue fragments of the trachea were separated from larger pieces using a 70 µm cell strainer. The trachea required a further processing of the tissue by grinding with the end of a 3 mL syringe plunger, followed by washing with 0.5 mM EDTA, for three repetitions in order to further separate the cells from cartilage and fatty tissue. The filtered trachea cells were spun for 5 minutes at 500 g at 21°C, and then the cells were suspended in complete RPM1 medium and counted using a haematocytometer.

Table 2.2. Scoring criteria used for determination of histological changes in lung

Score	Criteria
1	Para-bronchioles exhibit an inner ring of interrupted epithelia, indicating the presence of many airspaces close to the lumen, with multiple air exchange areas also present in the surrounding outer most tissue; mononuclear cell infiltration is at 25%.
2	Loss of air exchange areas closest to the lumen of the para-bronchioles as a result of infiltrating mononuclear cells; mononuclear cell infiltration is at 50%.
3	Mononuclear cell infiltration is at 75%, resulting in a loss of most, if not all, air exchange areas located outside the periphery of the para-bronchiole, and few remaining of those closest to the lumen of the para-bronchioles.
4	Massive mononuclear cell infiltration (>75%), with some cells visible in the lumen of the para-bronchioles, and little to no air exchange areas visible around the lumen.

2.8 Flow cytometry technique

Briefly, the mononuclear cells isolated from spleen (1-2 $x10^6$ cells) and lungs (1-2 $x10^6$ cells) and total cells isolated from trachea (1-2 $x10^5$ cells) were washed with 1% BSA (bovine serum albumin) fraction V (OmniPur, EMD, Darmstadt, Germany) made in PBS and centrifuged for 10 minutes at 211 g (4º C) and then suspended in 100 µL of

1:100 chicken serum (diluted in 1% BSA) for Fc blocking. Following centrifugation once again, cells were re-suspended in the dark with a final concentration of 0.5 µg/mL (100 uL) phycoerythrin (PE)-labelled mouse anti-chicken KUL01 (SouthernBiotech, Birmingham, Alabama, USA) or 0.5 ug/mL allophycocyanin (APC)-labelled mouse anti-chicken CD44 (SouthernBiotech, Birmingham, Alabama, USA) monoclonal antibodies, with respective isotype controls or 1% BSA (unstained controls) on ice for 30 minutes. Finally, cells were washed twice with 1% BSA. Flow cytometry samples were analysed with a BD LSR II (BD Biosciences, Mississauga, ON, Canada). Excitation was performed with a 488 nm argon-ion laser and the emission collected using a 660/20 nm band pass filter for APC conjugates and 585/42 nm BP filter for PE conjugates.

2.9 RNA extraction and complementary DNA (cDNA) conversion techniques

RNA was extracted from the trachea and lungs of infected and uninfected chickens by a single-step method using Trizol (Invitrogen Canada Inc., Burlington, ON, Canada) according to the manufacturer's protocol. Briefly, 5 mm (40 mg) of unwashed trachea or lung tissue preserved in RNAlater were homogenized in 1 mL of Trizol using a Pro200 Power Homogenizer (Diamed, Mississauga, ON). Subsequent chloroform extraction, isopropanol precipitation, and 75% ethanol wash were carried out precipitating the RNA. The RNA pellet was dissolved in 20 µL of RNAse-free water. RNA concentration was quantified using Nanodrop 1000 spectrophotometer at 260 nm wavelength (ThermoScientific, Wilmington, DE, USA). Reverse transcription of extracted RNA (2000 ng) was carried out using 10X RT random primers (High Capacity

cDNA Reverse Transcription Kit, Invitrogen Life Technologies, Carlsbad, CA) according to the manufacturer's instructions. The cDNA product was then diluted with 80 µL of RNAse-free water to a final concentration of 20 ng/µL.

2.10 Conventional PCR technique

For quantification of the IBV genome load, target and reference genes were PCR-amplified from cDNA preparations using primers listed in Table 2.3, cloned, and used to generate standard curves. For the preparation of the standards, relevant fragments were amplified using the primers and the following cycling parameters: denaturation at 94°C for 3 minutes, followed by 31 cycles of 94°C for 45 seconds, 55°C for 30 seconds, and 72°C for 45 seconds. The final extension was done at 72°C for 10 minutes.

Table 2.3. PCR primers used in conventional and real time PCR techniques

Primer Name	**Sequence (5' – 3')**	**Fragment (bps)**	**Reference**
IBV N	F- GACGGAGGACCTGATGGTAA R- CCCTTCTTCTGCTGATCCTG	206	(Kameka *et al.*, 2014)
β-actin	F- CAACACAGTGCTGTCTGGTGGTA R- ATCGTACTCCTGCTTGCTGATCC	205	(Villanueva *et al.*, 2011)

2.11 Preparation of constructs as standards

PCR products were run at 100 V for 1 hour and 15 minutes on a 1.5% agarose gel and extracted using QIAquick Gel Extraction Kit (Qiagen Inc.) according to the manufacturer's instructions. The extracted DNA was then cloned into the pCR®2.1-TOPO® vector and amplified through transformation of One Shot® *Escherichia (E.) coli*, followed by blue/white colony screening (TOPO TA Cloning kit Top 10, Invitrogen, Burlington, ON, Canada). The subsequently positive white cloned colonies had their plasmids extracted using the QIAprep spin miniprep kit (Qiagen Inc.), as per the manufacturer's instructions. The extracted plasmids were screened using EcoR1 restriction enzyme (Invitrogen, Burlington, ON, Canada) and the positive clones were submitted to the University of Calgary's Automated DNA Sequencing Services to be sequenced. The Basic Local Alignment Search Tool (BLAST) program (NCBI, Bethesda, MD, USA) was used to determine the accuracy of the target gene insert.

2.12 Real-time (q) PCR technique

Before running the qPCR reaction, both uninfected and infected samples collected from each individual animal were run using conventional PCR to confirm a lack of IBV amplification within the uninfected tissues. All the cDNA preparations originating from IBV infected trachea and lungs were analyzed using qPCR assays in duplicates for each individual sample, alongside a dilution series of the plasmids used to generate a standard curve, also done in duplicates for each dilution used in the standard curve. The total ng of plasmid DNA was determined using the Nanodrop 1000 and then using the total bps

(insert + plasmid) of the plasmid, the copies/µL were calculated for the dilutions used to make the standards. All qPCR assays were conducted in a 96-well un-skirted, low profile PCR plate (VWR, Edmonton, AB) in a reaction volume of 20 µL. Fast SYBR® Green Master Mix (Invitrogen, Burlington, ON, Canada) containing AmpliTaq® Fast DNA Polymerase was used for this assay. The DNA intercalating SYBR® Green dye was used for detection in a CFX96 Real-Time System C1000 Thermal Cycler (Bio-Rad Laboratories, Mississauga, ON). In addition, 5 nM of each of the gene-specific primers and 9 µl of a 1:10 dilution series of plasmid DNA, or 20 ng of cDNA extracted from each sample and RNAse-free water were used in the reaction. A positive control (plasmid) and negative control (RNAse-free water) were included alongside the samples for each qPCR run. The optimum thermal cycling parameters for the IBV genome and housekeeping gene β-actin included pre-incubation at 95°C for 20 seconds; 40 cycles of amplification/extension at 95°C for 3 seconds, and 60°C for 30 seconds; melting curve analysis at 95°C for 10 seconds (Segment 1), 65°C for 5 seconds (Segment 2) and 9°C for 5 seconds (Segment 3). Fluorescent acquisition was done at 60°C for 30 seconds.

2.13 Data analyses

Quantification of IBV genome load by real-time PCR was done by calculating the number of IBV genome copies per 20 ng of trachea or lung cDNA. Using the standard curves generated by a serial dilution of plasmids as described previously, the copy numbers for both IBV and β-actin for each sample was calculated. The IBV copy number

was then divided by the β-actin copy number and the result multiplied by $1x10^6$ to be expressed as IBV genome copies per $1x10^6$ host cells (Chan *et al.*, 2007).

FlowJo version 7.6.4 (Ashland, OR, USA) was used to complete the flow cytometry data visualization and analysis. The two-tailed Student's t-test using Graphpad (GraphPad Prism 5 Software, La Jolla, CA) or the one-way analysis of variance (ANOVA) followed by Tukey's test using the statistical package, MINITAB® release 15 (Minitab Inc. State College, Pennsylvania, USA) were used as applicable for analysis of the data sets.

For only the trachea and lung lesion scores, the distribution of the data was determined using the Anderson-Darling test to check for normality. This test was used as the lesion scores are considered to be categorical data, and not linear, and thus may have been distributed in a non-normal fashion (Agresti, 2007). When the lesion scores were found to be normally distributed, they were subjected to a one-way ANOVA to test for significance. If the data was not normally distributed, then the samples were subjected to the nonparametric Kruskal-Wallis test. The Kruskal-Wallis test is considered an acceptable alternative to ANOVA, as it also looks to compare between different treatments and across a span of time, but for nonparametric data instead (McDonald, 2009)

The two-tailed student's t-test was used as this test is applied to situations where the mean can be either greater than or less than a given value (McDonald, 2009). The ANOVA was used as we are looking at a difference in treatments across a specific range of time, in which separate individuals were used at each time point and compared to the individuals at the other time points (McDonald, 2009). The Tukey's post hoc test

generally follows-up an ANOVA test to find means that are significantly different from one another by comparing all possible pairs of means and helps to control for Type I (false positive) errors (Maxwell and Delaney, 2004). Grubb's test (GraphPad Software Inc., La Jolla, CA, USA) was applied to all data sets and outliers removed before analyzing. The Grubb's test detects outliers from univariate data that is assumed to have come from a normally distributed population and an outlier is the largest absolute deviation from the sample mean (Maxwell and Delaney, 2004). Comparisons were considered significant at $P \leq 0.05$.

Chapter Three: Results

3.1 Aim #1.1: Determine the macrophage depletion efficiency using single treatment of clodronate encapsulated-liposomes

3.1.1 Establishment of flow cytometry technique for the quantification of avian macrophages

Anti-chicken KUL01 and CD44 antibodies were used to quantify the macrophages in lung and spleen mononuclear cell populations using flow cytometry. The level of non-specific binding of PE-labelled anti-chicken KUL01 (0.00%) and APC-labelled mouse anti-chicken CD44 (0.001%), as assessed against isotype controls, are displayed in Figures 3.1 A) and B), respectively. Figures 3.1 C) and D) display the specific quantification of macrophages from total cell population using PE-labelled mouse anti-chicken KUL01 and APC-labelled mouse anti-chicken CD44 antibodies in untreated chickens. Of the mononuclear cells isolated, 4.08% of cells in the spleen (Figure 3.1 C) and 4.22% in the lungs (Figure 3.1 D) were macrophages.

3.1.2 Macrophage depletion efficiency following single treatment of clodronate encapsulated-liposomes

At 1 dpt, clodronate-treated chickens had significantly lower numbers of ($p<0.0001$) macrophages compared to the PBS liposome treated control chickens (Figure 3.2 A-C) in spleen. At 4 dpt, clodronate encapsulated-liposome treated chickens also had

significantly lower macrophages in spleen when compared to the controls ($p=0.0045$, Figures 3.2 D-F). In contrast to 1 and 4 dpt, we noted that there was no significant difference between treated and control birds at 5 dpt ($p=0.054$) (Figures 3.2 G-I).

At 1dpt, clodronate-treated chickens had significantly lower number of macrophages ($p=0.013$) compared to the PBS liposome-treated control chickens (Figures 3.3 A-C) in lungs. At 4 dpt, clodronate encapsulated-liposome treated chickens also had significantly lower macrophages ($p=0.0523$) in the lung when compared to the controls (Figures 3.3 D-F). Similar to the spleen, at 5dpt, a difference was not observed in lung macrophages between clodronate-treated and PBS-treated control chickens ($p=0.991$, Figures 3.3 G-I).

3.2 Aim #1.2: Determine macrophage depletion efficiency following two clodronate liposome treatments four days apart

Since a single clodronate liposome treatment reduces macrophages in spleen and lungs at 4 but not 5 dpt, we next hypothesized that the two clodronate treatments 4 days apart may be effective in depleting macrophages significantly in spleen and lung for 6 days following the second treatment. As expected, clodronate liposome treated chickens had significantly lower macrophages in spleen when compared to the controls 6 days following last clodronate treatment ($p=0.0007$, Figure 3.4 A-C). Similarly, clodronate liposome treated chickens had significantly lower macrophages in lungs when compared to the controls 6 days following last clodronate treatment ($p<0.0001$, Figures 3.4 D-F).

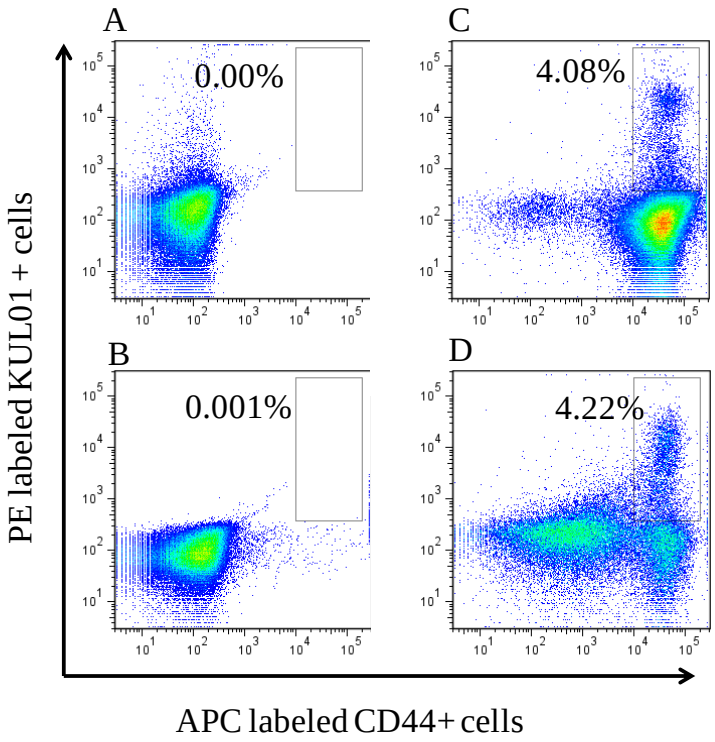

Figure 3.1. Optimized flow cytometry analysis of macrophages in the lung and spleen. Twenty-eight days old commercial chickens (n=2) were used to isolate mononuclear cells from spleen and lungs and to stain for macrophages (CD44+ KUL01+ cells) using PE-labelled mouse anti-chicken KUL01 and APC-labelled mouse anti-chicken CD44 monoclonal antibodies for flow cytometry. A) a representative FACS plot of isotype control for PE-labelled mouse anti-chicken KUL01 antibody, B) a representative FACS plot of isotype control for APC-labelled mouse anti-chicken CD44 antibody, C) a representative FACS plot showing CD44+ KUL01+ macrophages in spleen and D) a representative FACS plot showing CD44+ KUL01+ macrophages in lung.

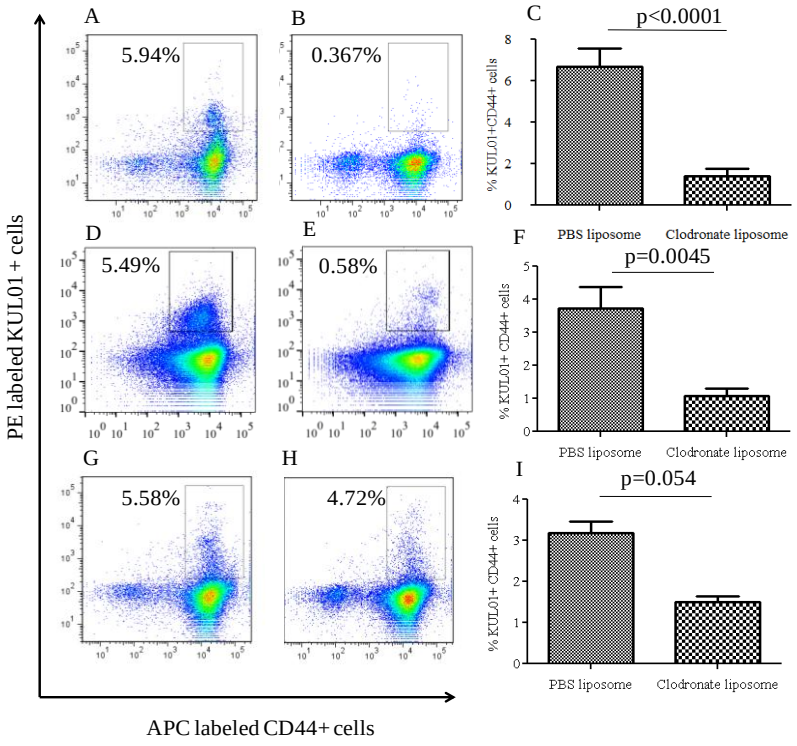

Figure 3.2 Flow cytometry analysis of spleen mononuclear cells from intra-abdominal clodronate and PBS treated chickens demonstrating macrophage depletion at 1 and 4 dpt, but not at 5dpt. A group of 8-12 days old commercial chickens were treated intra-abdominally once with 0.5 ml of clodronate encapsulated-liposomes or PBS encapsulated-liposomes. At 1, 4 or 5 dpt, spleen mononuclear cells were stained and analyzed as indicated in the materials and methods section for flow cytometry analysis. A-B) a representative FACS plot showing CD44+ KUL01+ macrophages in spleen of PBS or clodronate encapsulated-liposome treated birds at 1 dpt respectively; C) illustrates percentage CD44+ KUL01+ macrophages in spleen of clodronate encapsulated-liposome treated (n = 11) or PBS liposome treated (n = 10) birds at 1 dpt; D-E) a representative FACS plot showing CD44+ KUL01+ macrophages in spleen of PBS or clodronate encapsulated-liposome treated birds at 4 dpt, respectively; F) illustrates percentage

CD44+ KUL01+ macrophages in spleen of clodronate encapsulated-liposome treated (n = 5) or PBS liposome treated (n = 5) birds at 4 dpt; G-H) a representative FACS plot showing CD44+ KUL01+ macrophages in spleen of PBS or clodronate encapsulated-liposome treated birds at 5 dpt, respectively; I) illustrates percentage CD44+ KUL01+ macrophages in spleen of clodronate encapsulated-liposome treated (n = 8) or PBS liposome treated (n = 8) birds at 5 dpt; Figures C, F, and I correspond to pooled data originated from 2-3 independent experiments, and the error bars represent standard error of the mean (SEM). Grubb's test was applied to data and outliers removed from every sample group before using two-way Student's t-test to determine statistical significance between each treatment group.

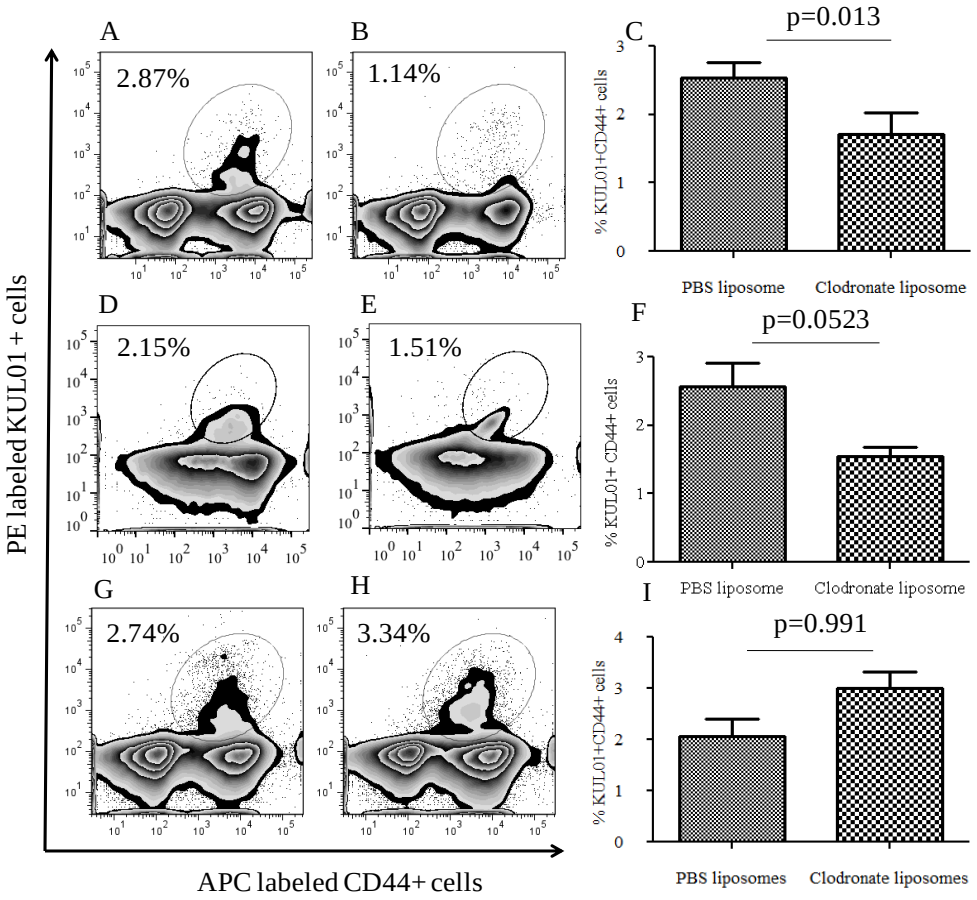

Figure 3.3 Flow cytometry analysis of lung mononuclear cells from intra-abdominal clodronate and PBS treated chickens demonstrating macrophage depletion 1 and 4 but not 5 dpt. Experimental design is the same as in Figure 3.2 legend. A-B) representative FACS plots showing CD44+ KUL01+ macrophages in lungs of PBS or clodronate encapsulated-liposome treated birds at 1dpt, respectively; C) illustrates percentage CD44+ KUL01+ macrophages in lung of clodronate encapsulated-liposome treated (n=7) or PBS liposome treated (n=7) birds at 1 dpt; D-E) representative FACS plot showing CD44+ KUL01+ macrophages in lungs of clodronate encapsulated-liposome treated birds at 4 dpt, respectively; and F) illustrates percentage CD44+ KUL01+ macrophages in lung of clodronate encapsulated-liposome treated (n=5) or PBS encapsulated-liposome treated (n = 5) birds at 4 dpt; G-H) representative FACS plots showing CD44+ KUL01+ macrophages in lungs of PBS or clodronate liposome treated birds at 5 dpt, respectively; I) illustrates percentage CD44+ KUL01+ macrophages in lung of clodronate encapsulated-liposome treated (n=5) or PBS encapsulated-liposome treated (n=5) birds at 5dpt. Figures C, F, and I correspond to pooled data originated from 2-3 independent experiments, and the error bars represent SEM. Grubb's test was applied to data and outliers removed from every sample group before using two-way Student's t-test to determine statistical significance between each treatment group.

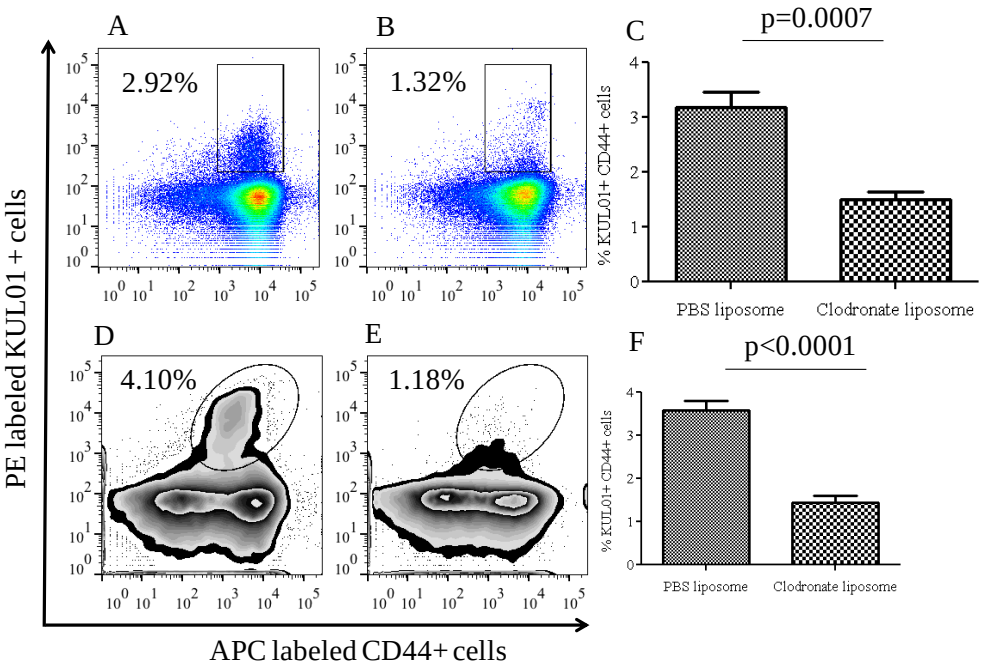

Figure 3.4 Flow cytometry analysis of spleen and lung mononuclear cells from chickens that were given 2 clodronate encapsulated-liposome treatments intra-abdominally demonstrating macrophage depletion 6 days following the second clodronate encapsulated-liposome treatment. Ten 11 days old commercial chickens were treated intra-abdominally twice 4 days apart with 0.5 ml of clodronate or PBS encapsulated-liposomes. Six days following the last treatment, spleen and lung mononuclear cells were isolated and stained as has been described in the materials and methods section. A-B) representative FACS plots showing CD44+ KUL01+ macrophages in spleen of PBS or clodronate encapsulated-liposome treated birds at 6 dpt following second treatment, respectively; C) illustrates percentage CD44+ KUL01+ macrophages in spleen of clodronate encapsulated-liposome treated (n=5) or PBS encapsulated-liposome treated (n=5) birds 6 day following the second treatment; D-E) representative FACS plot showing CD44+ KUL01+ macrophages in lung of PBS or clodronate encapsulated-

liposome treated birds at 6 dpt following the second treatment, respectively; and F) illustrates percentage CD44+ KUL01+ macrophages in lung of clodronate (n=5) or PBS liposome treated (n=5) birds 6 day following the second treatment, and the error bars represent SEM. Grubb's test was applied to data and outliers removed from every sample group before using two-way Student's t-test to determine statistical significance between each treatment group.

3.3 Aim #2.1: Establishment of an *in vivo* IBV infection model

3.3.1 *Clinical Observations*

Uninfected chickens showed no clinical signs. Although not all the IBV infected chickens developed respiratory signs such as coughing, sneezing, or rales, they all showed non-specific signs of infection, such as huddling together under the heat lamps, droopy wings, and depression. No scoring system was developed due to the significant lack of respiratory signs in IBV infected chickens.

3.3.2 *Quantification of IBV genome load*

3.3.2.1 Optimization of qPCR Standard Curves for IBV N and cellular β-actin genes

Using the plasmids generated as mentioned in the materials and methods, the copies/µL were determined for each dilution of the plasmid used in generating the standard curve. Figure 3.5 shows the amplification plot, dissociation curve, and resulting standard curve produced for both IBV N (A-C) and β-actin (D-F) genes inserted into their

respective plasmids. These standard curves were then used to calculate the IBV and β-actin copy numbers for all subsequent samples analyzed using qPCR.

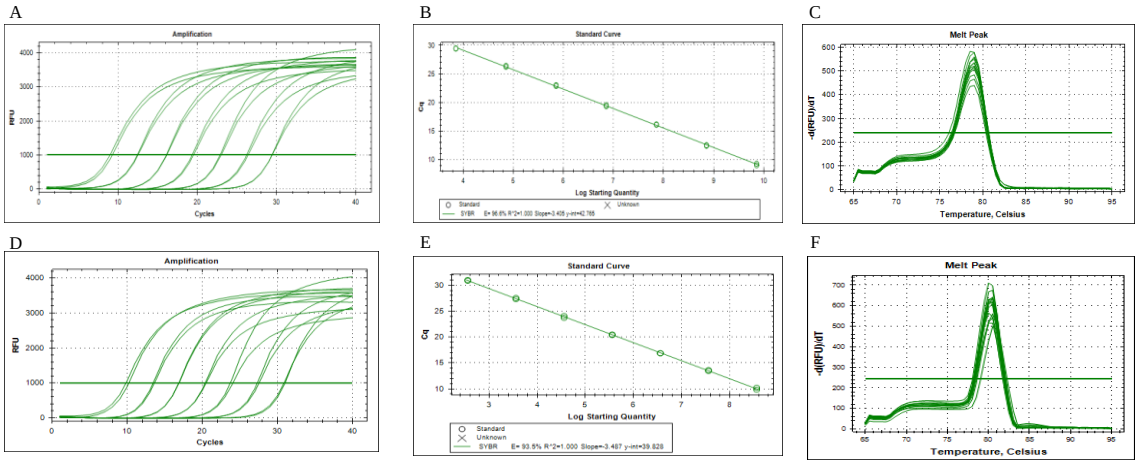

Figure 3.5. Optimization of standard curves generated for IBV N and β-actin gene expression. Plasmids produced using the protocol from the materials and methods were used to make a dilution series that were then ran in duplicate replicates to generate amplification plots, standard curves, and dissociation curves for both IBV N (A-C) and β-actin genes (D-F). Optimization was considered successful when efficiency of the standard curve was measured within the range of 90-110% and the reaction coefficient (R^2) found at around 0.999. The dissociation curve verified the absence of primer dimers within the reaction and a single specific product produced, due to the presence of a single narrow peak.

3.3.2.2 IBV Genome Load

To further quantify the change in IBV replication over the course of the infection, conventional PCR was first used to confirm the absence of an IBV N gene in uninfected tissues (Figure 3.6 A-B). After confirmation, the normalized IBV genome load was determined for infected lung and trachea at 4 and 7 dpi via qPCR for 20 ng of cDNA. Results indicate that there is no significant difference between the IBV genome loads of trachea (Figure 3.6 C, p=0.2036) or lung (Figure 3.6 D, p=0.4740) between 4 and 7 dpi.

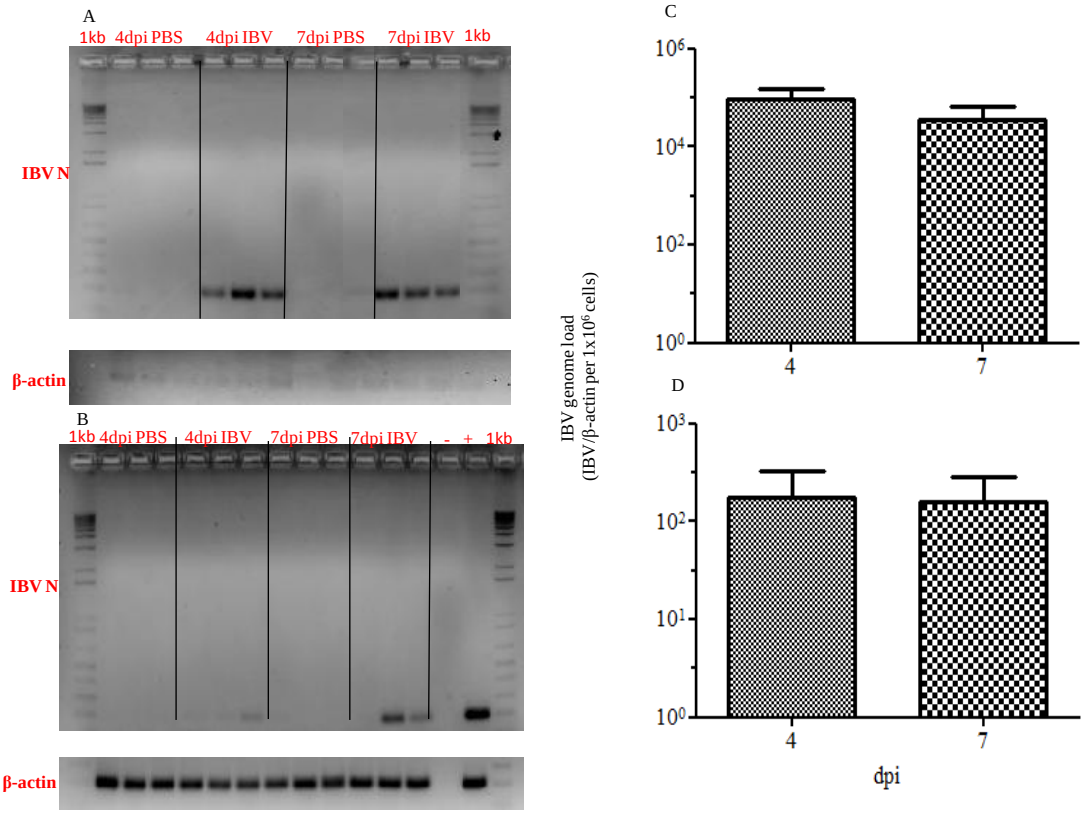

Figure 3.6. IBV genome load of trachea and lungs at 4 and 7 dpi in chickens infected with Conn A5968 strain of IBV**.** Twelve 6 days old chickens were infected intra-tracheally with the Conn A5968 strain of IBV and trachea and lung tissues were collected

at 4 and 7 dpi. There were three IBV-infected chickens at each time point and three PBS-treated chickens used as controls for each time point. Tissues were homogenized, the RNA extracted and converted to cDNA, and a conventional PCR ran to confirm the absence of IBV amplification in uninfected trachea (A) and lung (B) samples. A qPCR was used for only IBV infected tissues to determine IBV and β-actin genome loads as described in the materials and methods section. IBV genome loads for trachea (C) and lung (D) are presented and the error bars represent SEM. IBV genome load was normalized by dividing the genome load of IBV by the genome load of the housekeeping gene β-actin, with the result expressed as a product of $1x10^6$ cells. Grubb's test was applied to data and outliers removed from every group before using a two-way Student's t-test to determine statistical significance between each time point.

3.3.3 *Histopathology*

At both 4 dpi and 7 dpi, IBV infected trachea showed formation of lesions indicative of the replication of the virus within the epithelium of the tissue (Figures 3.7 C-D), when compared to uninfected controls at the same time points (Figures 3.7 A-B). These pathological changes include deciliation of epithelial cells, mononuclear cell infiltration into underlying mucosa, metaplasia of epithelium from simple columnar to squamous cells.

In comparison to trachea, the para-bronchioles in all IBV infected lungs also showed pathology indicative of an IBV infection (Figures 3.7 G-H) when compared to the uninfected controls at the same time points (Figures 3.7 E-F). These pathological

changes include massive mononuclear cell infiltration into area surrounding para-bronchioles, resulting in a loss of air exchange areas, with some mononuclear cell infiltration seen within the lumen of the para-bronchioles.

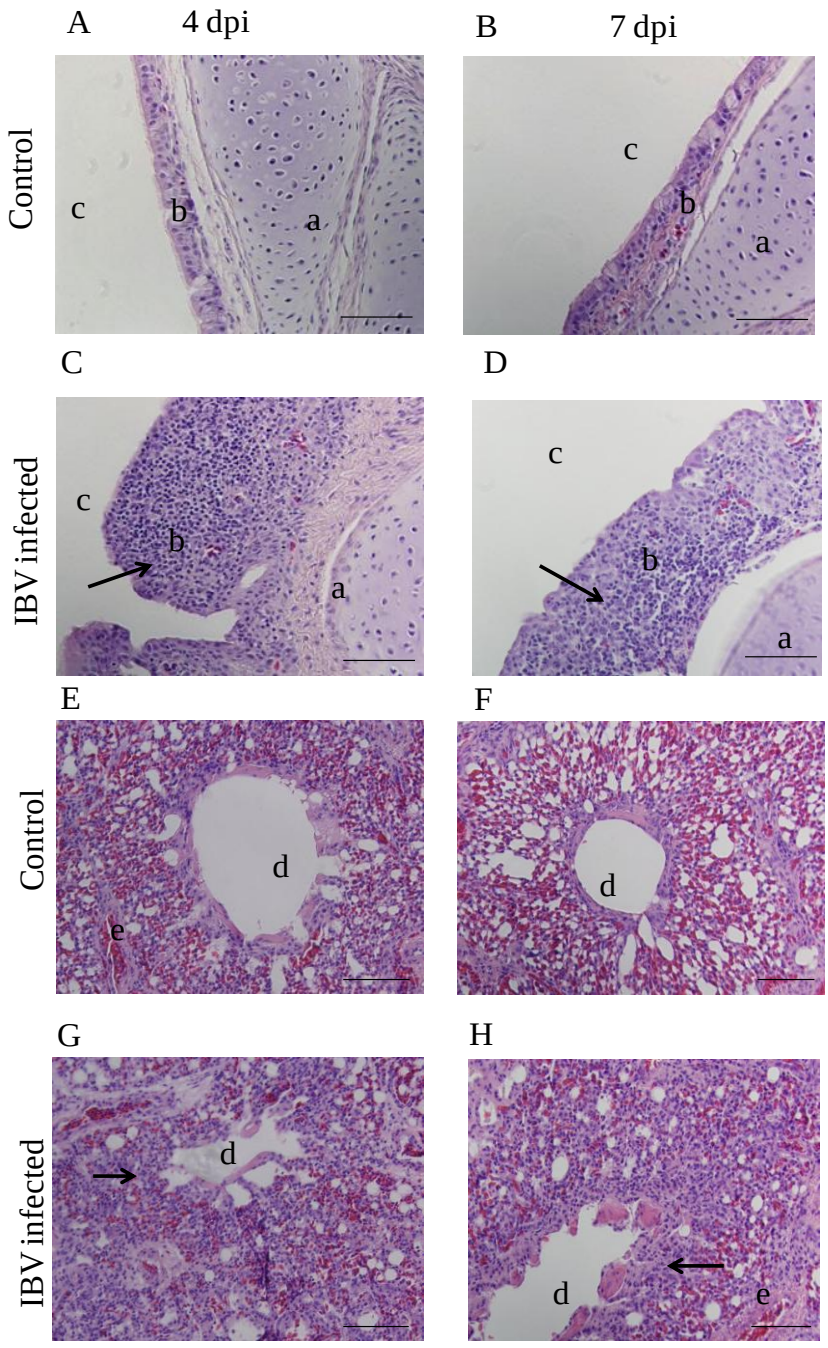

Figure 3.7. Representative histology images of trachea and lungs infected with Conn A5968 strain of IBV and uninfected controls at 4 and 7 dpi**.** Experimental design the same as in legend of Figure 3.5. Sections of trachea uninfected (A-B) and infected with IBV (C-D) are shown. a=tracheal cartilage, b=tracheal epithelium, c=tracheal lumen, d=Para bronchus, and e=intra-parabronchiole septa. Arrows indicate location of lesions in IBV infected tissues with mononuclear cell infiltration.

3.4 Aim #2.2: Determine what effect IBV replication has on macrophage numbers in trachea and lungs

3.4.1 *IBV genome load*

Normalized IBV genome load was determined for infected trachea and lung at 12 to 48 hpi via qPCR for 20 ng of cDNA. Conventional PCR was used to confirm an absence of IBV genome loads in uninfected tissues (data not shown). For trachea (Figure 3.8 A), there was no significant difference in the IBV genome loads between 12 and 48 hpi ($p=0.820$). In comparison, lung samples (Figure 3.8 B) also showed no significant difference in IBV genome loads from 12 to 48 hpi ($p=0.230$).

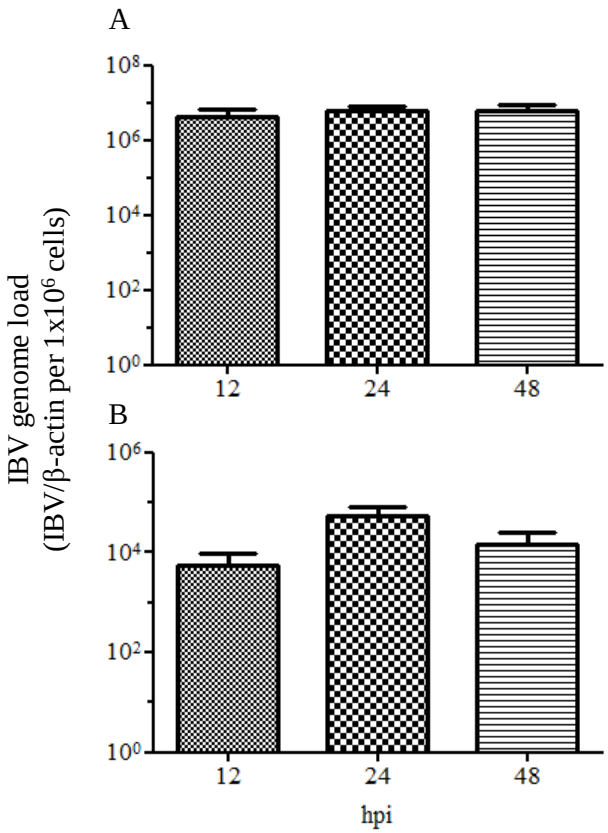

Figure 3.8. IBV genome load in trachea and lungs of chickens infected with Conn A5968 strain of IBV from 12 to 48 hpi. Chickens were infected intra-tracheally with the Conn A5968 strain of IBV at 6 days of age and trachea and lung tissues were collected at 12, 24, and 48 hpi. There were five IBV-infected chickens at each time point (six animals were sampled at 12 hpi) and five PBS-treated chickens used as controls for each time point. IBV genome loads for trachea (A) and lung (B) are presented and the error bars represent SEM. IBV genome load was normalized by dividing the genome load of IBV by the genome load of the housekeeping gene β-actin, with the result expressed as a product of $1x10^6$ cells. Grubb's test was applied to data and outliers removed from every sample group before using one-way ANOVA to determine statistical significance between each treatment group at each different time point.

3.4.2 *Macrophage counts*

The percentage of macrophages present in the representative FACS plots from tracheal samples collected from IBV infected and control chickens at 12, 24 and 48 hpi are illustrated in Figure 3.9 A-F. It was observed that macrophage numbers in the trachea only increased significantly ($p<0.0001$) in IBV infected chickens at 24 hpi when compared to control chickens. The percentage of macrophages present in the representative FACS plots from lungs of IBV infected of lung uninfected (E-F) and infected with IBV (G-H) also showed a significant increase in macrophage numbers at 24 hpi ($p=0.002$), but only when compared to uninfected controls at both 12 and 24 hpi.

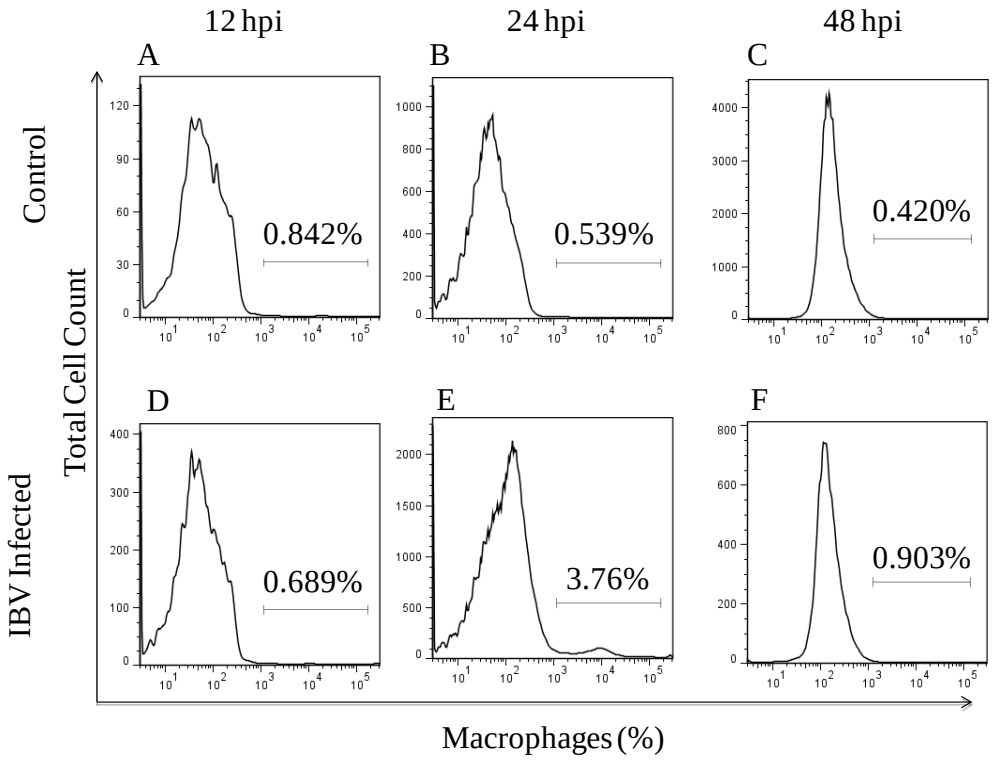

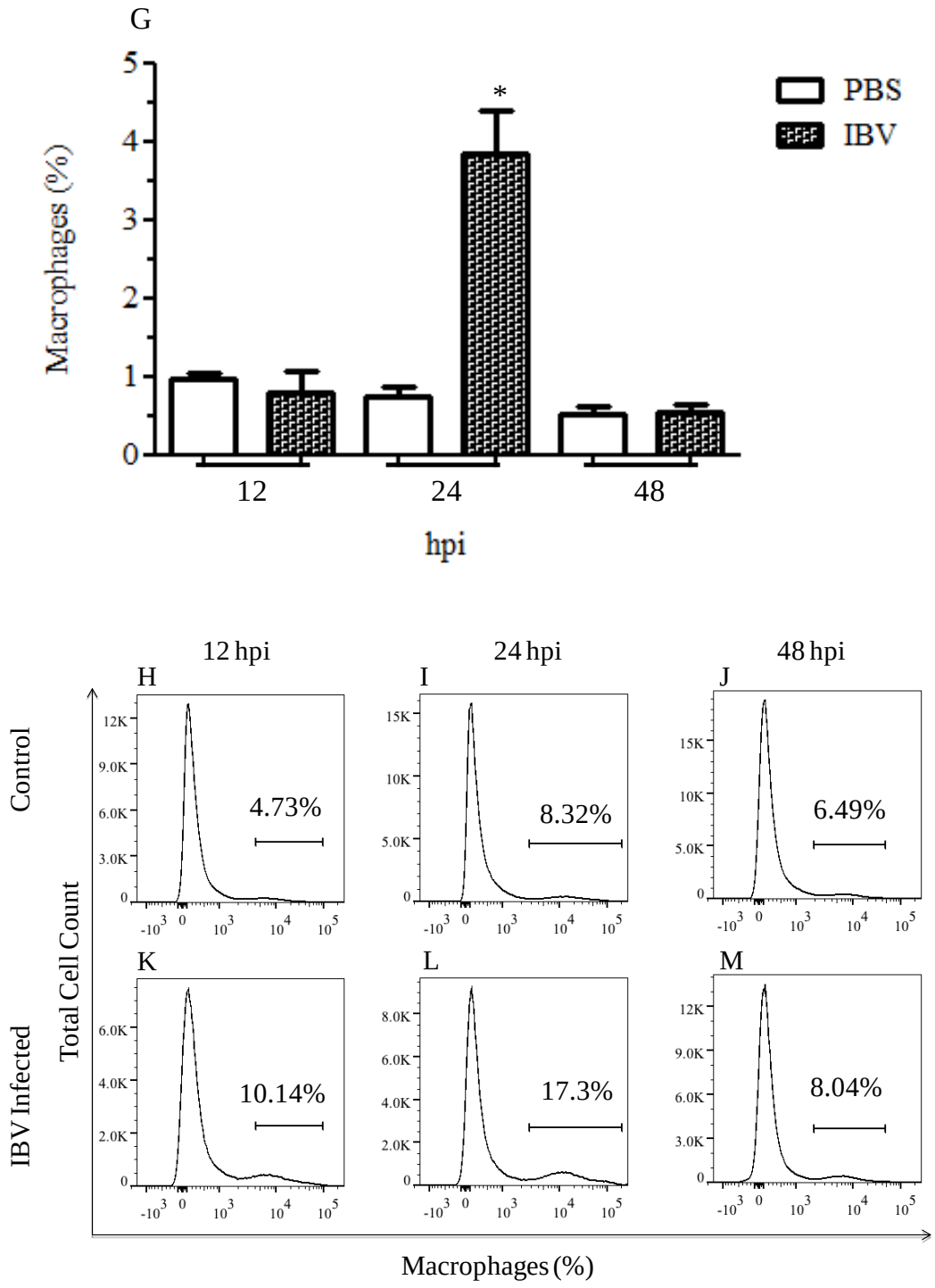
G
Macrophages (%)
PBS
IBV
*
12
24
48
hpi
12 hpi
24 hpi
48 hpi
Control
IBV Infected
Total Cell Count
H
I
J
K
L
M
4.73%
8.32%
6.49%
10.14%
17.3%
8.04%
Macrophages (%)

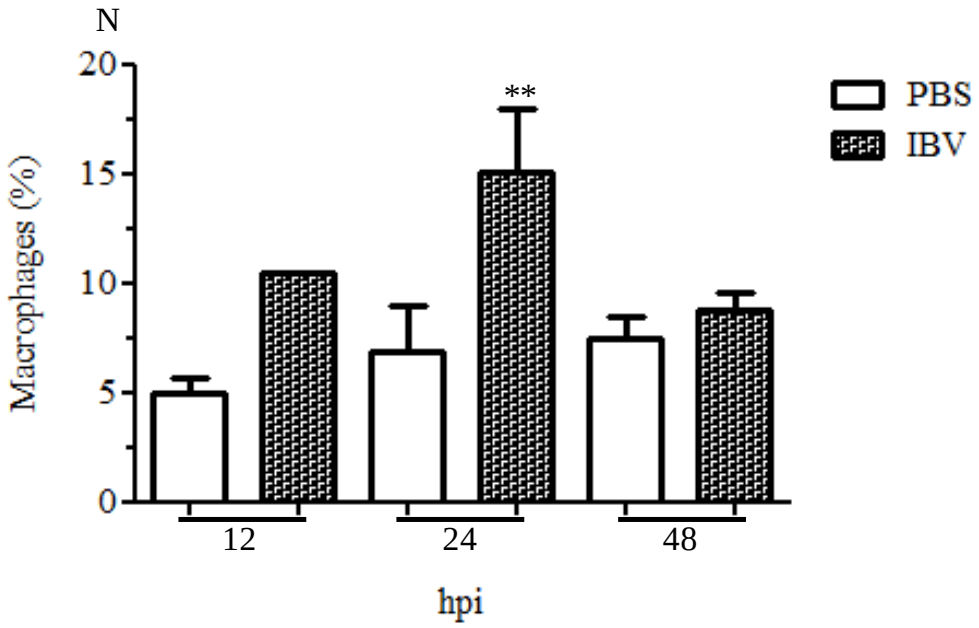

Figure 3.9. Quantification of macrophages present in trachea and lung during IBV infection from 12 to 48 hpi**.** Chickens were infected intra-tracheally with Conn A5968 at 6 days of age and trachea and lung tissues were collected at 12, 24, and 48 hpi. There were three IBV-infected and three PBS-treated chickens used at each time point for the lung macrophage quantification, and in a separate experiment with the same experimental design, four IBV-infected and five PBS-treated chickens used at each time point for quantification of macrophages in trachea. (A-C) represent the percent of macrophages in control trachea at 12, 24, and 48 respectively. (D-F) represent the percent of macrophages in IBV infected trachea for 12, 24, and 48 hpi, respectively. (H-J) represent the percent of macrophages in control lungs for 12, 24, and 48 hpi, respectively. (K-M) represent the percent of macrophages in IBV infected lungs for 12, 24, and 48 hpi, respectively. (G) and (N) are graphical representations of the percentage of macrophage numbers at each time point for trachea and lungs, respectively. Error bars represent SEM. * =

Significantly higher than all other treatment groups for trachea and ** = Significantly higher when compared to controls at 12 and 24 hpi in lung. Grubb's test was applied to data and outliers removed from every sample group before using one way ANOVA to determine statistical significance between each treatment group at each different time point.

3.4.3 *Histopathology*

Figure 3.10 (A-I) and (J-R) represent semi-quantitative data of histopathological scores used to describe IBV infected and control trachea and lung, respectively. In the trachea, we saw a significant increase in the scores over time, with the highest scores evident at 24 and 48 hpi for IBV infected tissues when compared to all other treatments ($p<0.0001$). For lung, there were also significant increases in the histopathological scores overtime, with IBV infected tissues have higher scores at both 24 and 48 hpi when compared to all other treatments ($p<0.0001$).

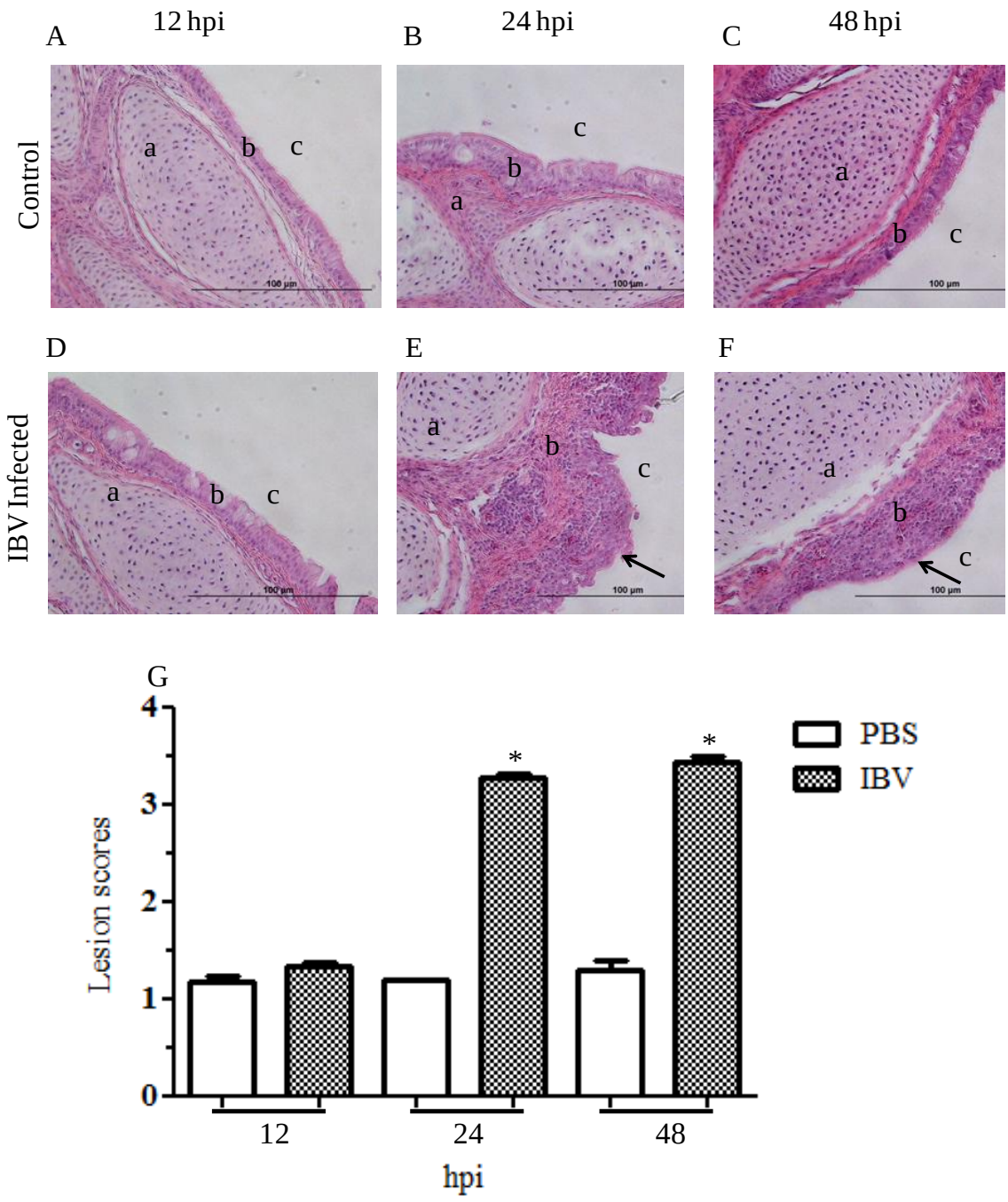
A
12 hpi
B
24 hpi
C
48 hpi
Control
a
b
c
D
E
F
IBV Infected
G
Lesion scores
0
1
2
3
4
12
24
48
hpi
PBS
IBV
*
*

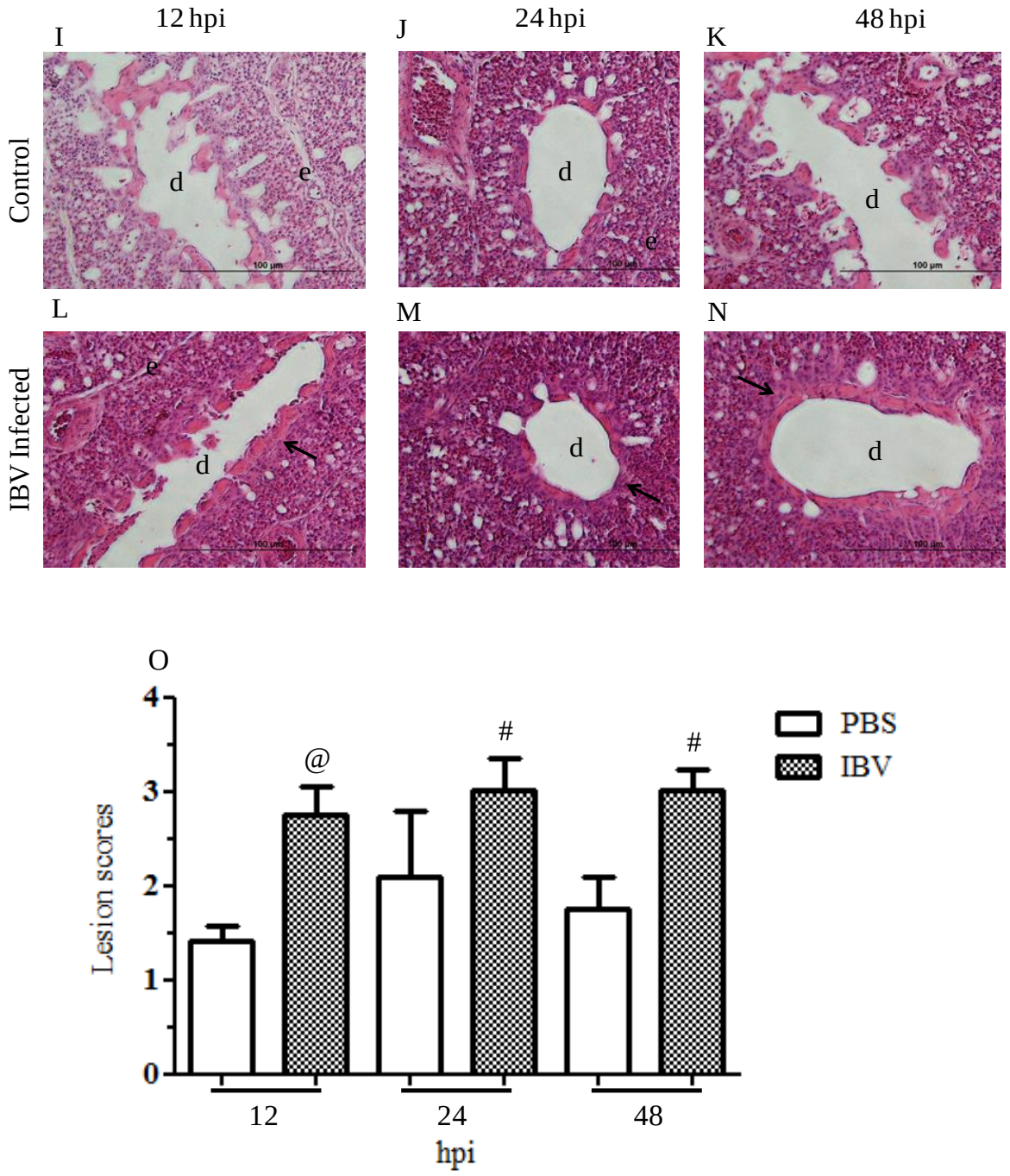

Figure 3.10. Representative histology images of trachea and lungs infected with Conn A5968 strain of IBV and uninfected controls. Chickens were infected intra-tracheally with Conn A5968 at six days of age and tracheas were collected at 12, 24, and 48 hpi.

There were five IBV-infected animals sampled at each time point (Only four tracheas were collected at 48 hpi) and two PBS-treated chickens sampled at each time point (five animals were sampled at 12 hpi). Sections of trachea uninfected (A-C) and infected with IBV (D-F) are shown, as well as sections of lung uninfected (I-K) and infected with IBV (L-N). The sections were stained with H & E. Scale Bar=100 μm. a=tracheal cartilage, b=tracheal epithelium, c=tracheal lumen, d=Para bronchus, and e=intra-parabronchiole septa. Blind scoring for both the trachea (G) and lung (O) was performed. Error bars represent SEM. * = Significantly higher than all other treatments for trachea, @ = Significantly higher than uninfected controls at 12, 24, and 24 hpi in lung, and # = Significantly higher than all other treatments for lung. Grubb's test was applied to data and outliers removed from every sample group. Anderson-Darling test was used to determine the distribution of the samples. Trachea samples were found not to be normally distributed and so the non-parametric Kruskal-Wallis test was used to determine if there were any significant differences between the groups. Lungs samples were found to be normally distributed, so the one-way ANOVA was used to determine statistical significance between each treatment group at each different time point. Arrows indicate location of lesions in IBV infected tissues with mononuclear cell infiltration.

3.5 Aim #3: Determine what effect macrophage depletion has on IBV replication in the chicken trachea

3.5.1 . *IBV genome load*

Normalized IBV genome load was determined for infected trachea at 1 to 3 dpi via qPCR for 20 ng of cDNA. Conventional PCR was used to confirm the absence of IBV genome loads within uninfected trachea (data not shown). For trachea, there was a significant difference in the relative IBV genome loads between the macrophage depleted and IBV infected group at 1 dpi and the untreated and IBV infected groups at 1, 2, and 3 dpi and the macrophage depleted and IBV infected group at 2 dpi ($p=0.045$). However, there was no significant difference between the macrophage depleted and IBV infected group at 1 dpi and the untreated and IBV infected group by 3 dpi

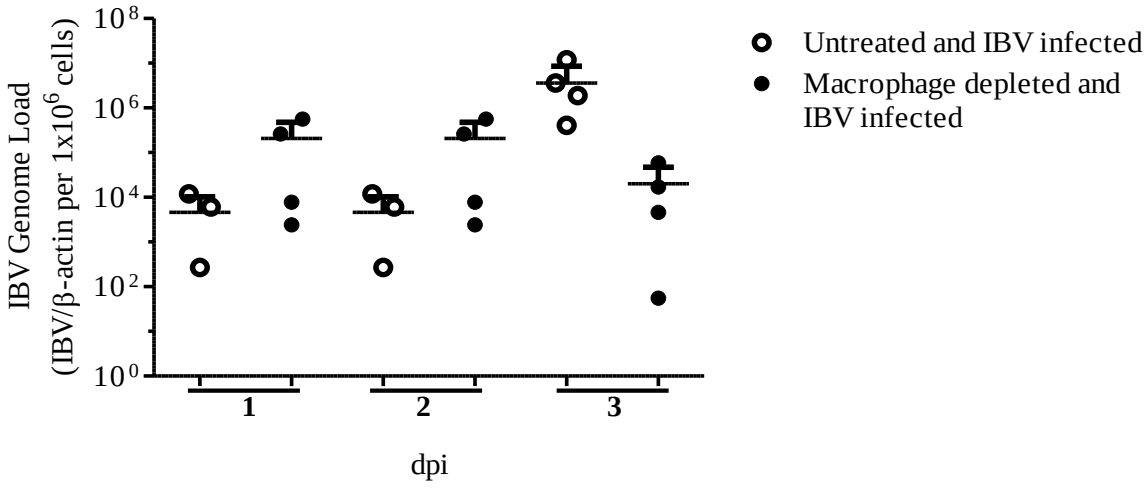

Figure 3.11. Normalized IBV genome load for untreated and IBV infected group and macrophage depleted and IBV infected group at 1, 2, and 3 dpi**.** Chickens were infected intra-tracheally with the Conn A5968 strain of IBV at 1 day of age and trachea were

collected at 1, 2, and 3 dpi. There were five untreated and IBV infected and five macrophage depleted and IBV infected chickens at each time point. There were four untreated and uninfected and macrophage depleted and uninfected chickens used as controls for each time point (only two animals were sampled at 3 dpi for the macrophage depleted and IBV infected group). IBV genome loads for trachea are presented and the error bars represent SEM. IBV genome load was normalized by dividing the genome load of IBV by the genome load of the housekeeping gene β-actin, with the result expressed as a product of $1x10^6$ cells. * = Significantly higher than untreated and IBV infected groups at 1, 2, and 3 dpi and macrophage depleted and IBV infected group at 2 dpi. Grubb's test was applied to data and outliers removed from every sample group before using one way ANOVA to determine statistical significance between each treatment group at each different time point.

3.5.2 *Macrophage counts*

The percentage of macrophages present in the representative FACS plots from tracheal samples collected from untreated and IBV infected and macrophage depleted and IBV infected chickens at 1, 2, and 3 dpi are illustrated in Figure 3.12 (A-I). Macrophage numbers in macrophage depleted and IBV infected group were found to significantly increase at 1 dpi when compared to the following groups: untreated and uninfected at 1, 2, and 3 dpi; untreated and IBV infected at 2 dpi; macrophage depleted and uninfected at 1 and 2 dpi; and macrophage depleted and IBV at 2 dpi ($p<0.0001$). Figure 3.12 (J) provide quantitative data to show the difference between the untreated and IBV infected

groups and macrophage depleted and IBV infected groups and the untreated and uninfected and macrophage depleted and uninfected control groups in terms of the percentage of macrophages at each time point for the trachea.

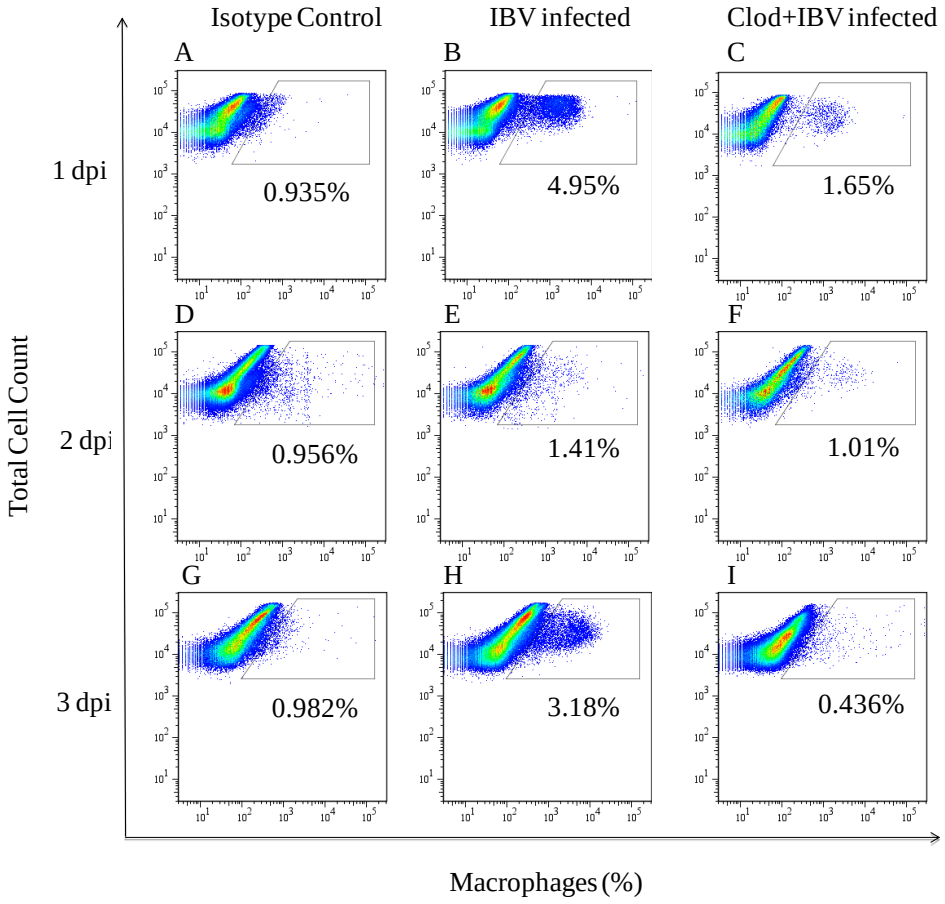

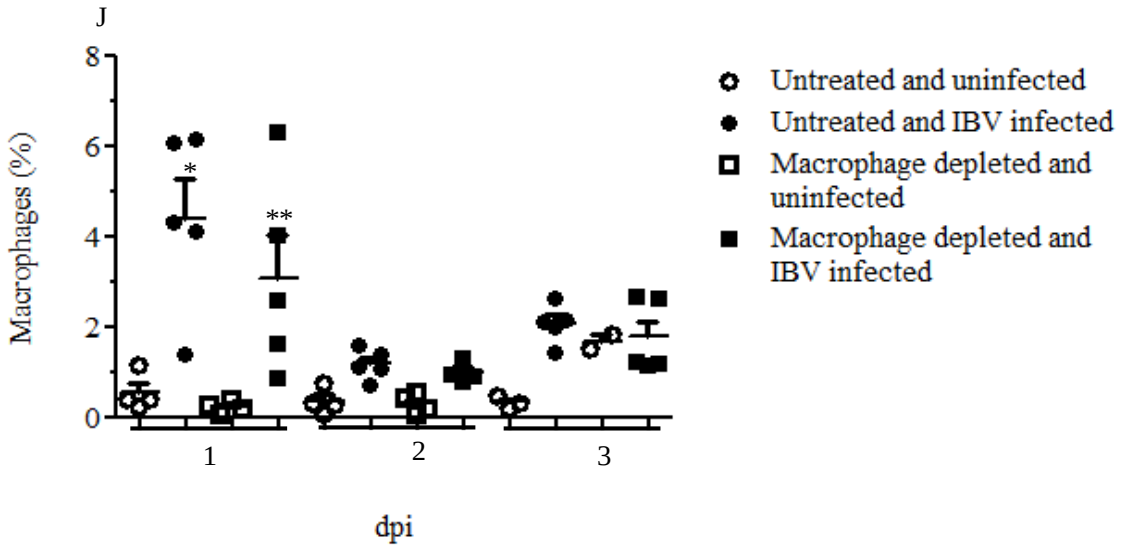

Figure 3.12. Quantification of macrophages present in trachea during IBV infection from 1 to 3 dpi between untreated and uninfected, untreated and IBV infected, macrophage depleted and uninfected, and macrophage depleted and IBV infected groups. Experimental design is the same as in Figure 3.10 legend. (A), (D), and (G) represent isotype controls used for the 1, 2, 3 dpi samples, respectively. (B), (E), and (H) represent the percent of macrophages in untreated and IBV infected trachea for 1, 2, and 3 dpi, respectively. (C), (F), and (I) represent the percent of macrophages in macrophage depleted and IBV infected trachea for 1, 2, and 3 dpi, respectively. (J) is a graphical representation of the percentage of macrophage numbers at each time point for trachea. Error bars represent SEM. * = Significantly higher than all other treatments, except for macrophage depleted and IBV infected group at 1 dpi, and ** = Significantly higher than untreated and uninfected groups at 1, 2, and 3 dpi; untreated and IBV infected group at 2 dpi; macrophage depleted and uninfected groups at 1 and 2 dpi; and macrophage depleted and IBV infected group at 2 dpi. Grubb's test was applied to data and outliers removed

from every sample group before using one way ANOVA to determine statistical significance between each treatment group at each different time point.

3.5.3 *Histopathology*

Figures 3.13 (A-D), (E-H), and (I-L) represent semi-quantitative data of histopathological scores used to describe untreated and uninfected, untreated and IBV infected, macrophage depleted and uninfected, and macrophage depleted and IBV infected tracheal groups at 1, 2, and 3 dpi, respectively. In the trachea, we saw a significant increase in the pathology when comparing the IBV infected groups to the uninfected groups, which retained relatively the same scores at each time point. While the IBV infected groups were higher than their uninfected counter parts at all three time points ($p<0.0001$), there was no significant difference between the untreated and IBV infected groups and the macrophage depleted and IBV infected group scores.

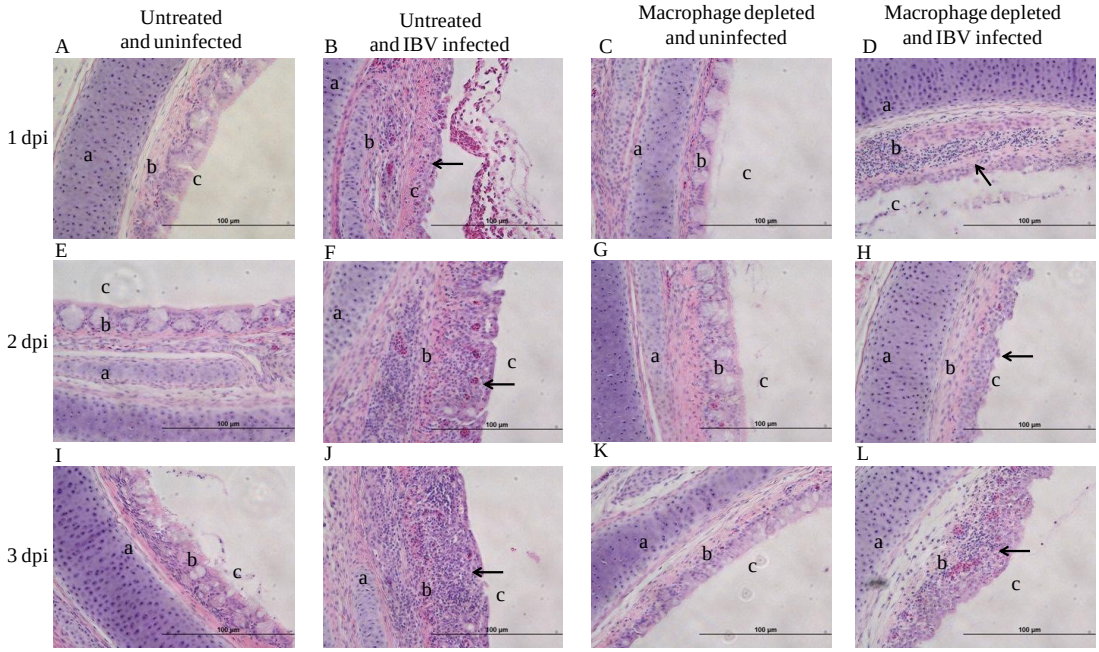

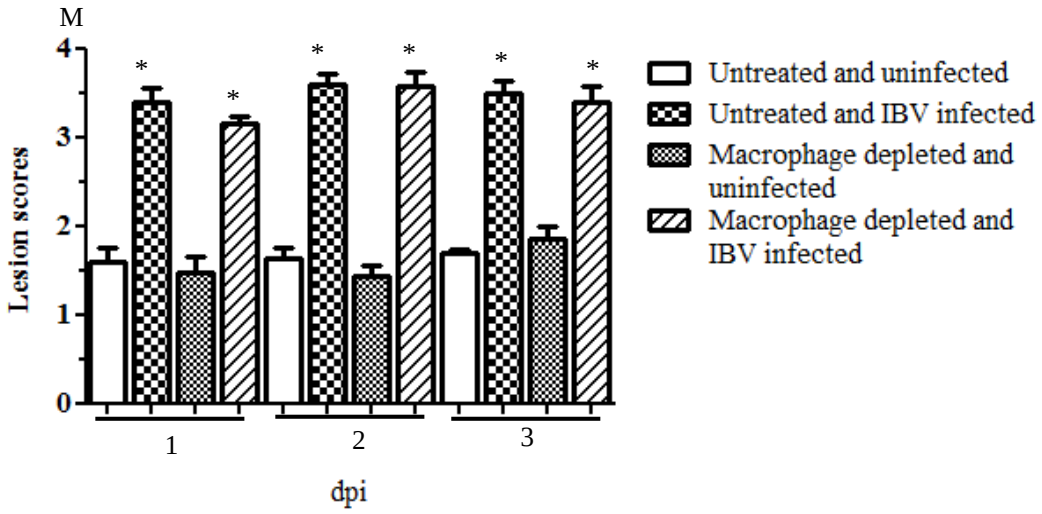

Figure 3.13. Representative histology images of trachea infected with Conn A5968 strain of IBV at 1, 2 and 3 dpi alongside macrophage depletion. Experimental design is the same as in Figure 3.10 legend. Sections of trachea from 1 (A-D), 2 (E-H) and 3 dpi (I-L) from untreated and uninfected, untreated and IBV infected, macrophage depleted and uninfected, and macrophage depleted and IBV infected groups are shown. The sections were stained with H & E. Scale Bar=100 µm. a=tracheal cartilage, b=tracheal epithelium, c=tracheal lumen. Blind scoring for the trachea (M) was performed. Error bars represent SEM. * = Significantly higher than untreated and uninfected groups and macrophage depleted and uninfected groups, but not significantly different from other likewise marked samples. Grubb's test was applied to data and outliers removed from every sample group. Remaining data was subjected to the Anderson-Darling test to determine the distribution of the data. The trachea data was found to be not normally distributed, so the nonparametric Kruskul-Wallis test was used to determine any significant differences between the different groups. Lung samples were found to be

normally distributed and the one way ANOVA was applied to determine any significant differences between samples across the time points.

Chapter Four: Discussion

The prevention and control of IB in poultry currently depends on vaccination. There are a number of vaccines are available that use live attenuated strains such as Mass, Conn, and Ark, and combinations of these strains provide protection against field strains (Cook *et al.*, 1999c). Live attenuated strains are generally used over killed strains when vaccinating against respiratory disease, as the live attenuated strains have lost their virulence and may only cause mild respiratory symptoms within the treated chicken while inducing high resistance (Maclachlan and Dubovi, 1974). In comparison, killed virus vaccines require multiple boosters in order to maintain host immunity and the adjuvants used in the vaccine could negatively impact the host following vaccination (Maclachlan and Dubovi, 1974). However, emergence of variant strains has become a challenge (Cavanagh, 2003) and these heterogonous IBV strains lead to IB outbreaks in vaccinated flocks and results in poultry production losses (Shimazaki *et al*., 2009; Xu *et al.*, 2007). In addition, strains used for vaccination can spread among individual birds within the flock (Matthijs *et al*., 2008), and change virulence during the bird to bird passage as a common occurrence (Farsang *et al*., 2002; Shimazaki *et al*., 2009). Moreover, vaccine driven increase of virulence has been documented for attenuated strains of IBV (Wang *et al*., 1993). These disadvantages associated with the current vaccines indicate the need for more reliable vaccines and/or other methods of disease control such as enhancing the host's innate immune response. In this regard, gaining a better understanding of the complexity of host-virus interactions, particularly host responses elicited against virulent IBV is an important prerequisite. Given the importance of macrophages in the host

response to many pathogens, we attempted to investigate the *in vivo* role of avian macrophages early during IBV infection at the respiratory tract.

Host responses in the chicken trachea following intranasal immunization of chickens using IBV vaccine strains such as attenuated or non-attenuated Mass IBV have shown an increase in the mRNA expression of innate immune genes following IBV immunization (Guo *et al*., 2008; Wang *et al*., 2006). The nature and extent of the innate host responses elicited by virulent IBV strains in the trachea and lung are also not known. It has also been shown that following immunization with the IBV Mass41 strain that the number of macrophages in bronchoalvelar lavage fluid is increased (Fulton *et al*., 1990; Fulton *et al*., 1993). However, it is not known whether these macrophages are mobilized from the trachea, lung, air sacs, or from all of these body compartments in response to IBV infection.

In order to support both hypotheses described in this thesis, we used three major techniques; qPCR, flow cytometry and conventional H&E staining. Conventionally, active viral infection in a tissue has been determined by demonstrating either the presence of viral antigens in tissues using immunohistochemical techniques or the presence of infectious virus in primary cell cultures by plaque assay. Due to limitations in these techniques relevant to IBV quantification, in that it immunohistochemistry is only semi-quantitative and IBV use in a plaque assay requires multiple viral passages in cell culture to become adapted, we used qPCR as a measure of IBV infection in the studies presented in this thesis. Although qPCR quantifies viral genome loads irrespective of whether the particle is living or non-living, it has been shown that IBV genome load correlates well with an active infection in trachea (Meir *et al.*, 2010). For the quantification of

macrophages from respiratory mucosa we chose flow cytometry over immunohistochemistry techniques, since the flow cytometry assay is more quantitative (Xu *et al*., 2002). The progression of IBV infection in trachea and lung was estimated semi-quantitatively using image analysis and lesion scoring of H & E stained histological sections.

In this study, I attempted to investigate the *in vivo* role of macrophages during IBV infection in chickens. The main hypotheses of our study were that 1) the replication of IBV in the trachea and lungs of the chicken is associated with an increase in the number of macrophages in the respiratory mucosa and that 2) the depletion of macrophages using clodronate encapsulated-liposomes, will result in an increase in IBV replication in these tissues, which will influence the resultant pathological outcomes when compared to uninfected controls. To support these hypotheses, our findings were three fold. Firstly, we provided phenotypic (quantitative) data that showed that two intra-abdominal treatments of clodronate encapsulated-liposomes 4 days apart results in depletion of macrophages for up to 10 days in the respiratory mucosa. Secondly, we found that IBV infection was associated with an increase in the number of macrophages present in the trachea and lung early during the infection. Finally, we showed clodronate encapsulated-liposome treatment leads to significant increase in the IBV genome load 1 day post-infection.

Before my MSc studies were undertaken, little was known about the efficacy of clodronate encapsulated-liposomes in depleting avian macrophages, particularly from the respiratory mucosa. Treatment of macrophages by clodronate encapsulated-liposomes has been performed in chickens in a number of earlier studies (Hala *et al*., 1998; Jeurissen *et*

al., 1998; Quere *et al.*, 2003; Rivas *et al*., 2003). Differences between our study and earlier studies are, firstly, that previous data have demonstrated an indirect analysis of effective macrophage depletion following clodronate encapsulated-liposome treatments (Hala *et al*., 1998; Quere *et al*., 2003; Rivas *et al.*, 2003). For example, some of these experiments focused on either the changes in nitric oxide (NO) levels in the blood or the progression of various diseases within the organs of the animal as a criterion of macrophage depletion. NO is released by cells in response to viral assault or in the presence of tumors (Koka *et al.*, 1995), and some experimental procedures showed NO concentration in serum decreasing in the chicken after treatment with clodronate encapsulated-liposomes within 3 days and returning to normal concentration by 9 days post-treatment (Quere *et al*., 2003). A decline in the resistance of chickens to MDV has also been used as an indicator of macrophage depletion after the administration of clodronate encapsulated-liposomes (Rivas *et al*., 2003). However, these results cannot directly correlate with clodronate-mediated macrophage depletion, since the source of NO can be other cell types such as DCs, NK cells, and mast cells (Baughman and Cook, 1999), and disease progression can be altered by a number of different pathways. Jeurissen and colleagues showed histological evidence of macrophage depletion from the spleen of chickens but their findings were limited by the lack of quantitative data important for calculating the effectiveness of clodronate function in chickens (Jeurissen *et al.*, 1998). In our first experiment, we obtained phenotypic (quantitative) data that demonstrates significant macrophage depletion, specifically from a secondary lymphoid organ, namely the spleen, and a non-lymphoid organ, the lung, following intra-abdominal administration of clodronate encapsulated-liposomes in chickens.

First, we used flow cytometry technique to quantify macrophage depletion by way of an anti-CD44 monoclonal antibody combined with antibody KUL01 (Mast *et al.*, 1998), effectively demonstrating that single clodronate encapsulated-liposome administration in chickens leads to significant macrophage depletion in lungs and spleen at 1 and 4 dpt, but not 5 dpt. Finally, we showed that two clodronate encapsulated-liposome treatments administered 4 days apart significantly deplete macrophages from spleen and lung for longer than single clodronate encapsulated-liposome treatment. One limitation to this protocol is that although the depletion was found to be significant, only around 30-50% of the macrophages in lung were actually depleted, which begs the question as to whether an IBV infection alongside this depletion efficiency will provide an accurate account of the functions that macrophages have, in comparison to a protocol that may produce a macrophage depletion efficiency of >80% instead.

IBV *in vivo* models are described previously (Alexander and Gough, 1977; Animas *et al.*, 1994; Grgic *et al*., 2008). In my second experiment, I established an IBV infection model infecting chicken via the intra-tracheal route using a Conn strain of IBV (A5968). We confirmed the establishment of infection in the trachea and lungs quantifying the IBV genome load and observing characteristic histological changes in these tissues. Using this model, I quantified the number of macrophages present in the trachea and lung early following IBV infection. Firstly, we observed quantified IBV genome loads in both the trachea and lung between 12 to 48 hpi. This presence of IBV genome at these time points was associated with histological scores that were also much higher in infected trachea and lungs when compared to uninfected tissues. Our IBV genome load data results are broadly in agreement with the work of Bronzoni and colleagues (2001) who used virus

isolation following infection with IBV Mass41 strain and showed a pattern of IBV replication similar to our observations; viral isolation didn't reveal an infection in either trachea or lungs of the chickens at 1 or 2 dpi, but saw an increase in IBV replication in both trachea and lung by 3 dpi (Bronzoni *et al*., 2001). The lack of detection of IBV replication before 72 hpi is potentially related to the use of virus isolation in their study, which is less sensitive, when compared to the more sensitive qPCR assay employed in our study (Wittwer and Kusakawa, 2004).

Macrophage numbers within the lungs and trachea of IBV infected chickens were found to significantly increase when compared to uninfected controls at 24 hpi. In chickens, macrophages are present within the tissue of the lung itself, lining the atria and infundibulae and providing a direct line of defence against respiratory infection (Abdul-Careem *et al.*, 2011) and can be mobilized to the lumen following viral infections (Cornelissen *et al.*, 2013). Similarly, Fulton and colleagues witnessed macrophage infiltration into the respiratory lumen of the IBV Mass41 infected chickens when collecting respiratory lavage fluid between 24 to 96 hpi (Fulton *et al*., 1993). Their study did not identify the source of these macrophages as trachea, lung, or air sacs, while our investigation indirectly indicates that macrophages may have been mobilised from the parenchyma of both the trachea and lung following IBV infection.

For the final experiment, macrophages were depleted using our optimized clodronate encapsulated-liposome protocol of two clodronate encapsulated-liposome injections spaced 4 days apart, followed by an IBV infection twenty-four hours following the second clodronate encapsulated-liposome treatment and the effect of said depletion on the progress of the IBV infection within the chicken trachea was determined. We

observed that IBV genome load within the trachea of clodronate encapsulated-liposome treated chickens were significantly higher than that of untreated chickens at 1 dpi, with the later two time points (2 and 3 dpi) recording no difference IBV genome loads between clodronate encapsulated-liposome treated chickens and controls. This observation made on IBV genome load could be explained firstly by the difference in macrophage numbers between macrophage depleted and un-depleted trachea. In the macrophage depleted group, macrophage numbers showed a lower trend at 1 dpi but not at 2 and 3 dpi. It is possible when the macrophages are lower, that the clearance of the virus infected cells is impaired, as was seen when comparing IBV genome loads of the macrophage depleted and untreated trachea at 1 dpi. In addition, both 2 and 3 dpi trachea have do not show a significantly higher IBV genome load, and the trachea at both time points shows a negligible difference in the number of macrophages counted when comparing between macrophage depleted and untreated chickens. Our 1 dpi IBV genome load data agrees with the data generated in experiments involving mammals, such as an infection of herpes simplex virus (HSV)-1 in the cornea of mice, which resulted in a 10^5 fold increase in viral titer when compared to the PBS liposome controls (Cheng *et al.*, 2000). Recently, it was also observed that viral titers were much higher in the lungs of ferrets who had their alveolar macrophages depleted by clodronate encapsulated-liposomes and followed by infection within H1N1 influenza virus and tissue collection at 3 dpi when compared to PBS encapsulated-liposome controls (Kim *et al.*, 2013). Secondly, it is possible that other cells of the innate immune response in the macrophage depleted trachea have been recruited to help clear the virus. One possible responsive cell type is the NK cells; Vervelde *et al* (2013) have shown that during an infection of IBV

Mass41, the NK cell population was found to increase at 1 dpi within the lungs of infected chickens (Vervelde *et al.*, 2013). The histological observations indicate that there is no visible difference between IBV infected macrophage depleted and un-depleted tracheas at 1, 2, or 3 dpi. Our observation on histological changes contrasts to the histological observations made in ferret lungs infected with H1N1 influenza virus (Kim *et al*., 2013). This discrepancy potentially is explained by a lack of significant macrophage depletion in trachea at 1, 2, and 3 dpi in our study.

In spite of the novel aspect of our work on *in vivo* characterization of interaction between macrophages and IBV, there were some limitations. We used chickens that ranged in age (1-12 days) for our experiments, which could have influenced the macrophage numbers, but the dose the of the clodronate encapsulated-liposomes wasn't adjusted to according to the age. This may have influenced the efficiency of the depletion of the macrophages. We chose the Conn strain of IBV specifically because it has been found to replicate in only the respiratory tissues of chickens, and no other areas of the body (Uenaka *et al*., 1998; Winterfield and Albassam, 1984). However, this isn't the case with the other strains such as Holte and Gray strains of IBV which can replicate in the kidneys (Chandra, 1987), or the Australian strains T and N1/88 of IBV, which have been found to replicate in the both kidneys, Harderian gland, and oviduct additional to the respiratory tissues (Chousalkar *et al.*, 2007). There is a possibility that these strains may use macrophages as one of the target cell of replication and as a means of spreading to other areas of the body (Nicholls *et al.*, 2003), and might therefore differ in their respective viral genome loads and consequent pathology if their source of replication was depleted by clodronate. Secondly, we employed qPCR for analyzing the magnitude of

IBV infection within the trachea and lung. Since qPCR measures genetic materials present in both living and non-living viral particles, we are unable to relate our data to an active IBV replication. One way of circumventing this problem would be to perform a plaque assay using primary cells such as chicken embryonic kidney cells (CEKs) or a cell line such as vero cells, both of which have been found to support IBV viral growth (Chasey and Alexander, 1976; Coria and Ritchie, 1973). The plaque assay relies on the mechanism that as the virus replicates within a cell monolayer, the cells lyse and form "holes" within the monolayer, which are visualized by staining with vital dyes such as crystal violet (Maclachlan and Dubovi, 2010). However, the virus collected from the tissues of infected birds cannot be directly grown in these cell culture systems; instead, virus inoculums must be adapted within embryonated eggs and in the cell culture system chosen (Chubb and Ma, 1974; Crawley and Fahey, 1956). This requirement of propagation of the virus in order to quantify the infectious virus particles for the plaque assay precluded the use of this assay in our experiments to quantify viral replication. Thirdly, although we observed statistically significant depletions of macrophages in the respiratory tract using intra-abdominal injection of clodronate encapsulated-liposomes, we achieved only partial depletion of macrophages (~20-40%) in both the trachea and lung when compared to spleen (~50-60%). Since we recorded significant increase in the IBV genome load in trachea 24 hours post clodronate treatment, a depletion that equaled the depletion in the spleen might have resulted a different picture in terms of IBV genome load and the pathology. Finally, it is well known that some functions of the immune system are redundant and depleting macrophages *in vivo* may mask the effect on the host due to the compensatory increase in other innate immune cells such as NK cells.

Taking the above into account, future studies should be performed to further characterize the role of macrophages during the IBV infection in the trachea and lung. Importantly, it is critical that we optimise a method for a more effective depletion of macrophages from the trachea and lung. Taking into account that some functions of the immune system are redundant, it is important that other innate immune cells are also characterized in the macrophage depletion model to allow for further understanding of our observations. Since there is only a single record that indicates that IBV does not replicate *in vitro* in avian macrophages (von Bulow and Klasen, 1983), verifying if IBV can replicate within avian macrophages either *in vitro* and *in vivo* will help understanding of the complexity of macrophage-IBV interaction. Field study experiments should also be preformed also well, as this experiment was limited in its use of SPF chickens, and field conditions would significantly impact commercial chickens in terms of the different pathogens they have been exposed to or different vaccines administered to them, which will also modulate the immune response. Overall, the findings of the studies presented here shed some light on the importance of macrophages in the immunity to IBV infection in respiratory tract of chickens.

Chapter Five: Conclusions

- A single intra-abdominal administration of clodronate encapsulated-liposomes is capable of significantly depleting macrophages from chicken spleen and lungs up to 4 dpt. The percentage reduction in macrophages is high in the spleen when compared to lungs which suggests that lung macrophage depletion using clodronate liposomes is partial.

- Two treatments of clodronate encapsulated-liposomes spaced 4 days apart allow for significant macrophage depletion within chicken spleen and lung 6 days following the second treatment. Although the reduction in macrophage count in clodronate encapsulated-liposome treated chickens is statistically significant, percentage reduction is partial in the lungs, as has been seen with single intra-abdominal administration of clodronate encapsulated-liposomes.

- As indicated by IBV genome load and histological changes in the trachea and lungs, the establishment of *in vivo* IBV infection model in SPF chickens was successful.

- As demonstrated using the established IBV infection model, IBV infection in chicken trachea and lung results in significant increase in the number of macrophages in these tissues, early following the infection peaking 24 hpi.

- Macrophage depletion using the optimized protocol with two clodronate encapsulated-liposome treatments resulted in no significant depletion of macrophages in trachea. However, we observed significantly higher IBV genome load in clodronate encapsulated-liposome treated and IBV infected trachea when compared to the IBV infected untreated trachea at 1 dpi, but not at 2 and 3 dpi. No difference was observed in histological changes in the trachea of IBV infected chickens with and without macrophage depletion.

- Further studies are necessary to optimize a technique of a more effective depletion of macrophages from respiratory tract and then to study the role of macrophages in the IB progression in trachea and lung of chickens. Further studies in the roles and functions of other innate immune cells, as well as the response of the adaptive immune response in a macrophage depletion model should also be undertaken.

5.1 Bibliography

Abdul-Careem, M.F., Firoz Mian, M., Gillgrass, A.E., Chenoweth, M.J., Barra, N.G., Chan, T., Al-Garawi, A.A., Chew, M.V., Yue, G., van Roojen, N., Xing, Z., Ashkar, A.A., 2011. FimH, a TLR4 ligand, induces innate antiviral responses in the lung leading to protection against lethal influenza infection in mice. Antiviral Res 92, 346-355.

Abdul-Careem, M.F., Haq, K., Shanmuganathan, S., Read, L.R., Schat, K.A., Heidari, M., Sharif, S., 2009. Induction of innate host responses in the lungs of chickens following infection with a very virulent strain of Marek's disease virus. Virology 393, 250-257.

Agresti, A., 2007. An introduction to categorical data analysis. Wiley Inter-Science, Gainesville, FL, USA.

Akira, S., 2001. Toll-like receptors and innate immunity. Adv Immunol 78, 1-56.

Albassam, M.A., Winterfield, R.W., Thacker, H.L., 1986. Comparison of the nephropathogenicity of four strains of infectious bronchitis virus. Avian Dis 30, 468-476.

Alberts, B., Johnson, A., Lewis, J., et al., 2002. The Adaptive Immune System. In, Molecular Biology of the Cell. Garland Science, City.

Alexander, D.J., Gough, R.E., 1977. Isolation of avian infectious bronchitis virus from experimentally infected chickens. Res Vet Sci 23, 344-347.

Alexopoulou, L., Holt, A.C., Medzhitov, R., Flavell, R.A., 2001. Recognition of double-stranded RNA and activation of NF-kappaB by Toll-like receptor 3. Nature 413, 732-738.

Ambali, A.G., Jones, R.C., 1990. Early pathogenesis in chicks of infection with an enterotropic strain of infectious bronchitis virus. Avian Dis 34, 809-817.

Anderson, D.P., Beard, C.W., Hanson, R.P., 1966. Influence of poultry house dust, ammonia, and carbon dioxide on the resistance of chickens to Newcastle disease virus. Avian Dis 10, 177-188.

Anderson, D.P., Wolfe, R.R., Cherms, F.L., Roper, W.E., 1968. Influence of dust and ammonia on the development of air sac lesions in turkeys. Am J Vet Res 29, 1049-1058.

Animas, S.B., Otsuki, K., Hanayama, M., Sanekata, T., Tsubokura, M., 1994. Experimental infection with avian infectious bronchitis virus (Kagoshima-34 strain) in chicks at different ages. J Vet Med Sci 56, 443-447.

Auriola, S., Frith, J., Rogers, M.J., Koivuniemi, A., Monkkonen, J., 1997. Identification of adenine nucleotide-containing metabolites of bisphosphonate drugs using ion-pair liquid chromatography-electrospray mass spectrometry. J Chromatogr B Biomed Sci Appl 704, 187-195.

Babcock, A.A., Toft-Hansen, H., Owens, T., 2008. Signaling through MyD88 regulates leukocyte recruitment after brain injury. Journal of Immunology 181, 6481–6490.

Bacon, L.D., Hunter, D.B., Zhang, H.M., Brand, K., Etches, R., 2004. Retrospective evidence that the MHC (B haplotype) of chickens influences genetic resistance to attenuated infectious bronchitis vaccine strains in chickens. Avian Pathol 33, 605-609.

Balaan, M.R., and Banks, D.E., 1998. Silicosis. In: Rom, W.N. (Ed.), Environmental and occupational medicine. Little Brown, Boston, MA, USA.

Baughman, R., Cook, L., 1999. Diagnostic quiz #33. Case no. 1. Florid cemento-osseous dysplasia. Todays FDA 11, 5C, 7C.

Bedard, P.A., Alcorta, D., Simmons, D.L., Luk, K.C., Erikson, R.L., 1987. Constitutive expression of a gene encoding a polypeptide homologous to biologically active human platelet protein in Rous sarcoma virus-transformed fibroblasts. Proc Natl Acad Sci U S A 84, 6715-6719.

Biebricher, C.K., Eigen, M., 2006. What is a quasispecies? Curr Top Microbiol Immunol 299, 1-31.

Biebricher, C.K., Eigen, M., Gardiner, W.C., Jr., 1984. Kinetics of RNA replication: plus-minus asymmetry and double-strand formation. Biochemistry 23, 3186-3194.

Binns, D.S., O'Brien, T.J., Hicks, R.J., Cook, M.J., Murphy, M., 1999. Experience of a 3-D, Large-Field-Of-View (LFOV) PET Scanner for the Localization Of Complex Partial Epilepsy. Clin Positron Imaging 2, 328.

Bitterman, P.B., Saltzman, L.E., Adelberg, S., Ferrans, V.J., Crystal, R.G., 1984. Alveolar macrophage replication. One mechanism for the expansion of the mononuclear phagocyte population in the chronically inflamed lung. J Clin Invest 74, 460-469.

Boltz, D.A., Nakai, M., Bahra, J.M., 2004. Avian infectious bronchitis virus: a possible cause of reduced fertility in the rooster. Avian Dis 48, 909-915.

Bom, H.S., Vansant, J.P., Pettigrew, R.I., Cooke, C.D., Votaw, J.R., Garcia, E.V., 1999. Determination of Myocardial Viability with ECG-Gated Fluorodeoxyglucose F-18 Positron Emission Tomography. Clin Positron Imaging 2, 183-190.

Bond, C.W., Leibowitz, J.L., Robb, J.A., 1979. Pathogenic murine coronaviruses. II. Characterization of virus-specific proteins of murine coronaviruses JHMV and A59V. Virology 94, 371-384.

Borucki, M.K., Allen, J.E., Chen-Harris, H., Zemla, A., Vanier, G., Mabery, S., Torres, C., Hullinger, P., Slezak, T., 2013. The role of viral population diversity in adaptation of bovine coronavirus to new host environments. PLoS One 8, e52752.

Boyle, P., Cooke, T., Halfacree, K., Smith, D., 1999. Integrating GB and US census microdata for studying the impact of family migration on partnered women's labour market status. Int J Popul Geogr 5, 157-178.

Bronzoni, R.V., Pinto, A.A., Montassier, H.J., 2001. Detection of infectious bronchitis virus in experimentally infected chickens by an antigen-competitive ELISA. Avian Pathol 30, 67-71.

Brune, K., Leffell, M.S., Spitznagel, J.K., 1972. Microbicidal activity of peroxidaseless chicken heterophile leukocytes. Infect Immun 5, 283-287.

Callison, S.A., Jackwood, M.W., Hilt, D.A., 2001. Molecular characterization of infectious bronchitis virus isolates foreign to the United States and comparison with United States isolates. Avian Dis 45, 492-499.

Calnek, B.W., Fahey, K.J., Bagust, T.J., 1986. In vitro infection studies with infectious laryngotracheitis virus. Avian Dis 30, 327-336.

Capua, I., Gough, R.E., Mancini, M., Casaccia, C., Weiss, C., 1994. A 'novel' infectious bronchitis strain infecting broiler chickens in Italy. Zentralbl Veterinarmed B 41, 83-89.

Casais, R., Dove, B., Cavanagh, D., Britton, P., 2003. Recombinant avian infectious bronchitis virus expressing a heterologous spike gene demonstrates that the spike protein is a determinant of cell tropism. J Virol 77, 9084-9089.

Casler, J.G., Cook, J.R., 1999. Cognitive performance in space and analogous environments. Int J Cogn Ergon 3, 351-372.

Cavanagh, D., 1983. Coronavirus IBV: further evidence that the surface projections are associated with two glycopolypeptides. J Gen Virol 64 (Pt 8), 1787-1791.

Cavanagh, D., Davis, P., Cook, J., Li, D., 1990. Molecular basis of the variation exhibited by avian infectious bronchitis coronavirus (IBV). Adv Exp Med Biol 276, 369-372.

Cavanagh, D., Davis, P.J., Cook, J.K., Li, D., Kant, A., Koch, G., 1992. Location of the amino acid differences in the S1 spike glycoprotein subunit of closely related serotypes of infectious bronchitis virus. Avian Pathol 21, 33-43.

Cavanagh, D., Elus, M.M., Cook, J.K., 1997. Relationship between sequence variation in the S1 spike protein of infectious bronchitis virus and the extent of cross-protection in vivo. Avian Pathol 26, 63-74.

Cavanagh, D., Mawditt, K., Britton, P., Naylor, C.J., 1999. Longitudinal field studies of infectious bronchitis virus and avian pneumovirus in broilers using type-specific polymerase chain reactions. Avian Pathology 28, 593-605.

Cavanagh, D., Naqi, S.A., 2003. Infectious bronchitis. Iowa State University Press, Iowa.

Champoux, J.J., Neidhardt, F.C., Drew, W.L., Plorde, J.J. , 2004. Intravascular infections, bacteremia, and endotoxemia. In: Ryan, K.J., Ray, C.G. (Ed.), Sherris Medical Microbiology. McGraw Hill, Toronto, Ontario, pp. 881-891.

Chan, P.K., Cheung, J.L., Cheung, T.H., Lo, K.W., Yim, S.F., Siu, S.S., Tang, J.W., 2007. Profile of viral load, integration, and E2 gene disruption of HPV58 in normal cervix and cervical neoplasia. J Infect Dis 196, 868-875.

Chandra, M., 1987. Comparative nephropathogenicity of different strains of infectious bronchitis virus in chickens. Poult Sci 66, 954-959.

Chasey, D., Alexander, D.J., 1976. Morphogenesis of avian infectious bronchitis virus in primary chick kidney cells. Arch Virol 52, 101-111.

Cheng, H., Tumpey, T.M., Staats, H.F., van Rooijen, N., Oakes, J.E., Lausch, R.N., 2000. Role of macrophages in restricting herpes simplex virus type 1 growth after ocular infection. Invest Ophthalmol Vis Sci 41, 1402-1409.

Chong, K.T., Apostolov, K., 1982. The pathogenesis of nephritis in chickens induced by infectious bronchitis virus. J Comp Pathol 92, 199-211.

Chousalkar, K.K., Roberts, J.R., Reece, R., 2007. Comparative histopathology of two serotypes of infectious bronchitis virus (T and n1/88) in laying hens and cockerels. Poult Sci 86, 50-58.

Chubb, R.C., Huynh, V., Law, R., 1987. The detection of cytotoxic lymphocyte activity in chickens infected with infectious bronchitis virus or fowl pox virus. Avian Pathol 16, 395-405.

Chubb, R.C., Ma, V., 1974. Some observations on the propagation of avian infectious bronchitis virus in tissue culture. Aust Vet J 50, 63-68.

Claassen, I., Van Rooijen, N., Claassen, E., 1990. A new method for removal of mononuclear phagocytes from heterogeneous cell populations in vitro, using the liposome-mediated macrophage 'suicide' technique. J Immunol Methods 134, 153-161.

Clementz, M.A., Chen, Z., Banach, B.S., Wang, Y., Sun, L., Ratia, K., Baez-Santos, Y.M., Wang, J., Takayama, J., Ghosh, A.K., Li, K., Mesecar, A.D., Baker, S.C., 2010. Deubiquitinating and interferon antagonism activities of coronavirus papain-like proteases. J Virol 84, 4619-4629.

Coleman, J.D., Cooke, M.M., Jackson, R., Webster, R., 1999. Temporal patterns in bovine tuberculosis in a brushtail possum population contiguous with infected cattle in the Ahaura Valley, Westland. N Z Vet J 47, 119-124.

Cook, A.K., Dorman, G., Redman, C.W., 1999a. A duplication of the descending colon presenting in pregnancy. J Obstet Gynaecol 19, 423.

Cook, C.J., 1999. Maternal behaviour in sheep (Ovis aries) following administration of opioid agonists. N Z Vet J 47, 67-70.

Cook, C.S., Wilkie, D.A., 1999. Treatment of presumed iris melanoma in dogs by diode laser photocoagulation: 23 cases. Vet Ophthalmol 2, 217-225.

Cook, G., Burton, L., Fields, K., 1999b. Reactive neuromuscular training for the anterior cruciate ligament-deficient knee: a case report. J Athl Train 34, 194-201.

Cook, J.K.A., Orbell, S.J., Woods, M.A., Huggins, M.B., 1999c. Breadth of protection of the respiratory tract provided by different live-attenuated infectious bronchitis vaccines against challenge with infectious bronchitis viruses of heterologous serotypes. Avian Pathology 28, 477-485.

Cook, K.A., Otsuki, K., Martins, N.R., Ellis, M.M., Huggins, M.B., 1992. The secretory antibody response of inbred lines of chicken to avian infectious bronchitis virus infection. Avian Pathol 21, 681-692.

Cooke, M.M., Buddle, B.M., Aldwell, F.E., McMurray, D.N., Alley, M.R., 1999. The pathogenesis of experimental endo-bronchial Mycobacterium bovis infection in brushtail possums (Trichosurus vulpecula). N Z Vet J 47, 187-192.

Coria, M.F., Ritchie, A.E., 1973. Serial passage of 3 strains of avian infectious bronchitis virus in African green monkey kidney cells (VERO). Avian Dis 17, 697-704.

Cornelissen, J.B., Vervelde, L., Post, J., Rebel, J.M., 2013. Differences in highly pathogenic avian influenza viral pathogenesis and associated early inflammatory response in chickens and ducks. Avian Pathol 42, 347-364.

Crawley, J.F., Fahey, J.E., 1956. Propagation of infectious bronchitis virus in tissue culture. Can J Microbiol 2, 503-510.

Crinion, R.A., Hofstad, M.S., 1972. Pathogenicity of four serotypes of avian infectious bronchitis virus for the oviduct of young chickens of various ages. Avian Dis 16, 351-363.

Cuadros, M.A., Santos, A.M., Martin-Oliva, D., Calvente, R., Tassi, M., Marin-Teva, J.L., Navascues, J., 2006. Specific immunolabeling of brain macrophages and microglial cells in the developing and mature chick central nervous system. J Histochem Cytochem 54, 727-738.

Cumming, R.B., Chubb, R.C., 1988. The pathogenesis of nephritis evoked by Australian IB viruses. In: *Proceedings of the 1st International Symposium on Infectious Bronchitis*, Rauischholzhausen, Germany, pp. 129-132.

Darbyshire, J.H., Peters, R.W., 1984. Sequential development of humoral immunity and assessment of protection in chickens following vaccination and challenge with avian infectious bronchitis virus. Res Vet Sci 37, 77-86.

Davis, M., Morishita, T.Y., 2005. Relative ammonia concentrations, dust concentrations, and presence of Salmoneua species and Escherichia coli inside and outside commercial layer facilities. Avian Dis 49, 30-35.

de Geus, E.D., Jansen, C.A., Vervelde, L., 2012. Uptake of particulate antigens in a nonmammalian lung: phenotypic and functional characterization of avian respiratory phagocytes using bacterial or viral antigens. J Immunol 188, 4516-4526.

Delamarre, L., Pack, M., Chang, H., Mellman, I., Trombetta, E.S., 2005. Differential lysosomal proteolysis in antigen-presenting cells determines antigen fate. Science 307, 1630-1634.

Delaplane, J.P., Stuart, H.O, 1939. Studies of infectious bronchitis. Rhode Island Agricultural Experiment Station, RI. Bulletin, 273.

Dolz, R., Pujols, J., Ordonez, G., Porta, R., Majo, N., 2006. Antigenic and molecular characterization of isolates of the Italy 02 infectious bronchitis virus genotype. Avian Pathol 35, 77-85.

Donaldson, K., Davis, J.M., James, K., 1982. Characteristics of peritoneal macrophages induced by asbestos injection. Environ Res 29, 414-424.

Erbeck, D.H., McMurray, B.L., 1998. Isolation of Georgia variant (Georgia isolate 1992) infectious bronchitis virus but not Ornithobacterium rhinotracheale from a Kentucky broiler complex. Avian Dis 42, 613-617.

Fagerland, J.A., Arp, L.H., 1993. Structure and development of bronchus-associated lymphoid tissue in conventionally reared broiler chickens. Avian Dis 37, 10-18.

Farnell, M.B., He, H., Genovese, K., Kogut, M.H., 2003. Pharmacological analysis of signal transduction pathways required for oxidative burst in chicken heterophils stimulated by a Toll-like receptor 2 agonist. Int Immunopharmacol 3, 1677-1684.

Farsang, A., Ros, C., Renstrom, L.H., Baule, C., Soos, T., Belak, S., 2002. Molecular epizootiology of infectious bronchitis virus in Sweden indicating the involvement of a vaccine strain. Avian Pathol 31, 229-236.

Ficken, M.D., Edwards, J.F., Lay, J.C., 1986. Induction, collection, and partial characterization of induced respiratory macrophages of the turkey. Avian Dis 30, 766-771.

Fink, K., Ng, C., Nkenfou, C., Vasudevan, S.G., van Rooijen, N., Schul, W., 2009. Depletion of macrophages in mice results in higher dengue virus titers and highlights the role of macrophages for virus control. Eur J Immunol 39, 2809-2821.

Foltz, J.F., 2008. Characterization of infectious bronchitis virus isolates discovered during the 2004 avian influenza outbreakof the Delmarva peninsula. In, Vol. Animal Science. University of Delaware, City, p. 102.

Fulton, R.M., Reed, W.M., DeNicola, D.B., 1990. Light microscopic and ultrastructural characterization of cells recovered by respiratory-tract lavage of 2- and 6-week-old chickens. Avian Dis 34, 87-98.

Fulton, R.M., Reed, W.M., Thacker, H.L., 1993. Cellular response of the respiratory tract of chickens to infection with Massachusetts 41 and Australian T infectious bronchitis viruses. Avian Dis 37, 951-960.

Fulton, R.M., Thacker, H.L., Reed, W.M., DeNicola, D.B., 1997. Effect of Cytoxan®-Induced Heteropenia on the Response of Specific-Pathogen-Free Chickens to Infectious Bronchitis. Avian Dis 41, 511-518.

Gilmour, P.S., Beswick, P.H., Brown, D.M., Donaldson, K., 1995. Detection of surface free radical activity of respirable industrial fibres using supercoiled phi X174 RF1 plasmid DNA. Carcinogenesis 16, 2973-2979.

Gobel, T.W., Chen, C.L., Shrimpf, J., Grossi, C.E., Bernot, A., Bucy, R.P., Auffray, C., Cooper, M.D., 1994. Characterization of avian natural killer cells and their intracellular CD3 protein complex. Eur J Immunol 24, 1685-1691.

Gomis, S., Babiuk, L., Godson, D.L., Allan, B., Thrush, T., Townsend, H., Willson, P., Waters, E., Hecker, R., Potter, A., 2003. Protection of chickens against Escherichia coli infections by DNA containing CpG motifs. Infect Immun 71, 857-863.

Gough, R.E., Alexander, D.J., 1979. Comparison of duration of immunity in chickens infected with a live infectious bronchitis vaccine by three different routes. Res Vet Sci 26, 329-332.

Grgic, H., Hunter, D.B., Hunton, P., Nagy, E., 2008. Pathogenicity of infectious bronchitis virus isolates from Ontario chickens. Can J Vet Res 72, 403-410.

Gross, W.B., Colmano, G., 1971. Effect of infectious agents on chickens selected for plasma corticosterone response to social stress. Poult Sci 50, 1213-1217.

Guillot, L., Le Goffic, R., Bloch, S., Escriou, N., Akira, S., Chignard, M., Si-Tahar, M., 2005. Involvement of toll-like receptor 3 in the immune response of lung epithelial cells to double-stranded RNA and influenza A virus. J Biol Chem 280, 5571-5580.

Guo, X., Rosa, A.J., Chen, D.G., Wang, X., 2008. Molecular mechanisms of primary and secondary mucosal immunity using avian infectious bronchitis virus as a model system. Vet Immunol Immunopathol 121, 332-343.

Hala, K., Malin, G., Dietrich, H., Loesch, U., Boeck, G., Wolf, H., Kaspers, B., Geryk, J., Falk, M., Boyd, R.L., 1996. Analysis of the initiation period of spontaneous autoimmune thyroiditis (SAT) in obese strain (OS) of chickens. J Autoimmun 9, 129-138.

Hala, K., Moore, C., Plachy, J., Kaspers, B., Bock, G., Hofmann, A., 1998. Genes of chicken MHC regulate the adherence activity of blood monocytes in Rous sarcomas progressing and regressing lines. Vet Immunol Immunopathol 66, 143-157.

Hamal, K.R., Burgess, S.C., Pevzner, I.Y., Erf, G.F., 2006. Maternal antibody transfer from dams to their egg yolks, egg whites, and chicks in meat lines of chickens. Poult Sci 85, 1364-1372.

Higgs, R., Cormican, P., Cahalane, S., Allan, B., Lloyd, A.T., Meade, K., James, T., Lynn, D.J., Babiuk, L.A., O'Farrelly, C., 2006. Induction of a novel chicken Toll-like

receptor following Salmonella enterica serovar Typhimurium infection. Infect Immun 74, 1692-1698.

Hiscox, J.A., Wurm, T., Wilson, L., Britton, P., Cavanagh, D., Brooks, G., 2001. The coronavirus infectious bronchitis virus nucleoprotein localizes to the nucleolus. J Virol 75, 506-512.

Ho, M.K., Springer, T.A., 1984. Preparation and use of monoclonal antimacrophage antibodies. Methods Enzymol 108, 313-324.

Hogue, B.G., Machamer, C. E., 2008. Coronavirus structural proteins and virus assembly. In: Perlman, S., Gallagher, T., Snijder, E. (Ed.), Nidoviruses. ASM Press, City, pp. 179-200.

Huang, A.Y., Golumbek, P., Ahmadzadeh, M., Jaffee, E., Pardoll, D., Levitsky, H., 1994. Role of bone marrow-derived cells in presenting MHC class I-restricted tumor antigens. Science 264, 961-965.

Ignjatovic, J., Galli, U., 1995. Immune responses to structural proteins of avian infectious bronchitis virus. Avian Pathol 24, 313-332.

Iqbal, M., Philbin, V.J., Withanage, G.S., Wigley, P., Beal, R.K., Goodchild, M.J., Barrow, P., McConnell, I., Maskell, D.J., Young, J., Bumstead, N., Boyd, Y., Smith, A.L., 2005. Identification and functional characterization of chicken toll-like receptor 5 reveals a fundamental role in the biology of infection with Salmonella enterica serovar typhimurium. Infect Immun 73, 2344-2350.

Jeurissen, S.H., Janse, E.M., 1989. Distribution and function of non-lymphoid cells in liver and spleen of embryonic and adult chickens. Prog Clin Biol Res 307, 149-157.

Jeurissen, S.H., Janse, E.M., Koch, G., de Boer, G.F., 1988. The monoclonal antibody CVI-ChNL-68.1 recognizes cells of the monocyte-macrophage lineage in chickens. Dev Comp Immunol 12, 855-864.

Jeurissen, S.H., Janse, E.M., van Rooijen, N., Claassen, E., 1998. Inadequate anti-polysaccharide antibody responses in the chicken. Immunobiology 198, 385-395.

Jia, W., Karaca, K., Parrish, C.R., Naqi, S.A., 1995. A novel variant of avian infectious bronchitis virus resulting from recombination among three different strains. Arch Virol 140, 259-271.

Johnson, M.A., Pooley, C., Ignjatovic, J., Tyack, S.G., 2003. A recombinant fowl adenovirus expressing the S1 gene of infectious bronchitis virus protects against challenge with infectious bronchitis virus. Vaccine 21, 2730-2736.

Joiner, K.S., Ewald, S.J., Hoerr, F.J., van Santen, V.L., Toro, H., 2005. Oral infection with chicken anemia virus in 4-wk broiler breeders: lack of effect of major histocompatibility B complex genotype. Avian Dis 49, 482-487.

Jones, R.C., Ambali, A.G., 1987. Re-excretion of an enterotropic infectious bronchitis virus by hens at point of lay after experimental infection at day old. Vet Rec 120, 617-618.

Kagan, E., Hartmann, D.P., 1984. Elimination of macrophages with silica and asbestos. Methods Enzymol 108, 325-335.

Kameka, A.M., Haddadi, S., Kim, D.S., Cork, S.C., Abdul-Careem, M.F., 2014. Induction of innate immune response following infectious bronchitis corona virus infection in the respiratory tract of chickens. Virology 450-451, 114-121.

Kant, A., Koch, G., van Roozelaar, D.J., Kusters, J.G., Poelwijk, F.A., van der Zeijst, B.A., 1992. Location of antigenic sites defined by neutralizing monoclonal antibodies on the S1 avian infectious bronchitis virus glycopolypeptide. J Gen Virol 73 (Pt 3), 591-596.

Kaspers, B., Lillehoj, H.S., Lillehoj, E.P., 1993. Chicken macrophages and thrombocytes share a common cell surface antigen defined by a monoclonal antibody. Vet Immunol Immunopathol 36, 333-346.

Kim, H.M., Kang, Y.M., Ku, K.B., Park, E.H., Yum, J., Kim, J.C., Jin, S.Y., Lee, J.S., Kim, H.S., Seo, S.H., 2013. The severe pathogenicity of alveolar macrophage-depleted ferrets infected with 2009 pandemic H1N1 influenza virus. Virology 444, 394-403.

Koch, G., Hartog, L., Kant, A., van Roozelaar, D.J., 1990. Antigenic domains on the peplomer protein of avian infectious bronchitis virus: correlation with biological functions. J Gen Virol 71 (Pt 9), 1929-1935.

Kodihalli, S., Sivanandan, V., Nagaraja, K.V., Shaw, D., Halvorson, D.A., 1994. Effect of avian influenza virus infection on the phagocytic function of systemic phagocytes and pulmonary macrophages of turkeys. Avian Dis 38, 93-102.

Koka, P., He, K., Zack, J.A., Kitchen, S., Peacock, W., Fried, I., Tran, T., Yashar, S.S., Merrill, J.E., 1995. Human immunodeficiency virus 1 envelope proteins induce interleukin 1, tumor necrosis factor alpha, and nitric oxide in glial cultures derived from fetal, neonatal, and adult human brain. J Exp Med 182, 941-951.

Koskela, K., Nieminen, P., Kohonen, P., Salminen, H., Lassila, O., 2004. Chicken B-cell-activating factor: regulator of B-cell survival in the bursa of fabricius. Scand J Immunol 59, 449-457.

Kusters, J.G., Jager, E.J., Niesters, H.G., van der Zeijst, B.A., 1990. Sequence evidence for RNA recombination in field isolates of avian coronavirus infectious bronchitis virus. Vaccine 8, 605-608.

Lai, M.M., 1987. Molecular biology of coronavirus 1986. Adv Exp Med Biol 218, 7-13.

Lane, T.E., Paoletti, A.D., Buchmeier, M.J., 1997. Disassociation between the in vitro and in vivo effects of nitric oxide on a neurotropic murine coronavirus. J Virol 71, 2202-2210.

Lee, C.W., Jackwood, M.W., 2001. Spike gene analysis of the DE072 strain of infectious bronchitis virus: origin and evolution. Virus Genes 22, 85-91.

Lehenkari, P.P., Kellinsalmi, M., Napankangas, J.P., Ylitalo, K.V., Monkkonen, J., Rogers, M.J., Azhayev, A., Vaananen, H.K., Hassinen, I.E., 2002. Further insight into mechanism of action of clodronate: inhibition of mitochondrial ADP/ATP translocase by a nonhydrolyzable, adenine-containing metabolite. Mol Pharmacol 61, 1255-1262.

Loudovaris, T., Calnek, B.W., Yoo, B.H., Fahey, K.J., 1991. Genetic susceptibility of chicken macrophages to in vitro infection with infectious laryngotracheitis virus. Avian Pathol 20, 291-302.

Maclachlan, J.N., and Dubovi, E. J. , 2010. Virus replication. In: Maclachlan, J.N., and Dubovi, E. J. (Ed.), Frenner's Veterinary Virology. Academic Press, Saint Louis, MO, USA, pp. 40-41.

Manrubia, S.C., Escarmis, C., Domingo, E., Lazaro, E., 2005. High mutation rates, bottlenecks, and robustness of RNA viral quasispecies. Gene 347, 273-282.

Martinet, W., Verheye, S., De Meyer, G.R., 2007. Selective depletion of macrophages in atherosclerotic plaques via macrophage-specific initiation of cell death. Trends Cardiovasc Med 17, 69-75.

Mast, J., Goddeeris, B.M., Peeters, K., Vandesande, F., Berghman, L.R., 1998. Characterisation of chicken monocytes, macrophages and interdigitating cells by the monoclonal antibody KUL01. Vet Immunol Immunopathol 61, 343-357.

Matthijs, M.G., Bouma, A., Velkers, F.C., van Eck, J.H., Stegeman, J.A., 2008. Transmissibility of infectious bronchitis virus H120 vaccine strain among broilers under experimental conditions. Avian Dis 52, 461-466.

Maxwell, S.E.a.D., H. D., 2004. Designing Experiments and Analyzing Data: A Model Comparison Perspective. Lawrence Erlbaum Associates, Mahwah, NJ, USA.

McDonald, J.H., 2009. Handbook of Biological Statistics. Sparky House Publishing, Baltimore, Maryland, USA.

McFarlane, J.M., Curtis, S.E., Simon, J., Izquierdo, O.A., 1989. Multiple concurrent stressors in chicks. 2. Effects on hematologic, body composition, and pathologic traits. Poult Sci 68, 510-521.

Meir, R., Maharat, O., Farnushi, Y., Simanov, L., 2010. Development of a real-time TaqMan RT-PCR assay for the detection of infectious bronchitis virus in chickens, and comparison of RT-PCR and virus isolation. J Virol Methods 163, 190-194.

Mew, D., Wat, C.K., Towers, G.H., Levy, J.G., 1983. Photoimmunotherapy: treatment of animal tumors with tumor-specific monoclonal antibody-hematoporphyrin conjugates. J Immunol 130, 1473-1477.

Mondal, S., Chang, Y.F., Balasuriya, U., 2012. Sequence analysis of infectious bronchitis virus isolates from the 1960s in the United States. Arch Virol.

Nagaraja, K.V., Emery, D.A., Jordan, K.A., Sivanandan, V., Newman, J.A., Pomeroy, B.S., 1984. Effect of ammonia on the quantitative clearance of Escherichia coli from

lungs, air sacs, and livers of turkeys aerosol vaccinated against Escherichia coli. Am J Vet Res 45, 392-395.

Nakamura, K., Yamada, M., Yamaguchi, S., Mase, M., Narita, M., Ohyama, T., 2001. Proliferation of lung macrophages in acute fatal viral infections in chickens. Avian Dis 45, 813-818.

Nauciel, C., Fleck, J., Martin, J.P., Mock, M., Nguyen-Huy, H., 1974. Adjuvant activity of bacterial peptidoglycans on the production of delayed hypersensitivity and on antibody response. Eur J Immunol 4, 352-356.

Nicholls, J.M., Poon, L.L., Lee, K.C., Ng, W.F., Lai, S.T., Leung, C.Y., Chu, C.M., Hui, P.K., Mak, K.L., Lim, W., Yan, K.W., Chan, K.H., Tsang, N.C., Guan, Y., Yuen, K.Y., Peiris, J.S., 2003. Lung pathology of fatal severe acute respiratory syndrome. Lancet 361, 1773-1778.

Okojie, P., Cook, P., 1999. Immediate and delayed complications of epidural analgesia in labour and delivery. J Obstet Gynaecol 19, 370-372.

Otsuki, K., Huggins, M.B., Cook, J.K., 1990. Comparison of the susceptibility to avian infectious bronchitis virus infection of two inbred lines of white leghorn chickens. Avian Pathol 19, 467-475.

Parvizi, P., Abdul-Careem, M.F., Mallick, A.I., Haq, K., Haghighi, H.R., Orouji, S., Heidari, M., Behboudi, S., Sharif, S., 2014. The effects of administration of ligands for Toll-like receptor 4 and 21 against Marek's disease in chickens. Vaccine 32, 1932-1938.

Paul-Clark, M.J., Gilroy, D.W., Willis, D., Willoughby, D.A., Tomlinson, A., 2001. Nitric oxide synthase inhibitors have opposite effects on acute inflammation depending on their route of administration. J Immunol 166, 1169-1177.

Pensaert, M., Lambrechts, C., 1994. Vaccination of chickens against a Belgian nephropathogenic strain of infectious bronchitis virus B1648 using attenuated homologous and heterologous strains. Avian Pathol 23, 631-641.

Perkins, P., Cooksley, C.D., Singletary, S.E., Cox, J.D., 1999. Differences in Breast Cancer Treatment and Survival Between Older and Younger Women. Breast J 5, 156-161.

Quere, P., Rivas, C., van Rooijen, N., 2003. Use of dichloromethylene bisphosphonate (Cl2MBP) to deplete macrophage function in the chicken. Br Poult Sci 44, 828-830.

Qureshi, M.A., Dietert, R.R., Bacon, L.D., 1986. Genetic variation in the recruitment and activation of chicken peritoneal macrophages. Proc Soc Exp Biol Med 181, 560-568.

Rafla, N.M., Cook, J.R., 1999. The effect of maternal exercise on fetal heart rate. J Obstet Gynaecol 19, 381-384.

Ramsey, D.T., Ewart, S.L., Render, J.A., Cook, C.S., Latimer, C.A., 1999. Congenital ocular abnormalities of Rocky Mountain Horses. Vet Ophthalmol 2, 47-59.

Ratanasethakul, C., Cumming, R.B., 1983. Effect of environmental temperature on the mortality in vaccinated chickens after challenge with Australian infectious bronchitis virus. Aust Vet J 60, 255-256.

Reyes, J.L., Terrazas, C.A., Alonso-Trujillo, J., van Rooijen, N., Satoskar, A.R., Terrazas, L.I., 2010. Early removal of alternatively activated macrophages leads to Taenia crassiceps cysticercosis clearance in vivo. Int J Parasitol 40, 731-742.

Rivas, C., Djeraba, A., Musset, E., van Rooijen, N., Baaten, B., Quere, P., 2003. Intravenous treatment with liposome-encapsulated dichloromethylene bisphosphonate (Cl2MBP) suppresses nitric oxide production and reduces genetic resistance to Marek's disease. Avian Pathol 32, 139-149.

Roscic-Mrkic, B., Schwendener, R.A., Odermatt, B., Zuniga, A., Pavlovic, J., Billeter, M.A., Cattaneo, R., 2001. Roles of macrophages in measles virus infection of genetically modified mice. J Virol 75, 3343-3351.

Rosenberger, J.K., Gelb, J., Jr., 1978. Response to several avian respiratory viruses as affected by infectious bursal disease virus. Avian Dis 22, 95-105.

Sahni, M., Guenther, H.L., Fleisch, H., Collin, P., Martin, T.J., 1993. Bisphosphonates act on rat bone resorption through the mediation of osteoblasts. J Clin Invest 91, 2004-2011.

Savill, J., Haslett, C., 1995. Granulocyte clearance by apoptosis in the resolution of inflammation. Semin Cell Biol 6, 385-393.

Schalk, H.M., Hawn, M.C., 1931. An apparently new respiratory disease of chickens. Journal of American Veterinary Medical Association 78, 413-422.

Sekimura, T., Zhu, M., Cook, J., Maini, P.K., Murray, J.D., 1999. Pattern formation of scale cells in lepidoptera by differential origin-dependent cell adhesion. Bull Math Biol 61, 807-827.

Shanmugasundaram, R., Selvaraj, R.K., 2013. In ovo injection of anti-chicken CD25 monoclonal antibodies depletes CD4+CD25+ T cells in chickens. Poult Sci 92, 138-142.

Shek, P.N., Lukovich, S., 1982. The role of macrophages in promoting the antibody response mediated by liposome-associated protein antigens. Immunol Lett 5, 305-309.

Shimazaki, Y., Watanabe, Y., Harada, M., Seki, Y., Kuroda, Y., Fukuda, M., Honda, E., Suzuki, S., Nakamura, S., 2009. Genetic analysis of the S1 gene of 4/91 type infectious bronchitis virus isolated in Japan. J Vet Med Sci 71, 583-588.

Sick, C., Schneider, K., Staeheli, P., Weining, K.C., 2000. Novel chicken CXC and CC chemokines. Cytokine 12, 181-186.

Siddell, S., Snijder, E.J., 2008. An introduction to *Nidoviruses*. In: Perlman, S., Gallagher, T., Snijder, E. (Ed.), Nidoviruses. ASM Press, Washington, D.C., pp. 1-14.

Smati, R., Silim, A., Guertin, C., Henrichon, M., Marandi, M., Arella, M., Merzouki, A., 2002. Molecular characterization of three new avian infectious bronchitis virus (IBV) strains isolated in Quebec. Virus Genes 25, 85-93.

Smith, H.W., Cook, J.K., Parsell, Z.E., 1985. The experimental infection of chickens with mixtures of infectious bronchitis virus and Escherichia coli. J Gen Virol 66 (Pt 4), 777-786.

Staines, K., Young, J.R., Hunt, L., Hammond, J.A., and Butter, C., 2012. An expanded mannose receptor family in avians is suggestive of a diversified functional repertoire. In: "12th Avian Immunology Research Group Conference Proceedings", Midlothian, Scotland, p. 37.

Sugano, S., Stoeckle, M.Y., Hanafusa, H., 1987. Transformation by Rous sarcoma virus induces a novel gene with homology to a mitogenic platelet protein. Cell 49, 321-328.

Sunderkotter, C., Nikolic, T., Dillon, M.J., van Rooijen, N., Stehling, M., Drevets, D.A., Leenen, P.J., 2004. Subpopulations of mouse blood monocytes differ in maturation stage and inflammatory response. J Immunol 172, 4410-4417.

Suzuki, K., Okada, H., Itoh, T., Tada, T., Mase, M., Nakamura, K., Kubo, M., Tsukamoto, K., 2009. Association of increased pathogenicity of Asian H5N1 highly pathogenic avian influenza viruses in chickens with highly efficient viral replication accompanied by early destruction of innate immune responses. J Virol 83, 7475-7486.

Tate, M.D., Pickett, D.L., van Rooijen, N., Brooks, A.G., Reading, P.C., 2010. Critical role of airway macrophages in modulating disease severity during influenza virus infection of mice. J Virol 84, 7569-7580.

Uenaka, T., Kishimoto, I., Uemura, T., Ito, T., Umemura, T., Otsuki, K., 1998. Cloacal inoculation with the Connecticut strain of avian infectious bronchitis virus: an attempt to produce nephropathogenic virus by in vivo passage using cloacal inoculation. J Vet Med Sci 60, 495-502.

Vallyathan, V., Shi, X.L., Dalal, N.S., Irr, W., Castranova, V., 1988. Generation of free radicals from freshly fractured silica dust. Potential role in acute silica-induced lung injury. Am Rev Respir Dis 138, 1213-1219.

Van Beek, E.R., Lowik, C.W., Papapoulos, S.E., 2002. Bisphosphonates suppress bone resorption by a direct effect on early osteoclast precursors without affecting the osteoclastogenic capacity of osteogenic cells: the role of protein geranylgeranylation in the action of nitrogen-containing bisphosphonates on osteoclast precursors. Bone 30, 64-70.

van Roeckel, H., Bullis, K.L., Flint, O.S., Clarke, M.K., 1942a. Massachusetts Agricultural Experiment Station, MA. Annual Report. Bulletin, 99-103.

van Roeckel, H., Bullis, K.L., Flint, O.S., Clarke, M.K., 1942b. Poultry disease control service. Massachusetts Agricultural Experiment Station, MA Bulletin 388, 99-103.

van Rooijen, N., Hendrikx, E., 2010. Liposomes for specific depletion of macrophages from organs and tissues. Methods Mol Biol 605, 189-203.

van Rooijen, N., Nieuwmegen, R., 1984. Elimination of phagocytic cells in the spleen after intravenous injection of liposome-encapsulated dichloromethylene diphosphonate. Cell Tissue Res 238, 355-358.

van Rooijen, N., Sanders, A., 1994. Liposome mediated depletion of macrophages: mechanism of action, preparation of liposomes and applications. J Immunol Methods 174, 83-93.

van Rooijen, N., Sanders, A., 1996. Kupffer cell depletion by liposome-delivered drugs: comparative activity of intracellular clodronate, propamidine, and ethylenediaminetetraacetic acid. Hepatology 23, 1239-1243.

van Rooijen, N., Sanders, A., van den Berg, T.K., 1996. Apoptosis of macrophages induced by liposome-mediated intracellular delivery of clodronate and propamidine. J Immunol Methods 193, 93-99.

van Roon, J.A., Bijlsma, J.W., van de Winkel, J.G., Lafeber, F.P., 2005. Depletion of synovial macrophages in rheumatoid arthritis by an anti-FcgammaRI-calicheamicin immunoconjugate. Ann Rheum Dis 64, 865-870.

Vervelde, L., Matthijs, M.G., van Haarlem, D.A., de Wit, J.J., Jansen, C.A., 2013. Rapid NK-cell activation in chicken after infection with infectious bronchitis virus M41. Vet Immunol Immunopathol 151, 337-341.

Vignuzzi, M., Stone, J.K., Arnold, J.J., Cameron, C.E., Andino, R., 2006. Quasispecies diversity determines pathogenesis through cooperative interactions in a viral population. Nature 439, 344-348.

Villanueva, A.I., Kulkarni, R.R., Sharif, S., 2011. Synthetic double-stranded RNA oligonucleotides are immunostimulatory for chicken spleen cells. Dev Comp Immunol 35, 28-34.

von Bulow, V., Klasen, A., 1983. Effects of avian viruses on cultured chicken bone-marrow-derived macrophages. Avian Pathol 12, 179-198.

Wang, F., Tao, W.A., Gozzo, F.C., Eberlin, M.N., Cooks, R.G., 1999. Synthesis of B- and P-Heterocycles by Reaction of Cyclic Acetals and Ketals with Borinium and Phosphonium Ions. J Org Chem 64, 3213-3223.

Wang, L., Junker, D., Collisson, E.W., 1993. Evidence of natural recombination within the S1 gene of infectious bronchitis virus. Virology 192, 710-716.

Wang, L., Junker, D., Hock, L., Ebiary, E., Collisson, E.W., 1994. Evolutionary implications of genetic variations in the S1 gene of infectious bronchitis virus. Virus Res 34, 327-338.

Wang, X., Rosa, A.J., Oliverira, H.N., Rosa, G.J., Guo, X., Travnicek, M., Girshick, T., 2006. Transcriptome of local innate and adaptive immunity during early phase of infectious bronchitis viral infection. Viral Immunol 19, 768-774.

Wang, Y., Mahajan, D., Tay, Y.C., Bao, S., Spicer, T., Kairaitis, L., Rangan, G.K., Harris, D.C., 2005. Partial depletion of macrophages by ED7 reduces renal injury in Adriamycin nephropathy. Nephrology (Carlton) 10, 470-477.

Warchol, M.E., Schwendener, R.A., Hirose, K., 2012. Depletion of resident macrophages does not alter sensory regeneration in the avian cochlea. PLoS One 7, e51574.

Watters, T.M., Kenny, E.F., O'Neill, L.A., 2007. Structure, function and regulation of the Toll/IL-1 receptor adaptor proteins. Immunol Cell Biol 85, 411-419.

Wilson, L., McKinlay, C., Gage, P., Ewart, G., 2004. SARS coronavirus E protein forms cation-selective ion channels. Virology 330, 322-331.

Winterfield, R.W., Albassam, M.A., 1984. Nephropathogenicity of infectious bronchitis virus. Poult Sci 63, 2358-2363.

Wittwer, C.T., and Kusakawa, N., 2004. Real-time PCR. In: Persing D.H., T.F.C., Versalovic J., Tang J.W., Unger E.R., Relman D.A., White, T.J. (Ed.), Molecular microbiology: diagnostic principles and practice. ASM Press, Washington, pp. 71-84.

Wu, Z., Hu, T., Kaiser, P., 2011. Chicken CCR6 and CCR7 are markers for immature and mature dendritic cells respectively. Dev Comp Immunol 35, 563-567.

Wurm, T., Chen, H., Hodgson, T., Britton, P., Brooks, G., Hiscox, J.A., 2001. Localization to the nucleolus is a common feature of coronavirus nucleoproteins, and the protein may disrupt host cell division. J Virol 75, 9345-9356.

Xu, C., Zhao, J., Hu, X., Zhang, G., 2007. Isolation and identification of four infectious bronchitis virus strains in China and analyses of their S1 glycoprotein gene. Vet Microbiol 122, 61-71.

Xu, Y., McKenna, R.W., Kroft, S.H., 2002. Comparison of multiparameter flow cytometry with cluster analysis and immunohistochemistry for the detection of CD10 in diffuse large B-Cell lymphomas. Mod Pathol 15, 413-419.

Yount, B., Denison, M.R., Weiss, S.R., Baric, R.S., 2002. Systematic assembly of a full-length infectious cDNA of mouse hepatitis virus strain A59. J Virol 76, 11065-11078.

Zikratov, G., Yueh, F.Y., Singh, J.P., Norton, O.P., Kumar, R.A., Cook, R.L., 1999. Spontaneous anti-Stokes Raman probe for gas temperature measurements in industrial furnaces. Appl Opt 38, 1467-1475.

Appendix

As the co-authors that contributed to the paper entitled " Clodronate treatment significantly depletes macrophages in chickens " Canadian Journal of Veterinary Research, in Press., we permit using materials in this paper as part of Amber Marie Kameka's thesis entitled "Effect of macrophage depletion on avian infectious bronchitis coronavirus infection" that will be submitted to the Faculty of Graduate Studies at University of Calgary in April 2014.

Co-Author's Name	Signature	Date
Siamak Haddadi		
Fathima Jesreen Jamaldeen		
Prima Moinul		
Xiao Tim He		
Fathima Hafsa Prem Nawazdeen		
Stephan Bonfield		
Shayan Sharif		
Nico van Rooijen		
Mohamed Faizal Abdul-Careem		
Dae Sun Kim		

As the co-authors that contributed to the paper entitled "Induction of innate immune response following infectious bronchitis corona virus infection in the respiratory tract of chickens" Virology 450-451, 114-121, we permit using materials in this paper as part of Amber Marie Kameka's thesis entitled "Effect of macrophage depletion on avian infectious bronchitis coronavirus infection" that will be submitted to the Faculty of Graduate Studies at University of Calgary in April 2014.

Co-Author's Name	**Signature**	**Date**
Siamak Haddadi		
Dae Sun Kim		
Susan Catherine Cork		
Mohamed Faizal Abdul-Careem		